REMOVAL OF LEAD (II) AND CADMIUM (II) IONS FROM WASTEWATER USING ACTIVATED CARBON DERIVED FROM *MACADAMIA INTERGRIFOLIA* NUTSHELL POWDER

AMOS KIMONDO KAMAU

MASTER OF SCIENCE

(Chemistry)

JOMO KENYATTA UNIVERSITY OF

AGRICULTURE AND TECHNOLOGY

2022

Removal of Lead (II) and Cadmium (II) Ions from Wastewater Using Activated Carbon Derived from *Macadamia Intergrifolia* Nutshell Powder

Amos Kimondo Kamau

A Thesis Submitted in Partial Fulfillment of the Requirements for the Degree of Master of Science in Chemistry of the Jomo Kenyatta University of Agriculture and Technology

2022

DECLARATION

This thesis is my original work and has not been presented for a degree award or any othe University.

Signature…… Date…….

Amos Kimondo Kamau

This thesis has been submitted for examination with our approval as supervisors

Signature…… Date…….

Prof. George Thuku Thiong'o, PhD

JKUAT, Kenya

Signature…… Date…….

Dr. Beatrice Katheu Kakoi, PhD

JKUAT, Kenya

DEDICATION

I dedicate this work to my entire family comprising of Mr. and Mrs. Kamau, John, Sam, Beth, Ruth, Ann, Lucy and Sarah.

ACKNOWLEDGEMENT

I thank God for giving me the strength and wisdom to achieve this dream. I also wish to thank my supervisors Prof. George Thiong´o and Dr Beatrice Kakoi for their guidance throughout the project. My sincere thanks to the departments of chemistry and Food Science and Technology (JKUAT) for giving space and facilities to undertake my research. I also thank Mr Mawili, Mr Nderitu and Mr Kamathi for their technical support. Last but not least, I wish to thank my colleagues Edwin Madivoli, Joyline Gichuki, Jackson Mutembei, Pius Kinoti, Ernest Maina, David Mutegi, Paul Kinyanjui, Sammy Wanakai, the late Japeth Njiema and Joel Ogilo for their advice during the difficult times. Special thanks goes to pastor in charge African Christian Church and School Ruiru Pastor Rose Nyambura Kamau for her endless support in prayers during my academic journey.

Lastly, I thank my entire family, my parents Mr and Mrs Elizaphan Kamau Mwangi, my siblings John, Sam, Beth, Ruth, Ann, Lucy and Sarah. I will always be grateful for their moral and financial support during my academic journey.

TABLE OF CONTENTS

LIST OF TABLES

LIST OF FIGURES

LIST OF APPENDICES

LIST OF PLATES

ABBREVIATIONS AND ACRONYMS

Ad (g)	Adsorbent dosage in grams
ANOVA	Analysis of Variance
Av (mg/L)	Averange equilibrium metal ions concentration in mg/L
DNA	Deoxyribonucleic Acid
Eq (mg/L)	Equilbirium metal ions concentration in mg/L
FAAS	Flame Atomic Absorption Spectrophotometer
FTIR	Fourier Transform Infra-red Spectrophotometer
In (mg/L)	Initial metal ions concentration in mg/L
SEM	Scanning Electron Microscope
UNICEF	United Nation International Childrens Fund
WHO	World Health Organization

ABSTRACT

Industrialization in developing countries has led to the release of toxic pollutants which has become a health challenge. Major sources of water contamination by toxic pollutants includes pharmaceuticals, residues from agrochemicals, dyes and heavy metals. Lead and Cadmium are heavy metals of great concern due to their high levels of toxicity even in minute concentrations. Convectional methods for the removal of heavy metal ions from aqueous solution are expensive. Adsorption using low cost activated carbon is a cheap and effective technique which removes heavy metal ions from water. In this study removal of Pb (II) ions and Cd (II) ions using activated carbon derived from *Macadamia intergrifolia* nutshell powder are reported. *Macadamia intergrifolia* nutshells were purchased for Kenya nut company in Kiambu county. Activated carbon was made by soaking two kilograms of *Macadamia intergrifolia* nutshell powder in 50 % phosphoric acid for 24 hours, which was then oven dried for 48 hours at 105°C. Dried sample was charred using a heating mantle at 300°C followed by iginition in an electrical muffle furnace at 550°C for 30 minutes. After cooling, the sample was washed with 0.1 HCl to remove ash content, and then washed with 0.1M NaOH to neutralize pH. Optimization parameters such as pH, sorbent mass, contact time and initial metal ion concentration were studied. The level of the two heavy metal ions before and after adsorption was determined using flame atomic absorption spectrophotometer . Adsorption of Pb (II) ions and Cd (II) ions were found to increase with increase in pH until the optimum pH of 4 and 5 for Pb (II) ions and Cd (II) ions respectively. Furthermore, adsorption of both metal ions was found to increase with increase in sorbent mass until the optimum sorbent mass of 0.4 and 0.3 grams for Pb(II) ions and Cd (II) ions respectively.The adsorption increased with increase in contact time. The optimum contact time for Pb (II) ions and Cd (II) ions were found to be 60 and 75 minutes respectively. Adsorption isotherm for both metal ions were found to fit well in the Langmuir model where maximum adsorption capacity was found to be 4.093 and 7.818 mg/g for Pb (II) ions and Cd (II) ions respectively. According to the Langmuir model values of 1/n for Pb (II) ions and Cd (II) ions were 0.627 and 0.598 respectively. This indicated a favorable reaction. Kinetics studies were found to fit well in the pseudo second order model where the value of equilibrium adsorption capacity was found to be 2.521 and 2.500 mg/g for Pb (II) and Cd (II) respectively. FT-IR of activated carbon analysis showed that the presence of OH at V_{max} 3389 cm^{-1}, COO- at V_{max} 2367 cm^{-1} , C=O at V_{max} 1593 cm^{-1} and POOH at V_{max} 1206 cm^{-1} . These functional groups may have been responsible for Pb(II) and Cd(II) ions adsorption onto activated carbon. Investigation on SEM on external morphology revealed that the surface of the activated carbon adsorbent had deep cavities and also irregular structures, which provided the binding sites for the attachment of Pb(II) ions and Cd(II) ions. The study showed that activated carbon derived from *Macadamia intergrifolia* nutshell powder has a good potential for use in the removal in Pb (II) and Cd (II) ions from wastewater.

CHAPTER ONE

INTRODUCTION

1.1 Background of the study

Water is the an important compound in human beings since it makes more than 60% of the human weight. Humans lose 5-10% of water daily due to various biological processes such as sweat loss, respiratory loss, faecal loss, urinary loss and metabolic production. Consequently, it is recommended that humans should drink 1.9 to 2.1 litres of water each day (Calvin *et al.*, 2012). According to (UNICEF., 2008) more than 3.4 million people die annually due to lack of safe drinking water. The most affected are children who have high chances of getting diseases as a result of their weak immune system. Pollutant discharge emanating from industrial waste increase pollution on water bodies (Lu *et al*., 2015). Water provides a conducive environment for biochemical reactions as it is a solvent media. Safe water is all important for human health and is one of the human basic needs. In developing and developed countries, water related illnesses such as cholera, typhoid and diarrhoea were eradicated when the population had access to safe drinking water (Jain., 2012). The most serious environmental health concern globally is the contamination of ground water by toxic heavy metals such as Pb (II) ions, Cd (II) ions, As (III) ions and Cr (VI) ions which when consumed,even at very low concentration,are detrimental to human health (Taboada-Castro *et al*., 2012). Plant nutrients and fertilizers which are applied for agricultural use causes heavy metal pollution to water and soil, and potentially this leads to increase in heavy metal ions concentration in soil and both surface and groundwater which may have adverse effects on human health (Chotpantarat *et al*., 2011). Due to increased environmental awareness and strict regulations regarding management of water, a number of industries have sought for the appropriate methods of water treatment before being discharged (Gupta *et al*., 2019).

1.1.1 Water crisis

High percentage of the landmass is made up of water but it is only 2.5% of this which constitutes freshwater which is required to sustain human life. However, the largest proportion of freshwater, two third, is found in permanent snow and glaciers.

This therefore, leaves only one third for the supply of increasing needs globally (Kumar *et al*., 2017). Water scarcity affects nearly all the countries in the world. In Kenya more than 17 million people, which accounts for 34% of the total population, do not have access to clean water. It has been reported that 10% deaths in Kenya are as a result of poor sanitation and water related diseases (Feng *et al*., 2011). Globally one-fifth of the world population do not have access to clean water. Furthermore, one-fourth of the world population which accounts to approximately 1.92 billion people live in countries which lack adequate infrastructure to draw water from aquifers and rivers to homesteads (Ochongo., *et al* 2019).

1.2 Statement of the problem

Approximately 1.92 billion people in the world do not have access to clean drinking water (Kariuki *et al*., 2017). Water pollution by heavy metals is one of the major health concerns globally. Thus, there is a great need for the removal of these and other chemical pollutants from water. Conventional methods which have been used for wastewater treatment such as membrane filtration, chemical precipitation, ion exchange and phytoremediation, are costly in terms of purchasing and maintenance. Thus, there is increasing need for the development of low-cost methods for removal of heavy metal ions from water. Natural materials, agricultural wastes, industrial wastes and activated carbon have been studied as the low-cost adsorbents for the removal of heavy metal ions from water (Renu *et al.,* 2017). Application of these low-cost adsorbents require a great understanding of their adsorption isotherms and kinetic properties.

1.3 Justification

Conventional methods for removal of heavy metal ions from water are expensive both to buy and maintain and also, they are not environmentally friendly. Consequently, the use of natural materials, agricultural wastes industrial wastes and activated carbon provides biodegradable, readily available and non-toxic alternative to low-cost adsorbents. Activated carbon derived from *Macadamia intergrifolia* nutshell derived products have the potential to remove heavy metal ions from water. Therefore, application of low cost activated carbon derived from *Macadamia intergrifolia* nutshells for the removal of Pb (II) ions and Cd (II) ions would address

the challenge faced in water and wastewater management in the developing countries.

1.4 Hypothesis

Activated carbon derived from *Macadamia intergrifolia* nutshell powder provide an effective way of removing heavy metal ions from wastewater

1.5 Objectives

1.5.1 General objective

To determine the efficacy of activated carbon derived from *Macadamia intergrifolia* nutshell powder in the removal of Pb (II) ions and Cd (II) ions from polluted water

1.5.2 Specific objectives

i. To prepare activated carbon from *Macadamia intergrifolia* nutshell powder.

ii. To characterize the activated carbon derived from *Macadamia intergrifolia* nutshell powder in terms of functional group and external morphology.

iii. To determine the optimum conditions of pH, optimum adsorbent dose, optimum contact time and optimum initial concentration for the removal of Pb (II) ions and Cd (II) ions from wastewater using activated carbon derived from *Macadamia intergrifoli*a nutshell powder.

iv. To determine the equilibrium, rate and mechanism of Pb (II) and Cd (II) ions adsorption onto activated carbon derived from *Macadamia intergrifolia* nutshell powder through adsorption isotherms and kinetic studies.

1.6 Significance of the study

Method of disposing industrial waste is a major concern in Kenya. Poor management of waste leads to environmental pollution and thus posing danger to public health. The study is aimed at comimg up with the cheaper adsorbent for the removal of Cd (II) ions and Pb (II) ions from wastewater, by using industrial waste products. Therefore, this study has converted an industrial waste into a cost effective adsorbent and has also enhanced the use of green chemistry.

1.7 Scope and limitation of the study

i. The study was restricted to activated carbon by activation with phosphoric acid and not from other activating agents.

ii. The study focused on the activation temperature of 550°C only.

iii. The research focused on the two heavy metal ions, that is Pb (II) ions and Cd (II) ions. Other heavy metal ions and pollutants were not considered**.**

CHAPTER TWO

LITERATURE REVIEW

2.1 Heavy metals

Heavy metals such as Pb (II), Zn (II), Cd (II) and Cr (VI) occur naturally, they have a density which is five times more than water and have high atomic weight. In the periodic table, they are classified under the categories of transition elements, lanthanides, actinides and some metalloids (Singh *et al*., 2011). Heavy metals are used in various fields such as medical, industrial purposes and in the microbial fuel cell for the purpose of electricity generation (Birry *et al.*, 2011; Lyu *et al.*, 2017). The following regulations for the standards for domestic water (NEMA., 2006) and (WHO., 2006) were put in place as shown in Table 2.1

Table 2.1: WHO and NEMA standards for domestic water

Parameter	**NEMA Guide Value (max allowable)**	**WHO Guide Value (max allowable)**
pH	6.5-8.5	6.5-8.5
Pb	0.05 mg/L	0.01 mg/L
Cd	0.01 mg/L	0.003 mg/L

However, exposure of non-essential heavy metals, even in minute concentrations, is detrimental to human health (Cai *et al*.,2015). Sources of heavy metal contamination include human activities such as use of heavy metal containing compounds for agricultural and domestic uses such as; use of fertilizer containing heavy metals, eating contaminated food and cigarrete smoking (Chaney., 2015), industrial activities such as combustion of petroleum products and burning of coal in power plants (Njuguna *et al*., 2017), mining and smelting activities (Li *et al*., 2014) among others. Various natural phenomena such as rocks and mineral breakdown by

weathering and eruption of volcanoes also contribute to pollution of streams, rivers and lakes (Vrhovnik *et al*., 2013).

Cadmium is a heavy metal with an atomic number of 48 and mass number 112 it is above Zn and below Hg in the periodic table with a divalent cation character when forming complexes with other elements (Wedepohl 1995). It is a toxic metal of great environmental concern. Cadmium distribution in the earth's crust is in the mean concentration of 0.1 mg/kg where the highest levels of cadmium are believed to be in the marine phosphates and sedimentary rocks at an average distribution of 15mg/kg (Symolyakov., 2012). Industrial application of cadmium include manufacture of television screens, alloy production, manufacture of cosmetics and pigments and paints production (Bernhoft., 2013). Sources of cadmium exposure to water bodies includes waste incineration near water bodies and use of phosphate fertilizers which may the find their way into the water bodies through erosion (Mohod and Dhote 2013). Humans may be exposed to cadmium through cigarette smoking and eating contaminated food. Cadmium is found in minute concentrations in seeds, grains, leafy vegetables and potatoes (Meharg *et al.,* 2013). Working in industries where cadmium is the primary metal, emission of effluents containing cadmium from industries and use of phosphate fertilizers containing cadmium are other means by which humans can be exposed to cadmium (Satarug *et al*., 2010). Symptoms of high cadmium exposure include; pain in the abdomen, vomiting, muscle cramps, loss of consciousness and irregular movement of the body which occurs after 15-30 minute of exposure (Rahimzadeh *et al.,* 2017). Depending on the route of poisoning, high cadmium concentration in human body causes injuries in the pulmonary, renal and hepatic systems, coma or even gastrointestinal tract infection (Järup and Åkesson., 2009). Cadmium induces generation of oxygen containing compound, causing damages to the cells which further causes damage of single stranded DNA. Damage to the single stranded DNA disrupts nucleic acid and protein synthesis (Pan *et al.*, 2010). Cadmium compounds are believed to be carcinogenic where they are believed to be the main cause of lung cancer (Kim *et al*., 2015).

Lead occurs naturally in minute concentrations in the earth's crust. It is a bluish grey metal whose atomic number is 82 and mass number 207 (Wedepohl., 1995).

Applications of lead include manufacture of lead acid battery , ammunitions, solders and pipes and in the making of x-ray shield devices (Assi *et al*., 2016). Anthropogenic sources that cause lead exposure to the environment are application of lead-based compounds for agricultural and domestic use, and emission of lead fumes from industries. Lead exposure to humans can be through the inhalation of dust particles containing lead, or by taking food or water contaminated by lead (Pizzol *et al*., 2010). Human lead absorption mainly depends on age and physiological status. Adults can absorb 35 to 50% of lead by drinking water while young children can absorb more than 50% through drinking water (Pastorelli *et al*., 2012). Lead may be found in drinking water through the leaching of lead containing pipes, solders and faucets which are commonly found during plumbing of older buildings. High concentration of lead in water is found during mining and also industrial wastewater during processes such as lead melting and printing of books (Wani *et al.*, 2015). Food which have been grown in the soil that has been contaminated with lead can lead to Pb (II) ions adsorption, and consequently leading to accumulation in the parts of edible plants and consequently leading to its harmful effects in the human body (Kinuthia *et al.,* 2020). Human absorbs high concentration of Pb (II) ions through consuming contaminated food and water (Pastorelli et al. 2012). Previous studies have shown that, after human have been exposed to Pb (II) ions, the metal ions accumulate in the soft tissues such as kidneys and liver and finally into the bones and teeth. Cd (II) ions has a half life of fifteen to thirty days in the blood and ten to thirty years in the bones (Singh et al. 2011). Enhancement of Pb (II) ions in the body is due to the deficient of Zn (II) ions and Ca (II) ions. Early symptoms of human lead exposure are dullness, loss of memory, headache and irritability. The main target for the lead exposure in humans are the endocrine systems, reproductive systems, kidney and liver (Colina *et al*. 2019; Mason *et al*., 2014)

2.1.1 Previous studies on heavy metal pollution in water and wastewater

Studies by (Sayo *et al*., 2020) reported high concentration of Zn (II), Cd (II) and Cu (II) ions in the sewage effluent from Embu sewage treatment plant. The levels of heavy metal ions in the sewage effluents were found to be higher than the

recommended levels for wastewater to be used for irrigation. It was also reported that, high concentration of heavy metal ions in the soil which was irrigated by the sewage effluents led to the accumulation of heavy metal ions in edible plants.

(Akenga *et al*., 2019) Studied the effects of heavy metal ions in the irrigation water, soil and managu (*Solanum nigrum*) from Homahills in Homabay county. It was reported that irrigated water had higher levels of manganese ion which exceeded the world health organization limit. It was also reported that there were high levels of $Mn^{2+,}$ $Pb^{2+,}$ Cd^{2+} and Fe^{3+} in *Solanum nigrum* which exceeded world health organisation limits.

(Kosgei *et al*., 2019) studied the concentration of heavy metal ions in water and its effects in the accumulation on the organs of *Oerochromis nicotixus* and *Clarias galiepinus* from Lake Victoria Kenya. It was reported that, although heavy metal ions concentration was low in fish and water, there was a high potential of metal toxicity which might be severe to future generations, depending on the extent on the influx of domestic and industrial wastewater into the lake as a result of human activities in the surrounding areas.

2.1.2 Heavy metal removal from wastewater

Various conventional method have been used for the removal of heavy metal ions from wastewater. The methods include; membrane filtration, chemical precipitation, ion exchange, phytoremediation, solvent extraction and floatation. These methods are briefly explained in the following subsections.

2.1.2.1 Membrane filtration

Membrane filtration entails the use of filter membranes which permit some particles to pass through the filter membranes but does not permit others to pass through. Examples of membrane filtration include; ultrafiltration, nanofiltration and reverse osmosis. Ultrafiltration entails heavy metal ions removal from aqueous solutions by allowing the passage of water and low molecular weight solutes while restricting the passage of the macromolecules, which have larger size than the pores of the filter (Qiu and Mao., 2013).

Nanofiltration entails the use of nanosized filter membranes which have a particle diameter of 0-10 nm. Particle which have sizes greater than the pores of nanosized membranes do not pass through the filter membrane which enhances heavy metal removal (Gherasim *et al.,* 2013). Reverse osmosis entails application of applied pressure to overcome the osmotic pressure. It entails the application of semi permeable membrane. Particles which have pores greater than the size of semi permeable membrane do not pass through the pores which allows heavy metal ions removal (Ortega *et al.*, 2008). Disadvantages of membrane filtration are formation of chemical sludge and high cost of buying and maintenance (Wei *et al.,* 2003).

2.1.2.2 Chemical precipitation

Chemical precipitation involves the reaction in which chemical precipitates reacts with heavy metal ions forming a precipitate. The precipitate formed is then separated with water by sedimentation or filtration. When filtration is complete water is then decanted ready for use (Meunier *et al.*, 2006). Calcium hydroxide and sodium hydroxide have been used to precipitate copper and chromium whereas iron sulphide have been used to precipitate copper, lead and cadmium(Zhu *et al.*, 2012). The general equation for the precipitation process is where metal ions react with hydroxide ions to form metal hydroxide precipitate.

$$M^{2+} + 2OH^{-} \rightarrow M(OH)_2 \quad \text{.....(2.1)}$$

The main disadvantage of chemical precipitation is costly disposal due to the formation of secondary waste such as gypsum and metal hydroxide sludge (Wang *et al.,* 2005).

2.1.2.3 Ion exchange

This involves the process of reversible exchange of ions. It involves application of ion exchange resin which can be either natural or synthetic. Ion exchange resin possesses cationic exchangers which are able to exchange ions with positively charged metal ions in aqueous solutions. The most commonly used cationic exchangers are $–SO_3H$ and –COOH (Kim and Benjamin., 2004; Rengaraj *et al*., 2001). Disadvantages of ion exchange resin is that it is expensive to buy. Further, there is selective removal of metal cations if there happens to be large quantities of

monovalent or divalent metal ions such as Na (I) ions and Ca (II) ions (Ran *et al.*, 2017).

2.1.2.4 Phytoremediation

This involves application of certain plant to remove sediments, clean up soil and removal of metal ions from soil and also from contaminated water. It includes phyroexctraction, phytostabilization, rhizofiltration and phytovolatilization (Ali *et al*, 2013). Phyroexctraction involves absorption of heavy metal ions by plant root and then transferring them to the shoots. The metal ions are then removed by harvesting (Lombi *et al*., 2001). Phytostabilization involves use of plant roots to limit the movement of metal ions in the soil. The plant purposes to prevent the soil erosion thus hindering the transfer of metal ions to other areas (Jadia and Fulekar., 2009). Rhizofiltration involves application of certain plants which are found in both terrestrial and aquatic environment, these plants absorb, concentrates and precipitates heavy metal ions from their polluted sources to the plant roots. Rhizofiltration is mainly applied in ground water and in the surface water where there is low contaminant concentration (Ullah *et al*., 2015). Phytovolatilization involves use of certain plants to remove heavy metal ions from soil. The metals ions after removal are volatilized and the discharged into the environment (Mahar *et al.,* 2016). Disadvantages of phytoremediation as a method of heavy metal removal includes; incomplete metal removal, high reagent energy requirement, time consuming and difficulty in the regeneration of plant for further biosorption (Wei *et al*., 2003).

2.1.2.5 Solvent extraction

Solvent extraction entails removal of metal ions in aqueous solution by dissolving the aqueous solution with another organic solvent which is more soluble. Removal of heavy metal ions by solvent extraction involves three steps namely; extraction step, scrubbing step and stripping step. In extraction step the aqueous solution containing the metal is mixed with the organic phase which contains the extracant. The metal ions in the aqueous solution reacts with the extracant which are then transferred to the organic phase, the aqueous phase is removed to be recycled for the purpose of removing other metals in solution. The organic phase moves to the scrubbing step where the other metal ions and impurities are removed from the organic phase

containing metal ions by using the appropriate aqueous solution. The loaded organic phase free of other metal ions and impurities then goes to the stripping step where the metal ions are removed from the organic phase in salt form. They are then converted to their corresponding oxides or free metals by processes such as evaporation or electrolysis (Fenglian and Qui., 2011). Examples of organic solvents used includes vegetable oil, kerosene, toluene, hexane and chloroform based organic solvents. Disadvantages of solvent extraction involves high cost of the organic solvents, and the equipment, and is also time consuming.

2.1.2.6 Floatation

Floatation involves removal of heavy metal ions from aqueous solutions by introduction of collectors or surfactants, which are negatively charged compared to metal ions being removed which are positively charged. Use of collector raises the surface hydrophobicity which in turn raises the separation of hydrophobic and hydrophilic particles. Increase in the concentration of the hydrophilic and hydrophobic particles floats the ion surfactants leading to the precipitate formation thus enhancing heavy metal ions removal. The main disadvantage of floatation is that it is only effective at very low concentrations (Deliyanni *et al*., 2017; Kyzas and Matis., 2018).

2.1.2.7 Adsorption

Adsorption is a separation process. In adsorption the metal ions adhere to the interior or the exterior surface of the adsorbent (Momčilović *et al.*, 2011).

2.1.3 Mechanism of adsorption using various sorbents

There are various mechanisms involved in metal ions sorption onto the adsorbent surfaces such include; ion exchange, physical adsorption and chemisorption. Ion exchange involves the replacement of alkali metals, alkaline earth cations, protons and other positively charged ions present in algae, bacteria and other plants with the heavy metal ions (Cheng *et al.*, 2011; Tao and Fletcher., 2013).

Physical adsorption involves formation of weak van der waals forces between the metal ions and the adsorbent in which no exchange of electrons takes place (Tripathi and Ranjan., 2015). In chemisorption, most adsorbents contain negatively charged

organic functional groups and this groups react with metal ions via the exchange of electrons leading to the formation of a chemical bond (Kakoi *et al*., 2016; Madivoli *et al*., 2016). Various sorbents have been tried for the removal of heavy metal ions from water. They include; natural materials, agricultural wastes and industrial wastes.

2.1.3.1 Removal of heavy metal ions by natural materials through chemisorption and ion exchange mechamism

Study by Kowanga *et al.,* (2016) revealed that *Moringa oleifera* seed powder is an effective adsorbent for the removal of Pb (II) ions and Cd (II) ions from aqueous solution. Fourier transform infrared spectrum for the *Moringa oleifera* revealed the presence of amino, carbonyl and carboxyl groups which were responsible for heavy metal ions adsorption. In his study, pseudo second order kinetics was prevalent and adsorption isotherm fitted well in Freundlich isotherms compared to other adsorption isotherms. Review of literature by Salehzadeh, (2013) showed that *xanthium penysyranium* is an effective biosorbent for the removal of Zn (II) ions, Cd (II) ions, Ni (II) ions, Co (II) ions and Fe (III) ions from aqueous solutions. It was found that at pH 4, initial concentration of 10 mg/l and contact time of 90 minutes, the percentage metal ions removal increased in the order $Zn^{2+}<Cd^{2+}<Cu^{2+}<Pb^{2+}<Ni^{2+}<Fe^{3+}<Co^{2+}$.

Research reports by Yu *et al*., (2013) revealed that natural bentonite can be used for the removal of Cu (II) ions, Zn (II) ions, Ni (II) ions and Co (II) ions from aqueous solutions. The study revealed that the kinetics data was best described by pseudo second order model, additional the values of thermodynamic parameters which included heat change, free energy and entropy for all metals were found to be temperature dependence. It was also found that adsorption for Cu (II) ions and Zn (II) ions was endothermic while for Ni (II) ions and Co (II) ions was found to be exothermic.

2.1.3.2 Removal of heavy metal ions by agricultural waste through chemisorption mechanism

According to Renu *et al.,* (2017), studied the removal of chromium from aqueous solutions using egg shells, calcined egg shell, wheat bran and modified wheat bran.

The study reported that the percentage removal for egg shell of 64 %, calcined egg shell of 70.19 %, wheat bran of 75.89 % and modified wheat bran of 96.9 %. Surchi, (2011) identified rice husk and tea waste as a low cost biosorbent for the removal of Pb (II) ions from aqueous solutions with percentage removal after 90 minutes of 90 % and 98 % respectively. The kinetic data for both biosorbents was found to fit well in the pseudo first order model while adsorption isotherms were best described by Freundlich model.

Ndungu *et al* (2014) studied the kinetic modelling of Cu^{2+}, Cd^{2+}, and Pb^{2+} onto a raw and modified *Atrocarpus heterophyllus* seed from a model solution. It was reported that, raw and modified jackfruit seed were efficient metal ions chelate in the study of adsorption of Cu^{2+}, Pb^{2+} and Cd^{2+}. Kinetic studies revealed that the adsorption of the three metal for the modified and raw jack fruit seeds best fitted in the pseudo second order model showing that chemical adsorption was prevalent.

2.1.3.3 Removal of heavy metal ions by industrial waste through chemisorption mechanism

.Study by Taha and Dakroury., (2007) revealed that cement kiln dust is an effective low cost adsorbent for the removal of Cd (II) ions, Al (III) ions, Co (II) ions and Zn (II) ions from wastewater. The study reported that maximum adsorption efficiency for Cd (II) ions of 165.94 mg/g, Adsorption isotherms data fitted well in Langmuir model an indication that monolayer adsorption was prevalent.

Wanja *et al*., (2015) studied the removal of Cu (II), Pb (II) and Cd (II) ions from aqueous solution using chemically modified avocado seed. It was reported that acid modified avocado seed and unmodified avocado seeds had differen efficicny levels in the removal of metal ions from aqueous solution. Adsorption isotherm data fitted well in the Freundlich isotherm while kinetic data fitted well in the Pseudo second order kinetics.

2.1.3.4 Removal of heavy metal ions by activated carbon through chemisorption mechanism

Study by Moreno-Piraján and Giraldo., (2012) shows that activated carbon derived from orange peel is a low cost adsorbent for the removal of Cr (III) ions, Cd (II) ions

and Co (II) ions from aqueous solution. It was reported that pH played an important role in the heavy metal ions removal. The maximum adsorption capacity for Cd (II) ions was found to be 26.87 mgg^{-1}, Cr (III) ions was 30.11 mgg^{-1} and Co (III) ions was 45.44 mgg^{-1}. The adsorption isotherm data was best described by Langmuir models while kinetic date best fitted in the pseudo second order model.

Asuquo *et al*., (2017) reported that mesoporous activated carbon is an effective adsorbent for the removal of Cd (II) ions and Pb (II) ions from aqueous solution. It was revealed that pseudo first order data best described Pb (II) ions adsorption as compared to Cd (II) ions adsorption. Langmuir models best described the adsorption isotherms for both metal ions with maximum loading capacity found to be 27.3 mgg^{-1} and 20.3 mgg^{-1} for Pb (II) ions and Cd (II) ions respectively. Mohammadi *et al*., (2010) revealed activated carbon derived from sea-buck thorn stones as a cheap adsorbent for the removal of Pb (II) ions from wastewater. It was reported that the adsorption data fitted well in the Freundlich and Langmuir equations, where maximum adsorption capacity for Pb (II) was found to be 51.81 mgg^{-1}. Desorption studies showed that activated carbon derived from sea-buckthorn stones can be recovered for further use.

Muvengei *et al*., (2017) Studied the removal of Pb^{2+} and Cd^{2+} from water using charcoal, activated carbon and ash derived from maize cobs. It was reported that, charcoal, activated carbon and ash from maize cobs are cheaper methods for the removal of Pb^{2+} and Cd^{2+} from aqueous solutions. Adsorption isotherms were found to fit well in the Freundlich model than the Langmuir model.

2.1.4 Knowledge gaps

Reviewed literature indicates that *Macadamia intergrifolia* nutshell derived products have been employed as the low cost adsorbents for the removal of hexavalent chromium from aqueous solutions (Pakade *et al*., 2017). However, the performance of activated carbon derived from *Macadamia intergrifolia* nutshell powder in the removal of Pb (II) ions and Cd (II) ions from wastewater has not been reported. Furthermore, previous studies have not determined the performance, equilibrium and

kinetic studies for Pb (II) ions and Cd (II) ions adsorption onto activated carbon derived from *Macadamia intergrifolia* nutshell powder. .

2.2 Adsorption isotherms

Adsorption is the accumulation of metal ions onto the adsorbent surface. It refers to the adherence of solid, liquid or gas to the solid surface. Adsorption occurs on gas–solid, solid-solid or in the liquid-solid. Isotherm refers to the variation in the metal ions adherence to the adsorbent surface with variation in the initial concentration at a constant temperature (Nethaji *et al*., 2013). Adsorption isotherms are therefore series of adsorption experiments which are performed at constant temperature. They are used to describe the state of balance created between the concentration of metal ions which is retained in the adsorbent surface and the concentration of the metal ions which has remained in the solution (Desta., 2013). They are used to describe the amount of heavy metal ions that a certain adsorbent can retain, they also describe the amount of metal ions remaining in the aqueous solution after the equilibrium is attained. Adsorption isotherms have constant values which describes the surface properties of a particular adsorbent (Repo *et al*., 2011). Various sorption isotherms used include; Langmuir, Freundlich, Jovanovic and Temkin sorption isotherm.

2.2.1 Langmuir sorption isotherm

Langmuir isotherm assumes the monolayer distribution of metal ions onto the adsorbent surface. It predicts that the adsorbent surface has a fixed number of attachment sites which have equal affinity for the interaction with the metal ions, once all the sites are saturated with the metal ions no further adsorption takes place (Seyed *et al*., 2013). Langmuir adsorption isotherms is based on the assumptions that., all the adsorption sites are equal, there is no reaction between the adsorbing metal ion, the same mechanism takes place during adsorption, and during adsorption metal ion occupies a single adsorption site thus there is no deposition of metal ions on top of the other (Fajardo *et al*., 2016 ; Kakoi *et al.,* 2016).

2.2.2 Freundlich sorption isotherm

Freundlich adsorption isotherms is used to describe the adsorption of the metal ions onto the heterogeneous adsorbent, and it is used to describe the strength of metal ions

adsorption towards the adsorbent surface. Freundlich isotherm predicts that increase in metal ions concentration in the solution leads to an increase in the concentration of the metal ions in the adsorbent surface (Sari and Tuzen., 2009; Kariuki e*t al*., 2016).

2.2.3 Jovanovic sorption isotherm

Jovanovic sorption isotherm is an extension of Langmuir adsorption isotherm. It predicts the monolayer coverage where there is mechanical contact between the adsorbed and the desorbed molecules. The mechanical contact arises as a result of binding vibrations which is experienced between the adsorbed molecules (Fajardo *et al*., 2016; kowanga *et al*., 2016).

2.2.4 Temkin sorption isotherm

Temkin sorption isotherms is used to describe the heavy metal ions-adsorbent interaction. It predicts that the heat of sorption decreases linearly with adsorbent coverage which is as a result of these interactions (Araújo *et al*., 2018; kowanga *et al*., 2016).

2.3 Kinetics studies

Kinetics studies is used in adsorption studies to determine the rate, path and the mechanism followed during the adsorption process (Sudha *et al*., 2007). Various kinetic adsorption models are used to describe metal ions adsorption onto activated carbon.

Pseudo first order kinetics model predicts that the rate at which the metal ions accumulates into adsorbent surface increases with increase in the number of attachment sites which are found in the adsorbent surface (Adamczuk and Kołodyńska., 2015).

Pseudo second order model predicts that the process of metal ions adherence onto the adsorbent surface is by the exchange of electrons between the metal ions and the adsorbent leading to the formation of a chemical bond (Simonin., 2016).

Intraparticle diffusion model is based on the porous nature of the adsorbent which determines the pore diffusion in addition to surface diffusion. It is also very useful in

the understanding of the diffusion mechanism which is used in the determination of the rate of adsorption (Moussout *et al*., 2018).

Elovich kinetic model is an extension of pseudo second order model. It predicts that the adsorbent surface is actually heterogeneous and thus the process of heavy metal ions accumulation onto the adsorbent surface is through the exchange of electrons between the adsorbent and the adsorbate on a heterogeneous surface leading to the formation of a chemical bond (Kowanga *et al*., 2016).

2.4 Method of analysis

Various methods of anslysis used includes., flame atomic absorption spectrophotometry, Fourier transform infra-red spectroscopy, SEM, mass spectrometry, and nuclear magnetic resonance spectroscopy.

2.4.1 Flame atomic absorption spectrophotometer (FAAS)

Flame atomic absorption spectrophotometer is an analytical tool that is used to determine the quantity of heavy metals by measuring the wavelength of the absorbed radiation. The FAAS works on the principle that when atoms which are in the ground state absorbs light energy, they move to the excited state. By measurement of the amount of light absorbed when atoms are in excited state, it becomes possible to quantitatively determine the concentration of the metal ions in the sample of interest (Lagalante., 1999). To determine the quantity of metal ions in a given sample, one needs to compare the concentration of the standards with the sample concentration, both of which have been prepared under the same matrix. This is done by using a calibration curve. Figure 2.1 shows the simplified diagram of flame atomic absorption spectrophotometer.

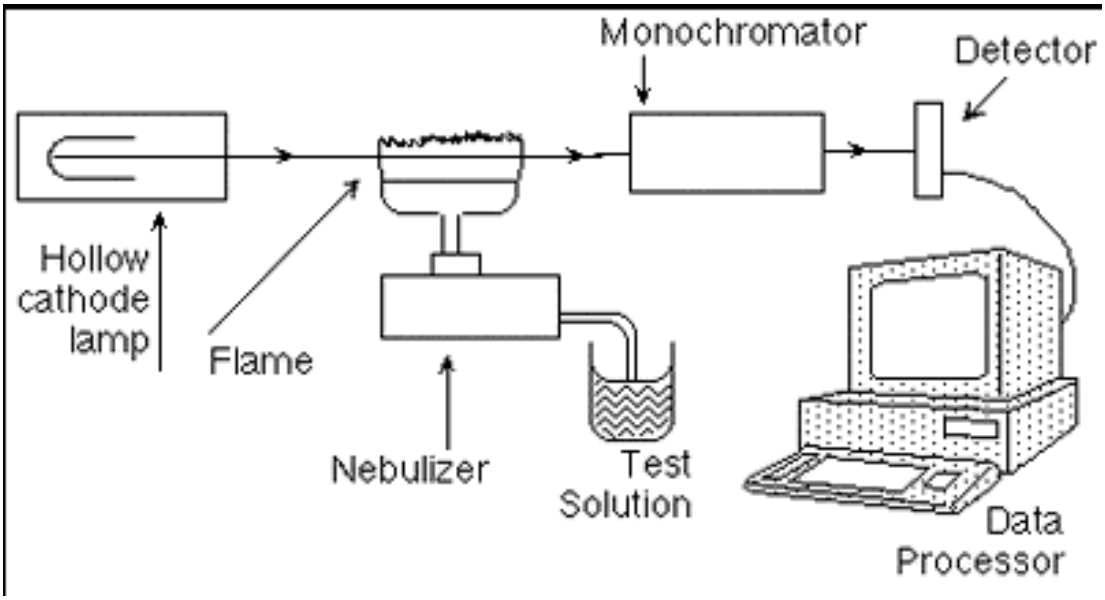

Figure 2.1: Simplified diagram of FAAS (Paul *et al.*, 2017)

Hollow cathode lamp is the light source in the flame atomic absorption spectrophotometer, each element has a characteristic wavelength of absorption. The light which is emitted from the hollow cathode lamp is directed to the part of the flame which have high concentration of atoms. The flame has a very wide path length which allows the detection of even the minute concentration of the samples. The light beam after leaving the flame then passes into the monochromator. The purpose of the monochromator is to select the desired wavelength of light which is then directed to the detector which converts the light energy into electric signal, which is read in the read out device (Boss and Fredeen., 1997). The components of flame atomic absorption spectrophotometer include; hollow cathode lamp, nebulizer, burner, flame, monochromator detector and read out device.

2.4.1.1 Hollow cathode lamp

The source of light in FAAS is the hollow cathode lamp. Each element absorbs light energy at a specific wavelength of light; thus, each element uses its specific hollow cathode lamp. Schematic diagram of hollow cathode lamp is shown in Figure 2.2.

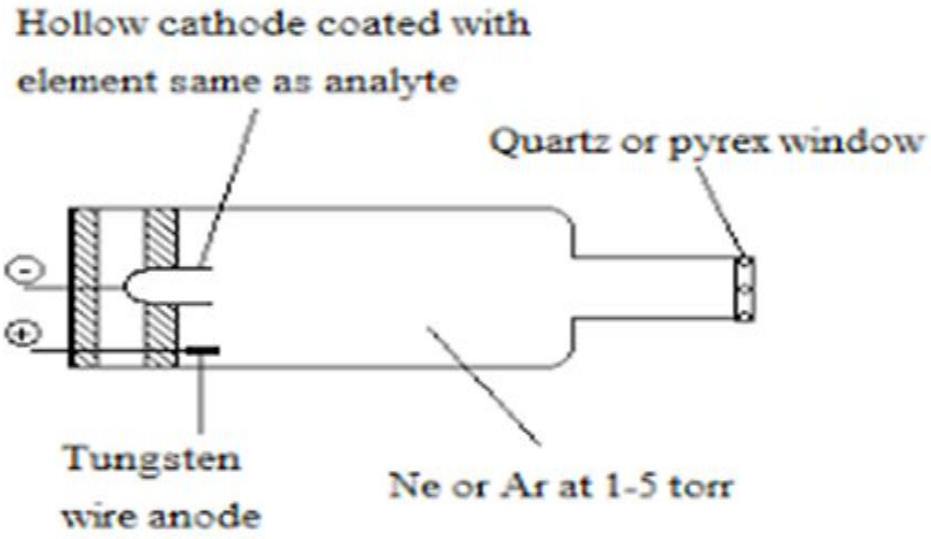

Figure 2.2: Hollow cathode lamp (Saini *et al*., 2018)

The hollow cathode lamp is covered by an envelope which contains inert gas such as argon. When the hollow cathode lamp is switched on, ionization takes place leading to the production of electrons. The emitted electrons move to the anode while the gas ions move to the cathode. Due to electron bombardment metal atoms present in the hollow cathode lamp are excited, after a period of 10^{-8} seconds the metal atoms return to the ground state where they emit line spectrum. The line spectrum is then directed to the part of the flame having high population of atoms. The metal atoms having the same emission as the line spectrum absorbs light energy and thus excited, the amount of radiation absorbed is determined which is thus used to determine concentration (Sharma and Tyagi., 2013).

2.4.1.2 Nebulizer

The role of the nebulizer is to draw the liquid from the sample bottle. The liquid sample is drawn from the sample bottle through a plastic tube to the nebulizer. In the nebulizer, the sample is broken into small droplets called the aerosol. The aerosol then mixes with the fuel and the oxidant which serves as a carrier gas to the flame. The high temperature in the flamein the flame breaks the sample into its individual atoms (Nagy *et al*., 2014). The simplified diagram of a nebulizer is shown in Figure 2.3.

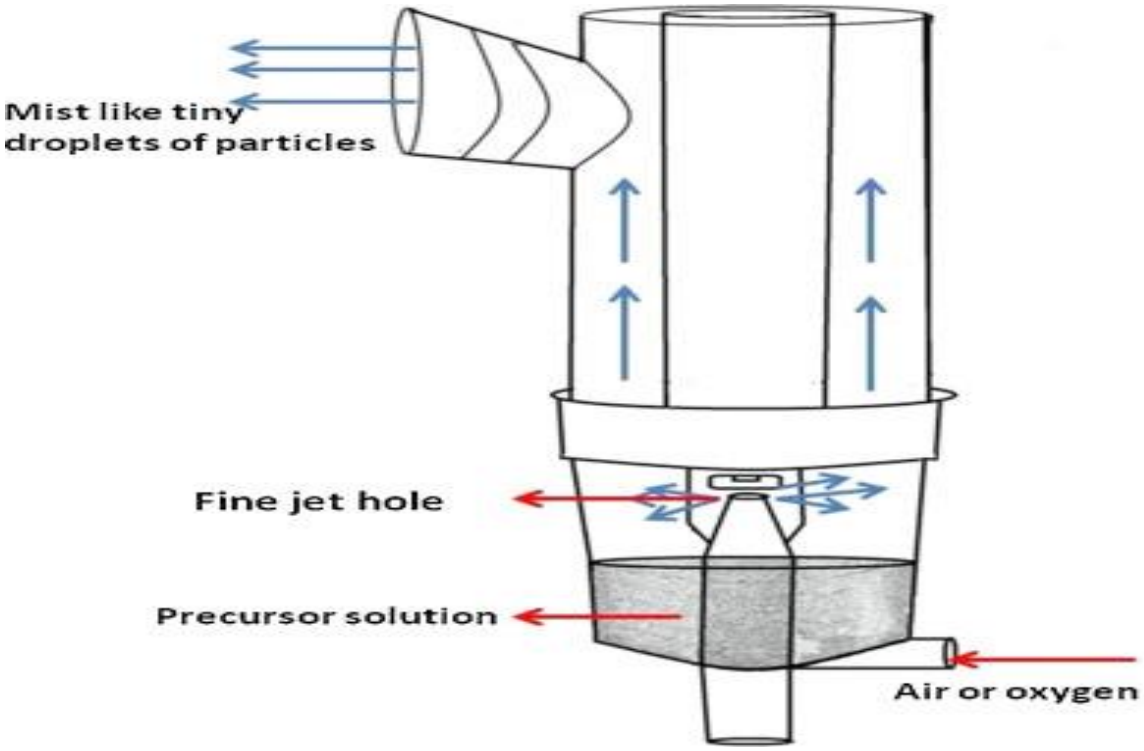

Figure 2.3: Simplified diagram of a nebulizer (Rocha *et al*., 2011).

2.4.1.3 Burner

Two types of burners are used in flame atomic absorption spectrophotometry, this includes total consumption burner and premix burner. Simplified diagrams of total consumption burner and premix burner is shown in Figures 2.4 and 2.5.

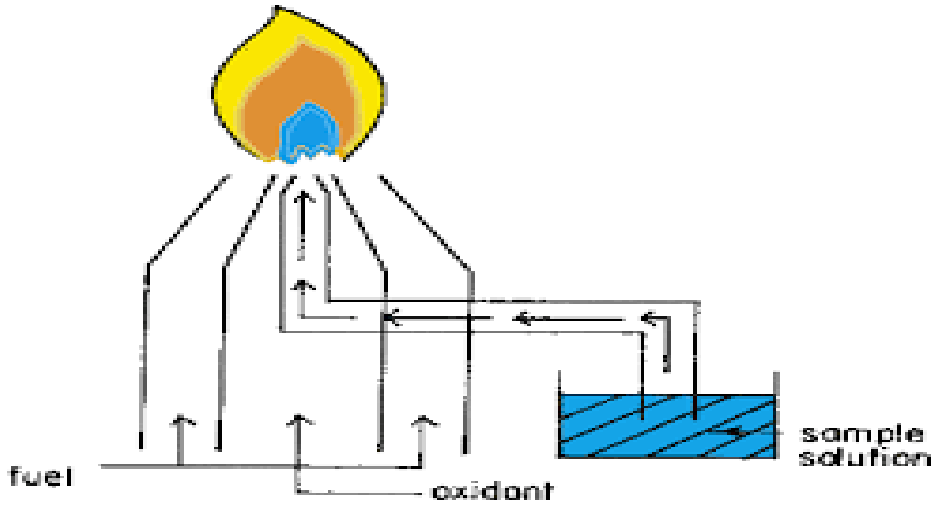

Figure 2.4: Simplified diagram of total consumption burner (Suryawanshi., 2019)

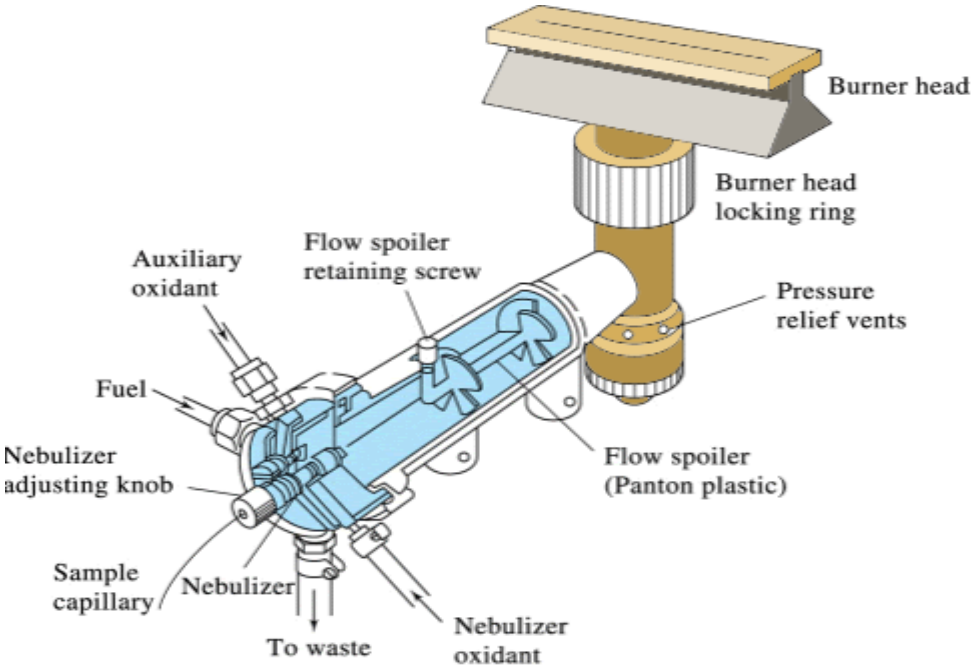

Figure 2.5: Simplified diagram of a premix burner (Fakayode *et al.*, 2012)

Total consumption burner works on a principle that the sample solution is pressurized to the flame due to the high pressure emanating from the fuel and the oxidant. Both the fuel, the sample and the oxidant are burnt at the tip of the burner before being introduced in the flame. The main advantage of total consumption burner is the ease in manufacturing and also since all the sample solution is allowed to enter the flame the data obtained thus represents the total representation of the sample of interest. The main disadvantage of total consumption burner is that it burns all the sample regardless of the drop size leading to a lot of noise. Total consumption burner has limited applications in flame atomic absorption spectrophotometry but is widely used in flame photometry (Kokot., 1955).

Premix burner is the most widely burner in flame atomic absorptin spectrophotometry. The sample solution, fuel and the oxidant are allowed to mix thoroughly before being introduced in the flame. It has a longer path length, less noise is produced and also it produces stable flame (Doroodmand and Mehrtash, 2015). It is the widely used burner in flame atomic absorption spectroscopy.

2.4.1.4 Flame

The type of flame used in FAAS consists of the fuel and the oxidant. Acetylene gas is the commonly used fuel while compressed air is used as the oxidant. With the above set of fuel-oxidant flame, a temperature of 2300 kelvins is attained. At temperatures of 3100 kelvins, flame burns so fast leading to incomplete atomization, and this leads to decrease in instrument sensitivity (Feng *et al*., 2011). For metals which cannot be atomized at lower temperatures nitrous oxide-acetylene oxidant flame is used. Several processes take place when sample is introduced in the flame, this includes; desolvation where the sample solution in form of aerosol is evaporated leaving the dry solid particles. This is followed by vaporization where dry solid particles are made to gaseous molecule. The gaseous molecule is then atomized where dissociation to free atoms takes place. Lastly, the free atoms are converted to free ions through a process of ionization(Paula *et al*., 2016).

2.4.1.5 Monochromator

Monochromator is used to isolate the desired wavelength of light. It selects a single resonance line from multiple lines which are emitted by the hollow cathode lamp. Simplified diagram of a monochromator is shown in Figure 2.6.

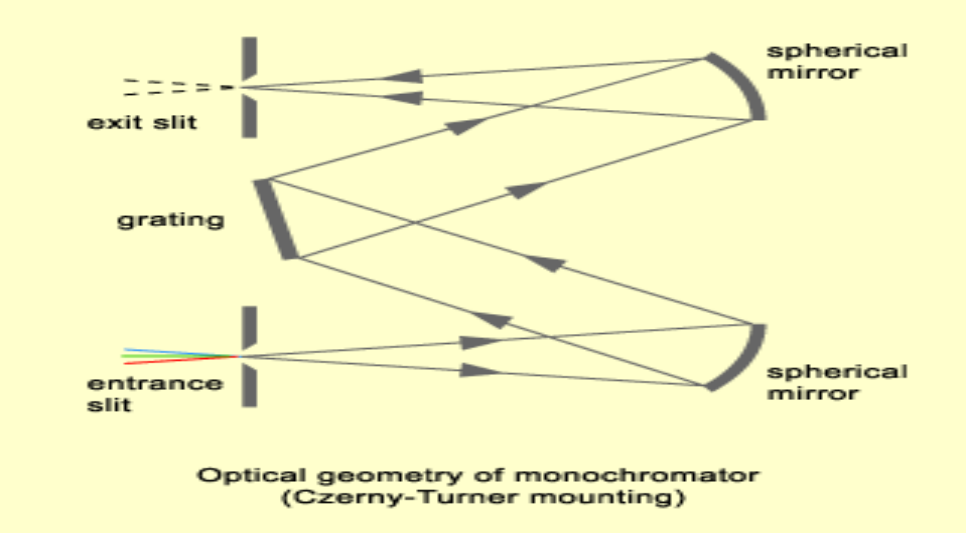

Figure 2.6: Simplified diagram of a monochromator (Paz-Rodríguez *et al*., 2015)

Monochromator contains a filter which isolates a specific narrow region wavelengths of light which moves to the detector while restricting all other wavelengths to pass through (Ciftci and Er, 2013). Components of a monochromator includes; entrance slit, collimating mirrors, dispersive device and exits slit. A specific beam of light emanating from the source enters the monochromator through the entrance slit. The beam of light is then directed to the dispersive device, two dispersive devices are used in flame atomic absorption spectrophotometer; this includes prism and gratings. In the dispersive device, the selected wavelength of light is dispersed at different angles. They are then directed to the exit slit, where only a specific wavelength of light passes through (Filho and Neto., 2009).

2.4.1.6 Detector

Detector converts light into electric signal. Flame atomic absorption spectroscopy uses photomultiplier tube as a detector. The simplified diagram of a photomultiplier detector is shown in Figure 2.7.

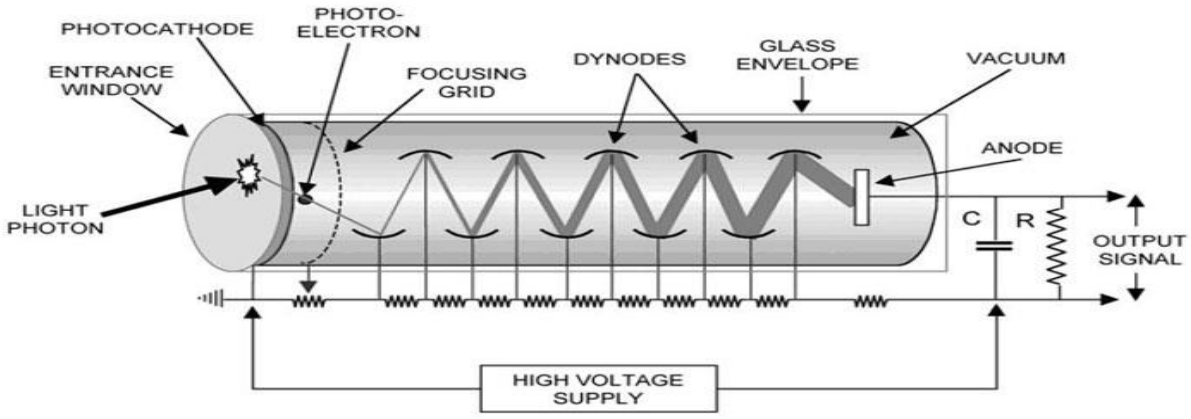

Figure 2.7: Simplified diagram of a photomultiplier tube detector (El-Ghussein *et al*., 2013)

The emitted light from the monochromator is directed to the detector and hits the first dynode. The dynode is coated with a material which a high potential for emitting secondary electron signal. The secondary electron signal from the first dynode is directed to the second dynode which increases the number of electron signal. The cycle is repeated after each dynode. There are about six to ten dynodes in a

photomultiplier tube. Ideally, photomultiplier tube converts light into electric signal, and amplifies the electric signal in the range of 10^3 to 10^6 (Lung *et al*., 2012) .

2.4.1.7 Read out device

The absorbance of the sample solution is then displayed in the read-out device usually a computer and then converted into concentration.

2.4.2 Fourier transform infrared spectroscopy

Fourier transform infra-red spectroscopy (FTIR) employs the infra-red region of the electromagnetic spectrum. The infra-red region has shorter frequency and longer wavelength than the visible region. The bonds between different elements absorb infra-red radiation at different frequencies which forms the basis for FTIR analysis.

2.4.2.1 Working principle of fourier transform infra-red spectroscopy

The block diagram of fourier trams infra-red spectrometer is shown in Figure 2.8.

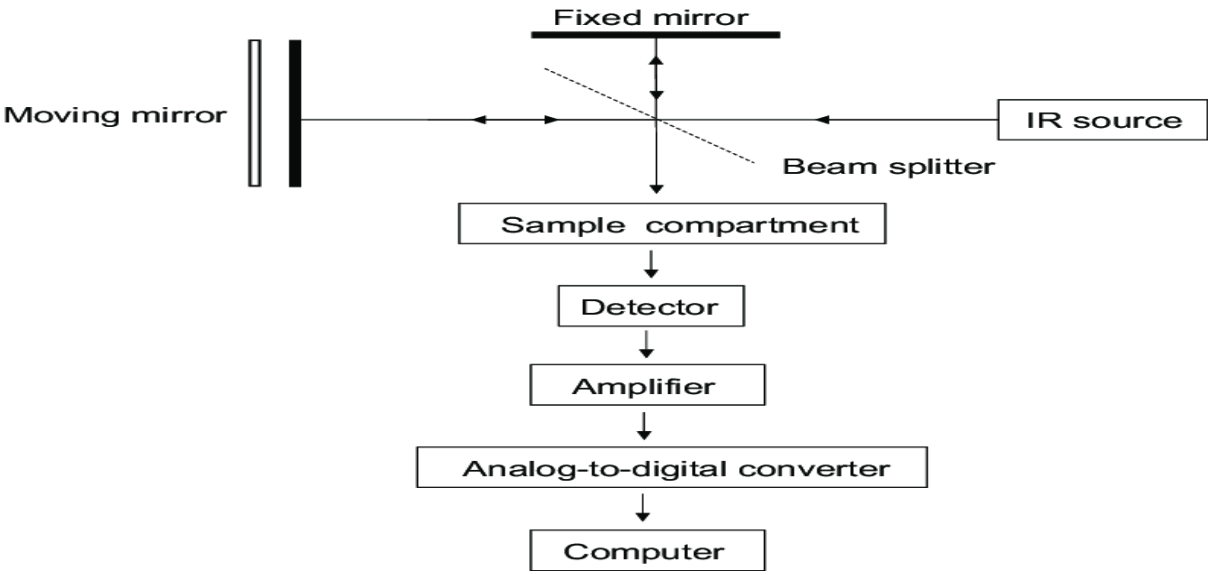

Figure 2.8: Block diagram of FTIR (Hashim *et al.*, 2010).

The source consisting of infra-red radiation is directed to the beam splitter. The beam splitter divides the infra-red beam into two halves where one half moves to the fixed mirror while the other half moves to the moving mirror which is sent at constant speed. The two beams are then reflected back and after combining an interference pattern is constructed. The interference pattern which is known as inferogram is directed to the sample holder. Some portion of the inteferogram is absorbed and

some is transmitted. The transmitted portion of the inferogram is directed to the detector and the inferogram signal is measured and then the measured signal amplified. The amplified inteferogram signal is directed to the analog to digital converter where it is digitalized and then to the computer where Fourier transformation takes place. Generally, the output of a graph is of percentage transmittance against wave number (Ganzoury *et al.*, 2015).

2.4.3 Scanning electron microscopy

Scanning electron microscopy (SEM) is used to detect and analyse the surface structures of the sample of interest

2.4.3.1 Working principle of scanning electron microscopy (SEM)

The simplified diagram of scanning electron microscope is shown in Figure 2.9.

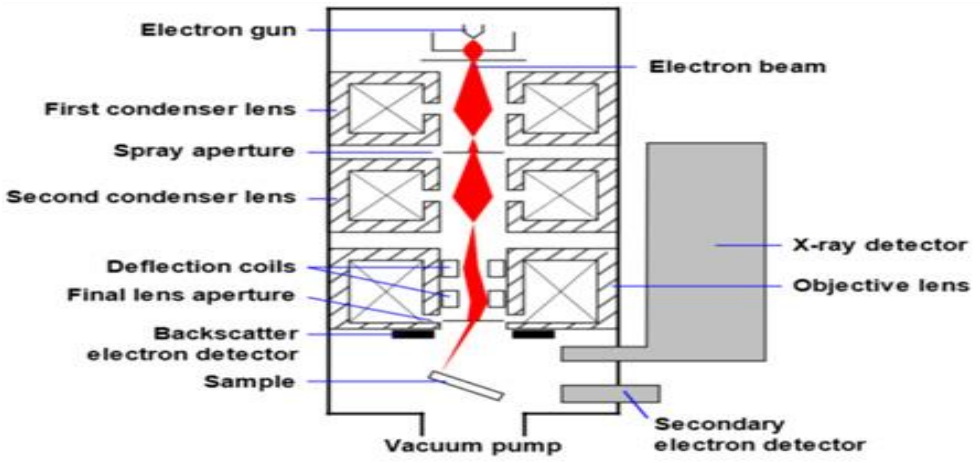

Figure 2.9: Simplified diagram of scanning electron microscope (Malik and Yadav., 2015)

The electron gun generates a beam of electrons down the column. The beam of electrons is then directed to the electromagnetic lenses which are wrapped with solenoid. Beam of electrons are then focussed onto the stage where the sample is placed. The interaction between the incident beam and the surface of the sample is determined by the acceleration rate of the incident electrons. Upon the incident electrons coming into contact with the sample, energetic electrons are released from the sample surface. This then leads to the formation of the scattering patterns which

gives information on the size, shape, texture and composition of the sample (Hossain *et al*., 2010).

CHAPTER THREE

MATERIALS AND METHODS

3.1 Study design

The research was carried out in four phases; the first phase involved sample collection and preparation. The second phase involved sample characterization using FTIR and SEM. The third phase involved preparation of stock solutions and working standards. The fourth phase involved optimization, adsorption and kinetic studies.

3.2 Instrumentation

Flame atomic absorption spectrophotometer (Model AA 7000- shimadzu AAS) using air-acetylene flame was used for Pb (II) ions and Cd (II) ions determination before and after adsorption. To determine the effect of pH on metal ions adsorption, pH measurement was done using pH meter (pH 211, Hanna instruments). The organic functional groups present in activated carbon which were responsible for heavy metal ions adsorption were determined using Fourier transform infrared spectrophotometer (Shimadzu, Japan, Model FTS-8000). Flame atomic absorption spectrophotometer conditions is shown in Table 2.1.

Table 3.1: FAAS instrumental conditions

Condition	Lead	Cadmium
Wavelength(nm)	283.3	228.8
Lamp current(mA)	10	8
Slit Width	0.7	0.7
Lamp mode	BGC-D_2	BGC-D_2
Flame type	Air-C_2H_2	Air-C_2H_2
Fuel gas flow rate (L/min)	10	8

3.3 Chemicals and reagents

All the chemicals used in this study were of analytical grade purchased from PY-REX East Africa limited with its branch located in Nairobi Kenya. Stock solutions of lead (1000 mg/L) was be made by dissolving 1.60 grams of $Pb(NO_3)_2$ in distilled

water in a 1000 mL volumetric flask and then adding water up to the mark. Cadmium ions stock solution was prepared by dissolving 1.86 grams of cadmium nitrate in distilled water and then topping up the solution to 1000 mL with distilled water. Working solutions were made by making the appropriate dilutions from the stock solutions through serial dilution using distilled water.

3.4 Sample collection preparation and pre-treatment

Activated carbon was prepared using modified method of Pakade *et al* (2017). Ten kilograms of *Macadamia intergrifolia* nutshells were sourced from Kenya nut company in Kamenu ward, Thika town constituency, Kiambu county Kenya. Five kilograms of the *Macadamia intergrifolia* nutshell was washed with deionized water to remove dirt. They were then oven dried at 105°C for 48 hours, were ground to a fine powder and then sieved using a standard sieve of 90 µm to 150 µm. Two kilograms of raw *Macadamia intergrifolia* nutshell powder was soaked in 50 % phosphoric acid for 24 hours, they were then oven dried for 48 hours at 105 °C. The dried sample was charred using a heating mantle at 300 °C for 24 hours followed by ignition in an electric muffle furnace at 550 °C for 30 minutes. The sample was left to cool, washed with 0.1M HCl to remove ash and then washed with 0.1M NaOH to raise the pH of the activated carbon to 7. It was then oven dried at 105 °C for 24 hours and kept in a stoppered bottle ready for use. Plate 3.1 shows the pictorial presentation of *Macadamia intergrifolia* nut shells.

Plate 3.1: Macadamia *integrifolia* nutshells

3.5 Characterization of activated carbon

3.5.1 FT-IR characterization

The KBR pellets were prepared by grinding 10 mg of activated carbon with 250 mg of KBR (FT-IR grade) and then pressed into a pellet using a Shimadzu hand press standard device at a pressure of 75 kN cm^{-2} to a pellet for 3 minutes. The scanning range was set from 400 to 4000 cm^{-1} while the spectral resolution was 4 cm^{-1}. The FT-IR spectrum analysis for activated carbon was done before adsorption and after adsorption to account for the shift of the absorption bands (Nethaji *et al*., 2013) .

3.5.2 Scanning electron microscope experimental protocol

SEM analysis of activated carbon was carried out at the department of chemistry in the University of Frebourg Switzerland. The scanning electron microscope was operated and an accelerating voltage of 11.0Kv at an aperture size of 50µm.

3.6 Optimization studies

Batch adsorption studies were carried out by keeping in equilibrium an amount of activated carbon in 50 mL of Pb (II) ions and Cd (II) ions at a specific pH, sorbent mass, contact time and a known metal ions concentration. Sample mixtures were then allowed to settle down for 30 minutes and then filtered using whatman no 42 filter paper. The filtrate was then analysed for the remaining Pb (II) ions and Cd (II) ions equilibrium concentrations after adsorption using Flame atomic absorption spectrophotometer model (AA-7000 Shimadzu Japan) with an air acetylene flame (Kakoi *et al*., 2016).

Determination of the percentage lead and cadmium ions removal after adsorption is done using equation 3.1;

$$\% \text{ Removal} = \left(\frac{C_O - C_e}{C_o}\right) * 100 \quad \ldots\ldots (3.1)$$

C_o is the initial concertation, and C_e is the equilibrium concentration in mg/L

Amount adsorbed at equilibrium is determined using equation 3.2;

$$q_e = \frac{V(C_o - C_e)}{W} \quad \ldots\ldots (3.2)$$

Where **qe** is amount adsorbed at equilibrium in mg/g, V is the volume of the solution in litres, C_o is the initial concentration in mg/L. C_e is the equilibrium concentration in mg/L and W is the weight of the adsorbent in grams (Kakoi *et al*., 2016).

3.6.1 Effect of pH variation

To determine effect of pH on Pb (II) ions and Cd (II) ions adsorption onto activated carbon, 0.5 grams of activated carbon was mixed with 50 mL of 4 mg/L of Pb(II) ions and 8 mg/L of Cd (II) ions, with each metal having its own pH kept in a different vessel based on the study done by (Onyancha *et al*., 2008). Solutions were adjusted to the pH of 2, 3, 4, 5, 6, 7, 8 and 10. The mixtures were then kept in a mechanical shaker which was set at 130 revolutions per second at a temperature of 25°C for 120 minutes. pH adjustment was done using 0.5 M NaOH and 0.5 M HNO_3. After the set time the sample mixtures were removed from the mechanical shaker and left to stand for 30 minutes and amount of metal ions remaining at

equilibrium determined using flame atomic absorption spectrophotometer. Experimental conditions were based on the studies done by (Kowanga *et al*., 2016; Madivoli *et al*., 2016). Analysis of Pb(II) ions and Cd(II) ions at various pH values was done in triplicate. Results for the effect of pH on metal ions adsorption are in section 4.3.1.

3.6.2 Effect of sorbent mass

Effect of sorbent mass on removal of Pb (II) ions and Cd (II) ions from aqueous solution was determined at optimum pH of 4 for Pb (II) ions and 5 for Cd (II) ions which was determined in section 3.6.1, 4 mg/L of Pb (II) ions and 8 mg/L of Cd (II) ions solution were mixed with various dosages (0.1, 0.2, 0.3, 0.4, 0.5, 0.6, 0.7, 0.8, 0.9 and 1 grams) of the activated carbon. The solutions were then kept in a mechanical shaker which was set at 130 revolutions per minute and 25°C for 120 minutes. After the set time, sample mixtures were then removed from the mechanical shaker and then allowed to settle for 30 minutes. Sample mixtures were then filtered using Whatman number 42 filter paper and the amount of metal ions remaining determined using flame atomic absorption spectrophotometer. Analysis of Pb (II) ions and Cd (II) ions at various values of adsorbent dosages was done in triplicate.

3.6.3 Effects of contact time

Optimum contact time determination was carried out by mixing 50mL of 4 mg/L of Pb (II) ions and 8 mg/L Cd (II) ions solution with the optimum pH of 4 for for Pb (II) ions and 5 for Cd (II) ions determined in section 3.6.1 and at optimum dosage of 0.4 grams for Pb (II) ions and 0.3 for Cd (II) ions determined in section 3.6.2. Sample mixtures were then kept in a mechanical shaker which was set at 130 revolutions per minute and at a temperature of 25 °C. Sample mixtures were then withdrawn at regular time intervals ranging from 15, 30, 45, 60, 75, 90, 105 and 120 minutes. Withdrawn sample mixtures were then allowed to settle for 30 minutes after which they were then filtered using Whatman number 42 filter paper. The amount of Pb (II) ions and Cd (II) ions remaining in equilibrium after various set time intervals was determined using flame atomic absorption spectrophotometer. All the analyses which were carried out at various time intervals were done in triplicate.

3.6.4 Adsorption isotherms and effect of initial metal ions concentration

The quantity of cadmium ions adsorbed (q_{eq}) as a function of initial Pb (II) ions and Cd (II) ions concentration was evaluated as follows; initial concentrations ranging from 4, 8, 12, 16, 20, 24, and 28 mg/L was mixed at the optimum pH of 4 for Pb (II) ions and 5 for Cd (II) ions determined in 3.6.1 and at optimum dosage of 0.4 grams for Pb (II) ions and 0.3 grams for Cd (II) ions which was determined in section 3.6.2 and optimum contact time of 60 minutes for Pb (II) ions and 75 minutes for Cd (II) ions determined in section 3.6.3 all having a fixed volume of 50 mL. The sample mixtures were then transferred to a mechanical shaker which was set at 130 revolutions per second and 25°C. They were then withdrawn after the optimum contact time of 60 and 75 minutes for Pb (II) ions and Cd (II) ions respectively which was identified in section 3.6.3. Sample mixtures were then allowed to settle for 30 minutes and then filtered using whatman number 42 filter paper. The level of metal ions concentration remaining at various initial concentrations was then determined using flame atomic absorption spectrophotometer. All the analyses at various time intervals were done in triplicate (Momčilović et al., 2011).

3.7 Kinetic studies

The rate and the mechanism for Pb (II) ions and Cd (II) ions adsorption onto the surface of the activated carbon was done as follows; Optimum initial concentration of 8 mg/L for both metal ions identified in section 3.6.4 was mixed with optimum dosages of 0.4 grams for Pb (II) ions and 0.3 grams for Cd (II) ions determined in section 3.6.2 and set at optimum pH of 4 for Pb (II) ions and 5 for Cd (II) ions determined in section 3.6.1 having a fixed volume of 50mL in each solution. Samples were then kept in a mechanical shaker which was set at 130 revolutions per second and a temperature of 25°C. Sample mixtures were then withdrawn at regular time intervals ranging from 15, 30, 45, 60, 75, 90, 105 and 120 minutes. Sample mixtures were then allowed to settle for 30 minutes and the filtered using Whatman number 42 filter paper. Equilibrium concentration of Pb (II) ions and Cd (II) ions solution at regular time intervals was determined using flame atomic absorption spectrophotometer and all the analysis done at regular time intervals were done in triplicate (Kowanga *et al.*, 2016).

3.8 Data analysis

Statistical analysis was done using Microsoft excel. Microsoft excel was used to determine the analysis of variance, mean and the standard deviation. Adsorptive isotherms were used to estimate the adsorptive capacity of activated carbon derived from *Macadmia intergrifolia* nutshell powder. Kinetic models were used to investigate the mechanism of adsorption and its potential in rate controlling step.

CHAPTER FOUR

RESULTS AND DISCUSSIONS

4.1 Characterization

4.1.1 Characterization of activated carbon using FTIR

The FT-IR spectrum of activated carbon is shown in Figure 4.1.

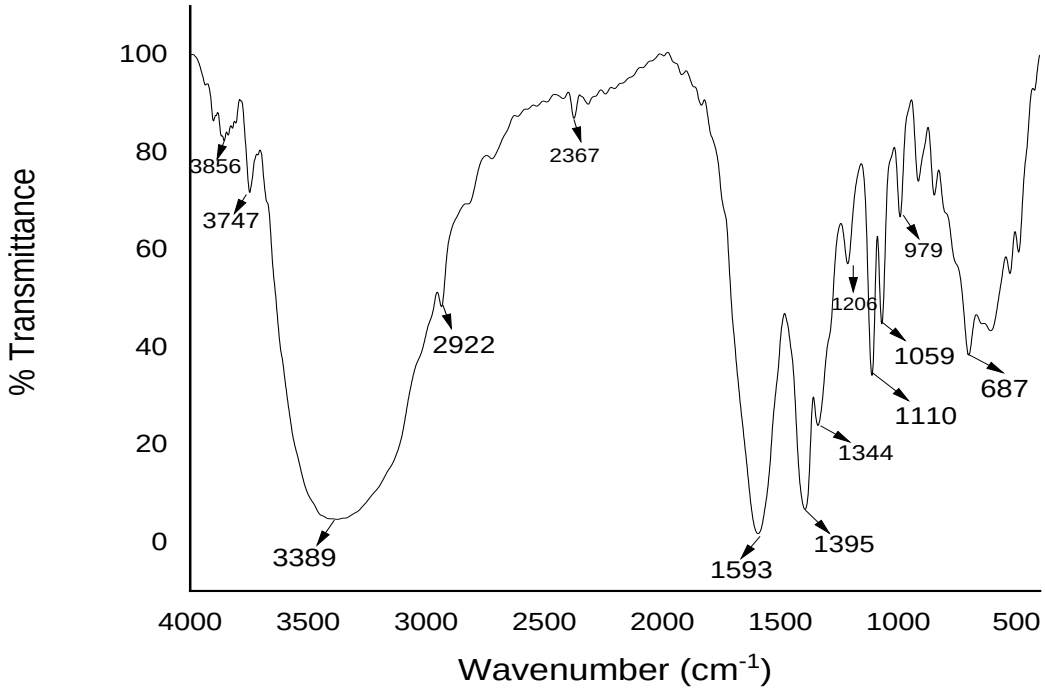

Figure 4.1: The FTIR spectrum of unloaded activated carbon

The weak absorption bands at V_{max} 3856cm^{-1} and V_{max} 3747cm-1 was due to the presence of the isolated silanols which might be present in the activated carbon (Huang Ma and Zhao., 2015). The broad absorption bands at V_{max} 3389cm^{-1} were attributed to the presence of OH stretching vibration of hydroxyl groups. The absorption band at V_{max} 2922cm^{-1} was attributed to CH stretching vibrations which is indicative of the presence of methyl groups (Shamsuddin *et al.*, 2016). The presence of band at V_{max} 2367 cm^{-1} was ascribed to the presence of COO- stretching. The absorption band at V_{max} 1593 cm^{-1} was attributed to the presence of C=O stretching vibrations (Sych et al. 2012). The band at V_{max} 1395 cm^{-1} was associated

with the aliphatic $-CH_3-$ bend while the peak at 1344 cm^{-1} was indicative of C-0 stretching vibrations which may be assigned to ethers, phenols, esters, acids or alcohols (Gupta *et al*., 2013). The band at 1206 cm^{-1} was associated with the stretching mode of the hydrogen bonded P-O and O-C which are found in P-O-C and P-OOH (Filho and Neto., 2009). The band at V_{max} 1110 cm^{-1} was associated with the ionized linkage P-O- which is found in phosphate esters it was also assigned to symmetric vibration in P-O-P. The band at V_{max} 979 cm^{-1} depicted the C-O bending vibrations associated with acids and alcohols whereas the peak at V_{max} 687 cm^{-1} was associated with in-plane ring deformation (Tongpoothorn *et al*., 2011).

The FT-IR spectra of loaded and unloaded Pb (II) ions and Cd (II) ions is shown in figure 4.2 and figure 4.3.

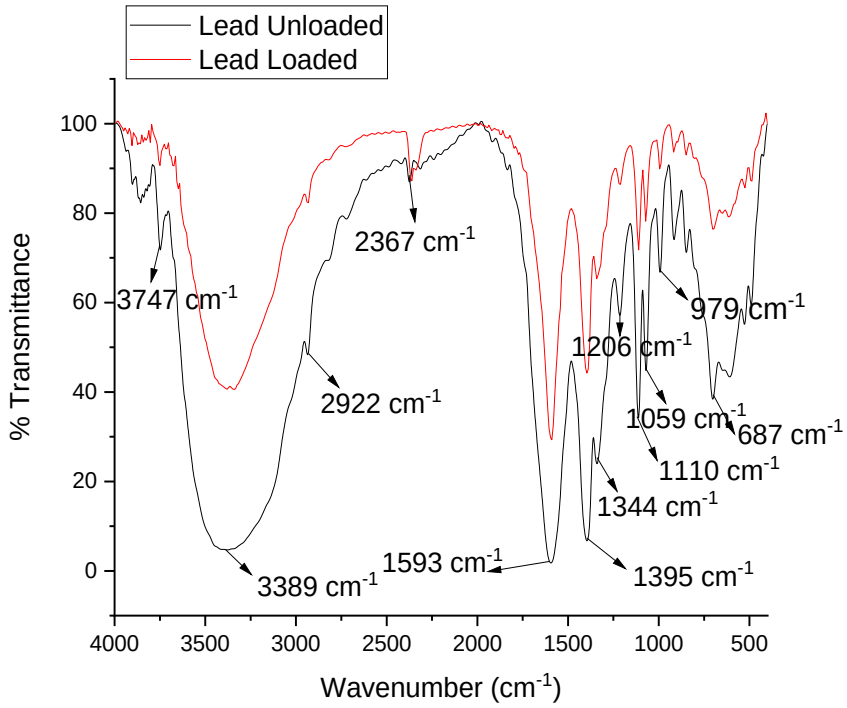

Figure 4.2: The FTIR spectrum of Pb (II) ions loaded and unloaded activated carbon

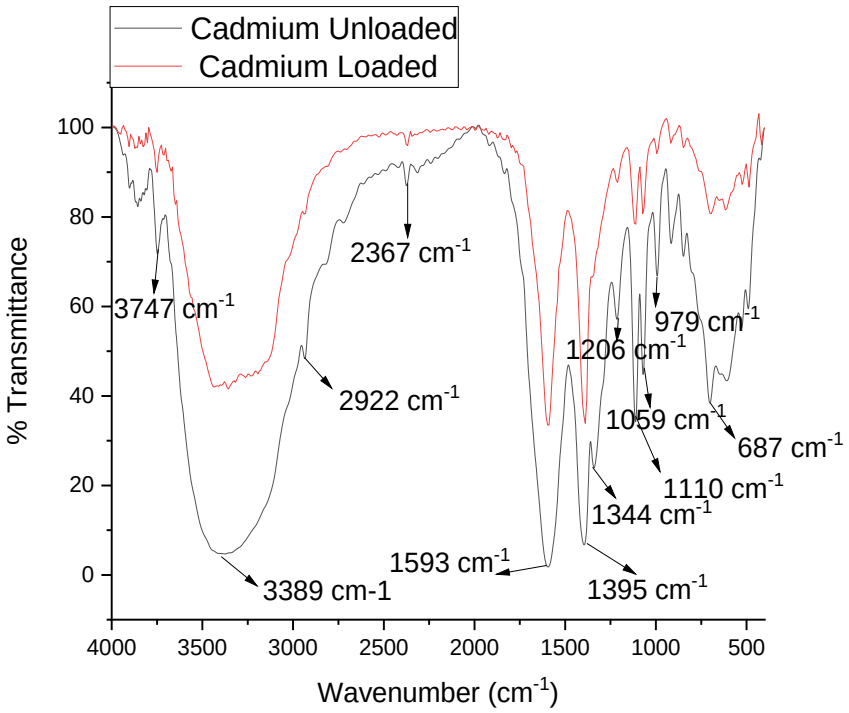

Figure 4.3: The FTIR spectrum of Cd (II) ions loaded and unloaded activated carbon

For both metal ions the broad bands at V_{max} 3389 cm^{-1} and 1593 cm^{-1} which is associated with O-H stretching and C=O respectively, there was an observed shift in energy to lower frequency. This was an indication of the involvement of the O-H and C=O in metal ions adsorption (Kowanga *et al.*, 2016).

4.1.2 Interpretation of scanning electron micrograph of activated carbon derived from *Macadamia Intergrifolia* nutshell powder

The SEM micrograph for activated carbon derived from *Macadamia Intergrifolia* nutshell powder is shown in Plate 4.2

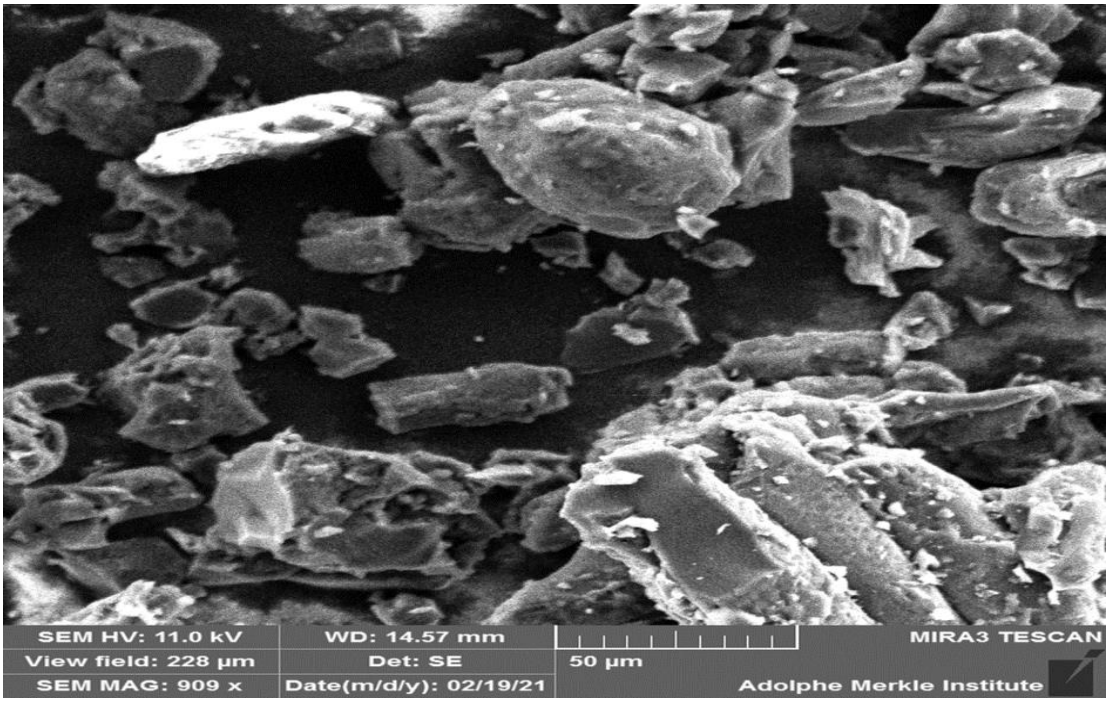

Plate 4.1: The SEM micrograph for activated carbon derived from *Macadamia intergrifolia* nutshell powder

Scanning electron microscopy (SEM) revealed the structure of activated carbon. The surface of the activated carbon adsorbent showed deep cavities and irregular structures. As shown in the SEM micrograph (Plate 4.1) for the activated carbon, crevices and cracks are visible. Therefore, after activation with phosphoric acid, most organic volatiles were eliminated, which consequently left ruptured surface of the activated carbon (Sekhararao *et al*., 2011). Pores of different shapes were also observed in the activated carbon surface. The deep cavities provided the binding sites for the attachment of Pb (II) ions and Cd (II) ions (Demiral., 2016). Irregular distribution of pore sizes is observed which gives a good possibility for the metal ions to be trapped and adsorbed. Variation in pore sizes provides a large surface area for the active sites for metal ions adsorption to take place (Ravindra *et al*., 2015).

4.2 Batch adsorptions studies

4.2.1 Effect of pH

The effect of pH on Pb (II) ions and Cd (II) ions accumulation onto activated carbon is shown in Figure 4.4.

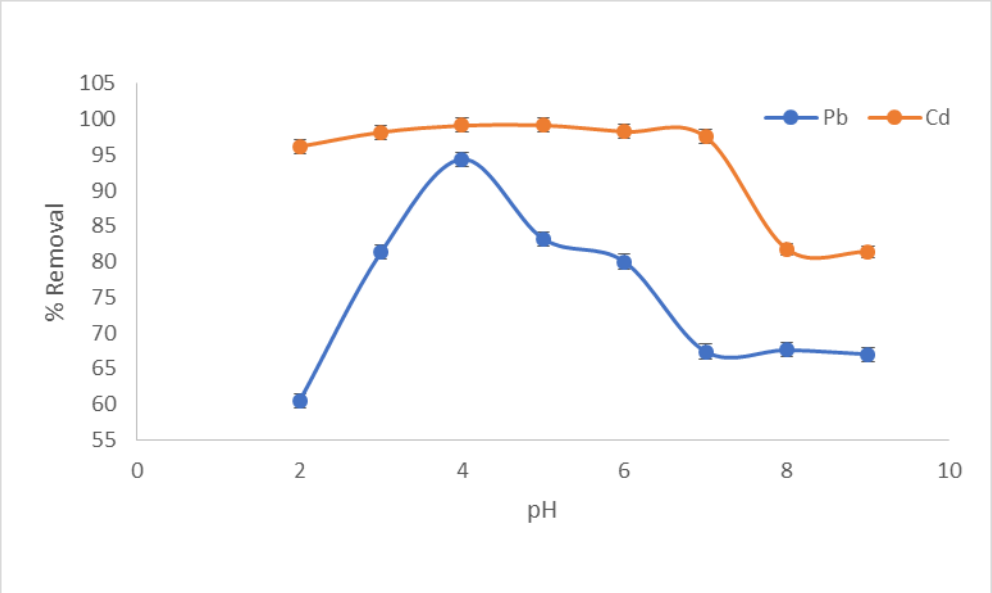

Figure 4.4: Effects of pH on lead (II) and cadmium (II) ions adsorption onto activated carbon

One of the most critical parameters in metal ions adsorption is pH. This is because pH has effect on the chemistry of the solution under study (Onyancha *et al.*, 2008). The influence of pH on Pb (II) ions and Cd (II) ions adsorption onto activated carbon was done in the range of 2-10. This range was based on the studies which were done and reported by (Chand *et al.*, 2014; Rubio *et al.*, 2013). From Figure 4.4, Pb (II) ions accumulation onto activated carbon was found to increase with increase in pH from 60.5% at pH 2 to 81.83% at pH 3 and then to an optimum 94.37 % at pH 4. Cd (II) ions accumulation onto activated carbon was found to increase from 96.15% at pH 2 to 98.16 at pH 3, then to 99.13% at pH 4 and finally to an optimum of 96.15% at pH 5 where there was maximum percentage metal ions removal. At very acidic pH there is protonation of H^+ onto the activated carbon surface, therefore the protonated H_3O^+ compete with metal ions for the active sites of the adsorbent (Moreno-Piraján and Giraldo., 2012).

The adsorption capacity for both metals increased as pH increased. This was due to the deprotonation of the activated carbon active sites. Thus, at pH 4 for Pb (II) ions and pH 5 for Cd (II) ions, metal ions were able to bind more strongly at leading to optimum adsorption capacity(Ge and Fan, 2011). Further increase in pH above the

optimum pH led to the decrease in the percentage metal removal which was found to decrease from the optimum 94.37% at pH 4 to 83.21, 79.99, 81.77 and 68.38 and 67.01% at pH 5,6,7,8 and 10 respectively for Pb (II) ions. For Cd (II) ions the percentage removal decreased from the optimum at pH 5 which was 99.13% to 98.23, 97.51, 81.77 and 81.39% at pH 6, 7, 8 and 10 respectively. At higher pH above 4 for Pb(II) and above 5 for Cd (II) ions, the COO- attracts the positively charged Pb^{2+} and Cd^{2+} and thus binding occurs. This therefore suggests that, the binding process was probably through the ion exchange mechanism involving electrostatic interaction between the negatively charged groups in the activated carbon and the Pb^{2+} and Cd^{2+} (Wanja *et al*., 2016). The decrease in percentage metal ions removal at pH greater than 7 was associated with the formation of low solubility $Pb(OH)_2$ and $Cd(OH)_2$ precipitate which interferes with the adsorption process since it restricts the movement of metal ions thus making it unavailable for adsorption (Feng *et al*., 2011). Statistical analysis revealed there was a significant difference ($P \leq 0.05$) in the metal ions adsorbed at different pH values. Analysis of variance study for both metal ions revealed that the value of F calculated for Pb(II) ions was 59.8736 and for Cd (II) ions was found to be 86.6950 which was found to be greater than F critical which was found to be 4.1709 (Appendices X-XI). This therefore revealed that the means at different pH values were significantly different from each other. The optimum pH obtained by both metal ions was used in subsequent experiment.

4.2.2 Effect of sorbent mass

Figure 4.5 shows the effects of sorbent mass on removal of Pb (II) ions and Cd (II) ions while keeping other parameters constant.

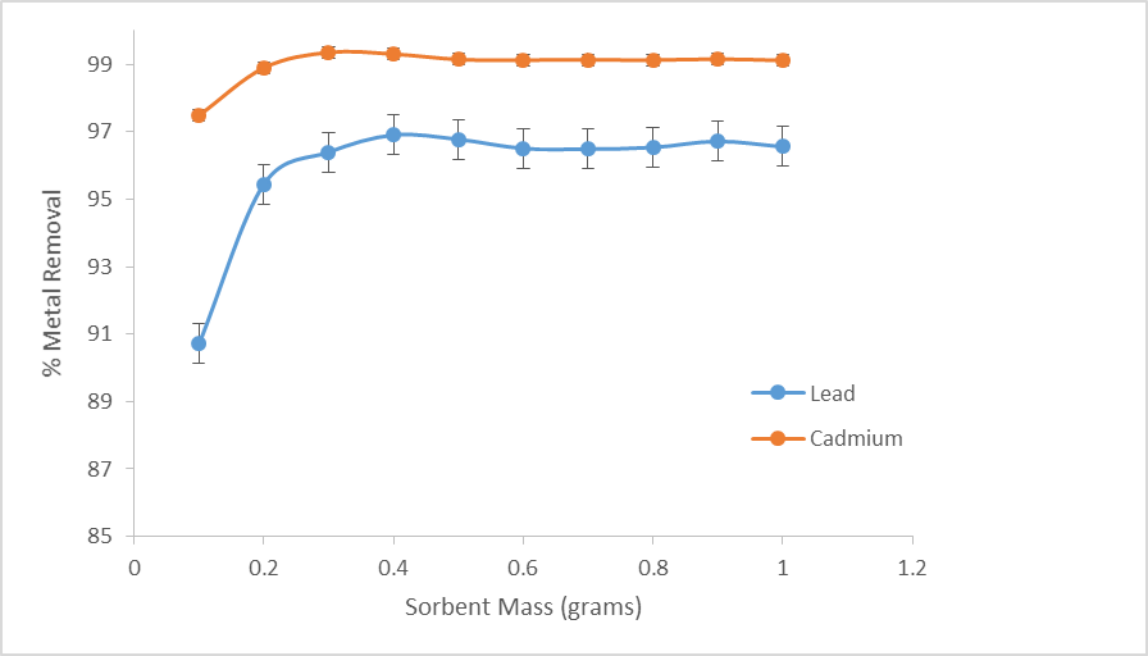

Figure 4.5: **Effect of sorbent mass on lead (II) and cadmium (II) ions adsorption onto activated carbon**

For Pb (II) ions, there was increased percentage removal with increase in sorbent mass up to 0.3 grams where the optimum percentage metal removal was found to be 96.91 %. For Cd (II) ions the percentage metal removal increased with increase in sorbent mass up to 0.4 grams where the optimum percentage metal removal was found to be 99.36 %. The increase in percentage metal removal with increase in sorbent mass was attributed to the increase in the surface area of the activated carbon attachment sites which were responsible for metal ions adsorption (Sahu *et al.*, 2018). Above the optimum dosage for both metal ions there was a slight decline in percentage metal ions removal. This is because higher values of adsorbent dosages causes shielding effect which occurs as a result of the overlapping of the metal ions adsorption sites, which hinders metal ions adsorption onto activated carbon surface (Malakahmad *et al.*, 2016; Kakoi *et al.*, 2016). Statistical analysis revealed that there was a significant difference ($P \leq 0.05$) in the amount of metal ions adsorbed with increased sorbent mass upto the optimum adsorbent dosage. Analysis of variance for both metal ions revealed that the value of F calculated for Pb(II) ions was 39.5903

and for Cd(II) ions was found to be 67.9667 which was greater than the value of F critical which was found to be 4.0982 (Appendices XII-XIII). This is an indication that the mean at different values of adsorbent dosages are significantly different from each other. The optimum sorbent mass was then used in the subsequent experiment

4.2.3 Effects of contact time

The effect of contact time on Pb (II) ions and Cd (II) ions adsorption is shown in Figure 4.6.

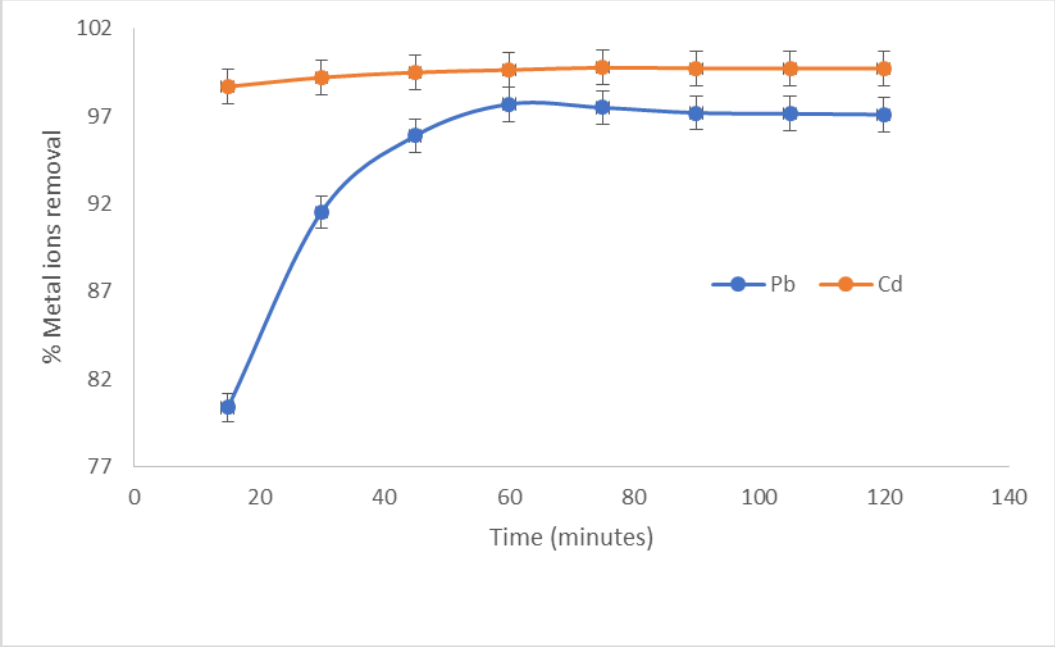

Figure 4.6: Effect of contact time on lead (II) and cadmium (II) ions adsorption onto activated carbon

The effect of contact time on Pb (II) ions and Cd (II) ions adsorption was determined by monitoring the attachment of metal ions onto activated carbon for 120 minutes. The optimum contact time for Pb(II) ions was 60 minutes which had 97.7 % removal while the optimum contact time for cadmium was 75 minutes which had 99.78 % removal. High values of percentage metal ion removal at lower values of contact time was due to the higher concentration difference between the metal ions in solution and the activated carbon surface (Afroze Sen and Ang., 2016). Increment in metal ions concentration adherence with increased contact time was as a result of net

movement of metal ions from the aqueous solution to the interior and exterior surface of the activated carbon (Mishra *et al*., 2012). At the optimum contact time, the rate of metal ions adsorption equalled the rate of metal ions desorption and thus there was no further movement of metal ions onto the activated carbon attachment sites (Vijayaraghavan and Sivakumar., 2011). Above the optimum contact time for both metal ions, there was a slight decline in metal ions removal. This was as a result of desorption which was as a result of the repulsion between the metal ions adsorbed and those in aqueous solution (Sekhararao *et al.,* 2011). Statistical analysis of the data revealed that there was a significant difference ($P \leq 0.05$) in the amount of Pb(II) ions and Cd(II) ions adsorbed with increase in contact time. Analysis of variance test for both metal ions revealed that the value of F calculated for Pb(II) ions was 85.9607 and for Cd(II) ions was found to be 86.6660 which was greater than the value of F critical which was found to be 4.1708 (Appendices XIV-XV). This implies that there was significant difference between the mean at different time intervals. The optimum contact time was used in subsequent experiment.

4.2.4 Effect of initial metal ions concentration

The effect of initial metal ions concentration on Pb (II) and Cd (II) ions removal is shown in Figure 4.7.

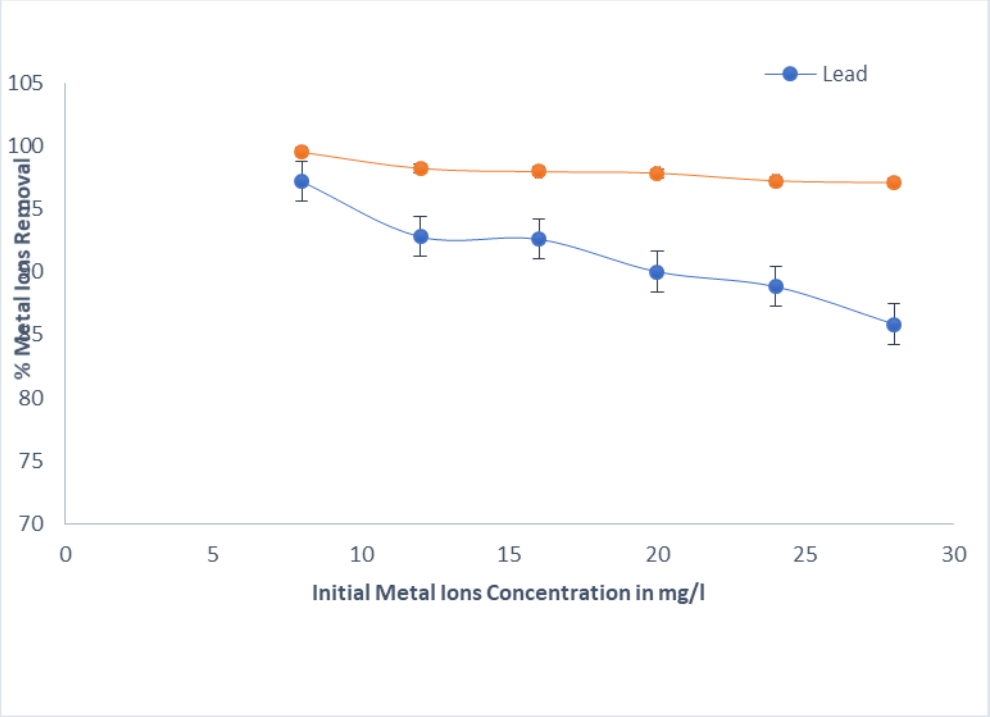

Figure 4.7: Effect of initial metal ions concentration on lead(II) and cadmium(II) ions adsorption onto activated carbon

Increase in initial metal ions concentration is the chief driving force which was able to overcome the mass transfer resistance of metal ions between the aqueous solution and the superficial layer of the activated carbon (Wasewar., 2010). Increase in metal ions concentration in solution above 8 mg/L for both the metal ions led to decrease in percentage metal ions removal. This was due to the reduction in the ratio of the unattached metal ions binding sites to the number of the metal ions in solution since a constant mass of sorbent has a fixed number of adsorption sites (Zewail and Yousef., 2015). Furthermore, the attachment sites which had higher affinity for metal ions were saturated. Consequently, there was an increase in mutual electrostatic interaction between the lower affinity adsorption sites and the unabsorbed metal ions (Gupta *et al.*, 2013). Adsorption capacities were found to increase with increased initial metal ions concentration and were fitted in the adsorption isotherms. Statistical analysis of the data revealed there was a significant difference ($P \leq 0.05$) in the Pb (II) ions and Cd (II) ions adsorbed at different values of initial concentrations. Analysis

of variance test for both metal ions revealed that the value of F calculated for Pb (II) ions was 62.3221 and for Cd (II) ions was found to be 76.1634 which was greater than the value of F critical which was found to be 4.2252 (Appendices XVI-XVII). This therefore showed that there was significant difference between the mean at different values of initial concentrations.

4.3 Adsorption isotherms

Various adsorption isotherms were used to describe the equilibrium created between the metal ions adsorbed on the adsorbent surface and the metal ions in solution. Raw data on adsorption isotherms for Pb (II) ions and Cd (II) ions adsorption are found in appendix XXX.

4.3.1 Langmuir adsorption isotherm

The linear form of Langmuir sorption isotherm is shown in equation 4.1.

$$\frac{C_e}{q_e} = \frac{1}{K_L q_{max}} + \frac{1}{q_{max}} \quad \text{.....(4.1)}$$

Where; C_e is the equilibrium concentration of the metal ions in mg/l, qe is the adsorption capacity at equilibrium, q_{max} is the optimum adsorption of the adsorbent when the surface is fully saturated by the adsorbate. The constant K_L is called the separation factor and is indicative of the direction of the reaction. When K_L is greater than 1 the reaction is said to be unfavourable, when K_L is equal to one reaction is said to be linear, when K_L is between 0 and 1 reaction is said to be favourable and when K_L is equal to 0 it indicates that the reaction is irreversible (Taha and Dakroury., 2007). A plot of c_e/q_e against c_e given in Figures 4.8 and 4.9. From the figures we get a straight line where $1/q_{max}$ and K_L are obtained from slope and intercept respectively (Rao *et al.*, 2010).

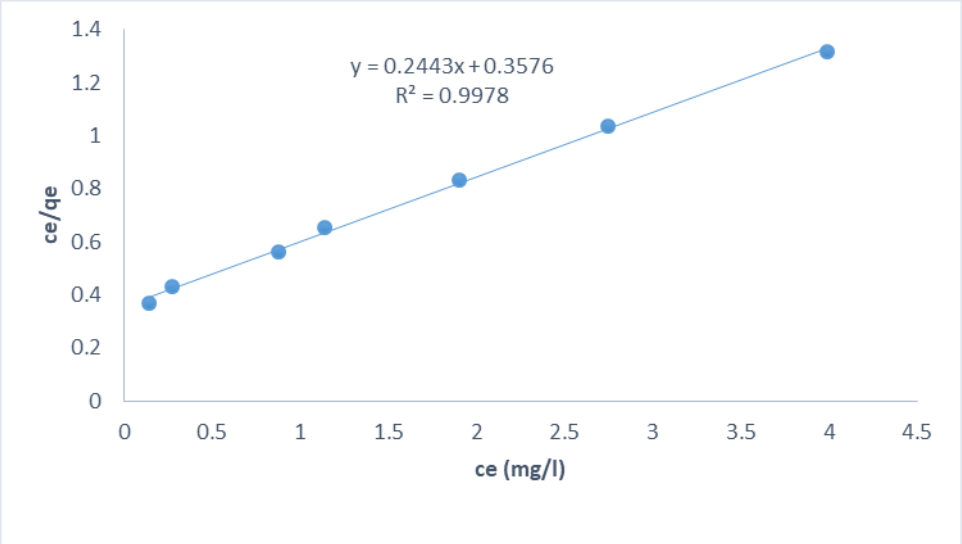

Figure 4.8: Linearized Langmuir isotherm for Pb (II) Ions adsorption onto activated carbon

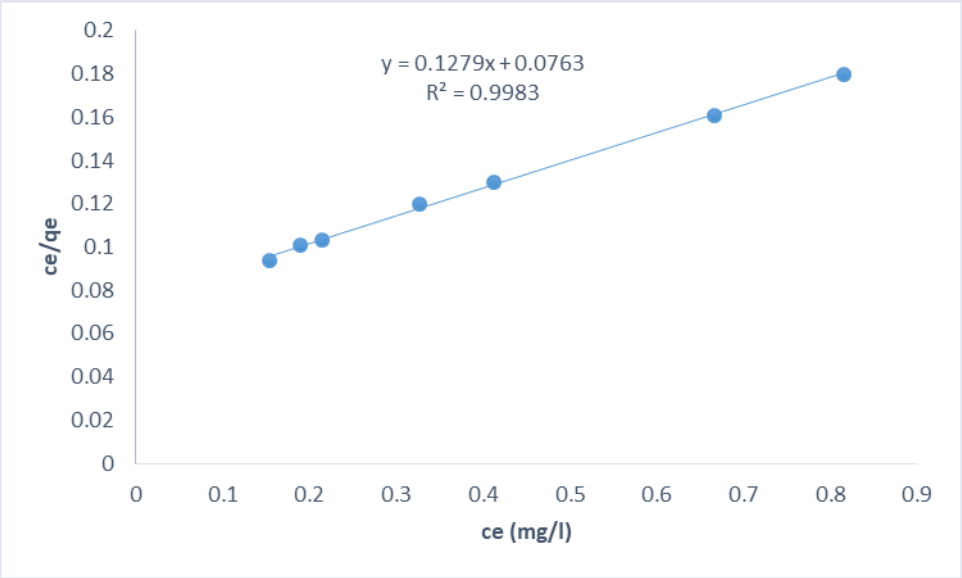

Figure 4.9: Linearized Langmuir isotherm for Cd (II) ions adsorption onto activated carbon

Langmuir isotherms parameters are shown in Table 4.1.

Table 4.1: Langmuir isotherm parameters for Pb (II) ions and Cd (II) ions adsorption

Lead		Cadmium	
$\frac{1}{qmax}$	K_L	$\frac{1}{qmax}$	K_L
R^2		R^2	
0.2443	0.3576	0.1279	0.0763
0.9978		0.9983	

4.3.2 Freundlich adsorption isotherm

Freundlich isotherm is shown in equation 4.2

$$q_e = K_F C_e^{1/n} \quad \text{..... (4.2)}$$

The linear form of the Freundlich equation is shown in equation 4.3

$$\text{Log}q_e = \text{Log}K_F + \frac{1}{n} \log c_e \quad \text{..... (4.3)}$$

q_e is the amount of adsorbate adsorbed per unit weight of the adsorbent in mg/g, K_F is the Freundlich constant which represents the quantity of the metal ions adsorbed onto the adsorbent surface for a unit equilibrium concentration, C_e is the equilibrium concentration in mg/l, n is a Freundlich constant which describes the strength of the bond. The smaller the $\frac{1}{n}$ the bigger the n and the stronger the bond. A plot of ln q_e versus ln c_e is shown in Figures 4.10 and 4.11. As can be seen in figure 4.10 and 4.11 there is a straight line where the slope gives $\frac{1}{n}$ and intercepts give K_F (Afroze *et al*., 2016; Alslaibi *et al*., 2013).

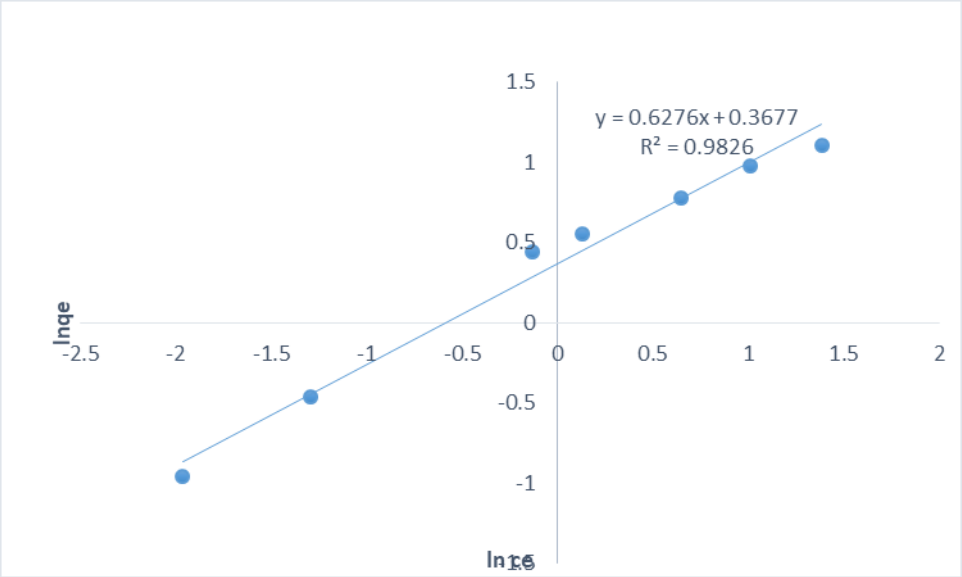

Figure 4.10: Linearized Freundlich isotherm for Pb (II) ions adsorption onto activated carbon

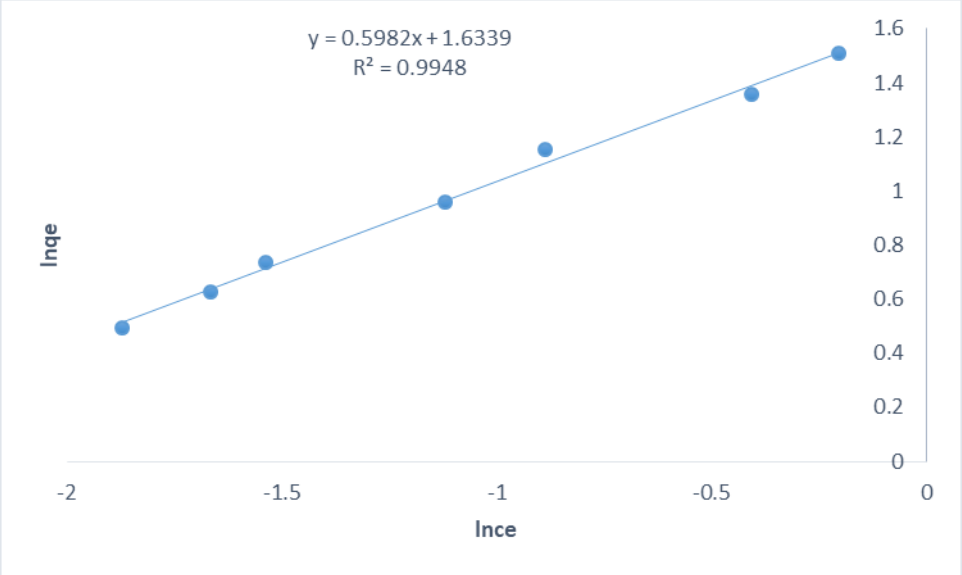

Figure 4.11: Linearized Freundlich isotherm for Cd (II) ions adsorption activated carbon

Freundlich isotherms parameters are shown in Table 4.2.

Table 4.2: Freundlich isotherm parameters for Pb (II) ions and Cd (II) ions adsorption

Lead		**Cadmium**	
$\frac{1}{n}$	K_F	$\frac{1}{n}$	K_F
R^2		R^2	
0.6276	0.3677	0.5982	1.6339
0.9826		0.9948	

4.3.3 Jovanovic adsorption isotherm

The linearized form of Jovanovic equation is shown in equation 4.4

$$\ln q_e = \ln q_{max} - K_J C_e \quad \text{.....(4.4)}$$

Maximum amount of adsorbate adsorbed per unit mass q_{max} of the adsorbent and K_J is Jovanovic constant which is associated with energy of adsorption. Figure 4.12 and 4.13 shows a plot of linearlized Jovanovic isotherm for Pb (II) and Cd (II) ions adsorption onto activated carbon.

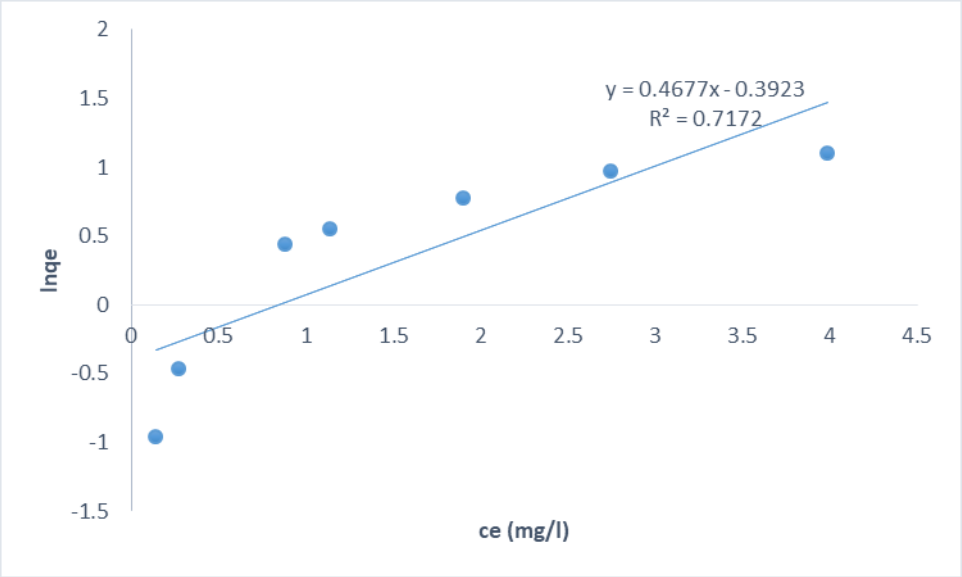

Figure 4.12: Linearized Jovanovic isotherm for Pb (II) ions adsorption onto activated carbon

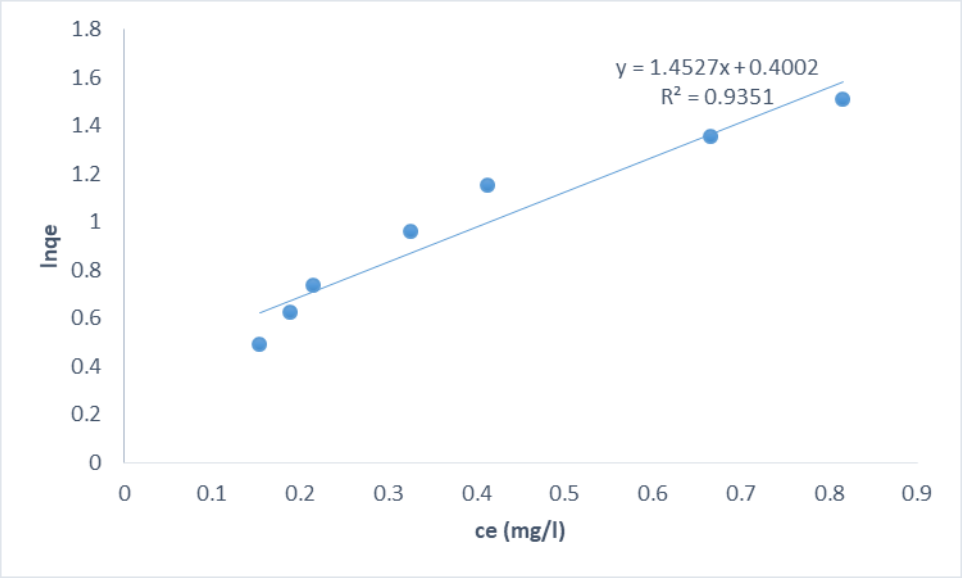

Figure 4.13: **Linearized Jovanovic isotherm for Cd (II) ions adsorption onto activated carbon**

Values of K_J and q_{max} were obtained from the slope and intercept respectively (Yousef *et al.*, 2016).

Jovanovic isotherms parameters are shown in table 4.3.

Table 4.3: **Jovanovic isotherm parameters for Pb (II) ions and Cd (II) ions adsorption**

Lead		**Cadmium**	
K_J	q_{max}	K_J	q_{max}
R^2		R^2	
0.4677	-0.3923	1.4527	0.4002
0.7172		0.9351	

4.3.4 Temkin adsorption isotherm

The linear form of Temkin isotherm is shown in equation 4.5.

$$q_e = BlnA + BlnC_e \quad \text{.....(4.5)}$$

where B is Temkin constant which is related to the heat of sorption, A is Temkin isothermal constant, T is absolute temperature in kelvins and R is molar gas constant and a plot of qe vs lnce in Figures 4.14 and 4.15 was drawn and the values of B and A were computed from slopes and intercepts respectively (Can *et al*., 2016). Figure 4.14 and 4.15 shows Temkin isotherm plot for Pb (II) and Cd (II) ions.

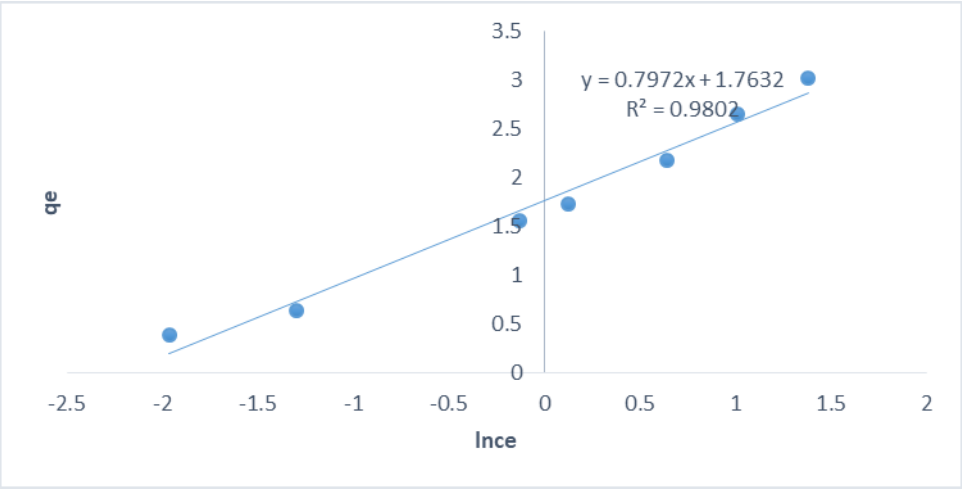

Figure 4.14: **Linearized Temkin isotherm for Pb (II) ions adsorption onto activated carbon**

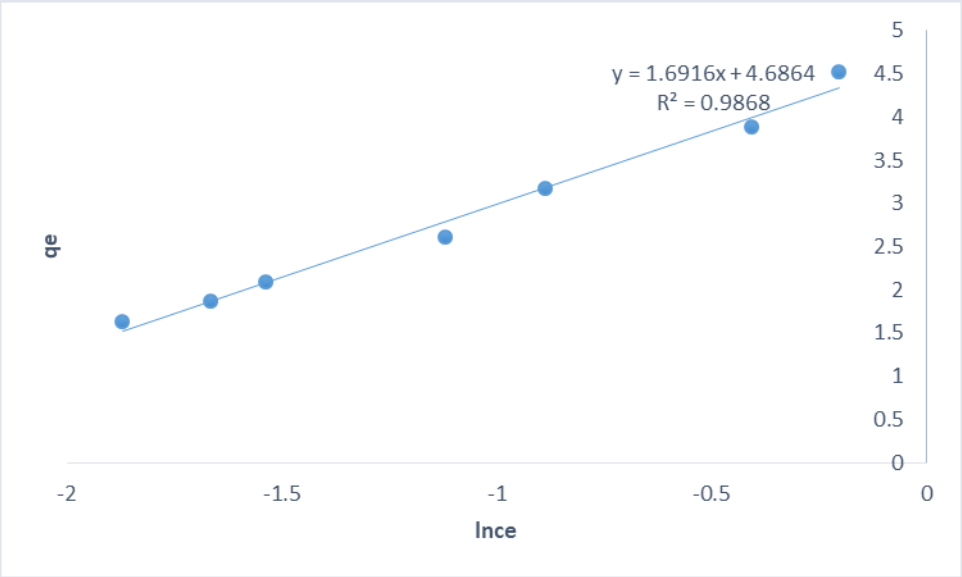

Figure 4.15: **Linearized Temkin isotherm for Cd (II) ions adsorption onto activated carbon**

Temkin isotherms parameters are shown in table 4.4.

Table 4.4: Temkin isotherm parameters for Pb (II) ions and Cd (II) ions adsorption

Lead		**Cadmium**		
A	B	A	B	R^2
R^2				
1.7632	0.7972	4.6964		1.6916
0.9802		0.9868		

Comparison of all adsorption isotherm parameters is shown in table 4.5.

Table 4.5: **Comparison of various sorption isotherm parameters for Pb (II) ions and Cd (II) ions adsorption**

Lead			**Cadmium**		
Langmuir Isotherm			**Langmuir Isotherm**		
q_{max}	K_L	R^2	q_{max}	K_L	R^2
1.5934		0.3576	7.8186		0.0763
0.9978			0.9983		
Freundlich isotherm			**Freundlich isotherm**		
n		K_F	n	K_F	R^2
R^2			1.6717		1.6339

4.093		0.3677	0.9948		
0.9826				**Jovanovic isotherm**	
	Jovanovic isotherm		K_J	q_{max}	R^2
K_J	q_{max}	R^2	1.4527		0.4002
0.4677		-0.3923	0.9351		
0.7172				**Temkin isotherm**	
	Temkin isotherm		A	B	R^2
A	B	R^2	4.6964		1.6916
1.7632		0.7972	0.9868		
0.9802					

Langmuir model fitted well in both metal ions where values of correlation coefficient (R^2) was found to be 0.9978 and 0.9983 for Pb (II) ions and Cd (II) ions respectively. According to the Langmuir model, values of maximum adsorption capacity (q_{max}) for Pb (II) ions and Cd (II) ions was found to be 4.09 mg/g and 7.18 mg/g respectively, values of separation factors (K_L) for Pb (II) ions and Cd (II) ions was found to be 0.3576 and 0.0763 respectively indicating favourable reactions (Taha and Dakroury., 2007). For Freundlich model, both metals gave a good correlation coefficient. Values of regression coefficients (R^2) for Pb (II) ions and Cd (II) ions ions was found to be 0.9826 and 0.9948 respectively. Overall adsorption capacity (K_F) for Pb (II) and Cd (II) ions were found to be 0.3677 and 1.6339 respectively. Values of n for Pb (II) ions was found to be 1.594 while for Cd (II) ions it was found to be 1.672, thus an indication of a favourable and heterogonous adsorption reaction of Pb (II) ions and Cd (II) ions onto the activated carbon (Afroze *et al*., 2016. Values of regression coefficient R^2 for Jovanovic model in both metal ions were 0.7172 for Pb(II) ions and 0.9351 for Cd (II) ions which were very low thus failed to describe well the adsorption of both metal ions onto activated carbon. The values of regression coefficient for the Temkin model was 0.9802 for Pb (II) ions and 0.9868 for Cd (II) ions. For Pb (II) ions the heat of adsorption (A) was found to be 1.7632 lg^{-1} while for Cd (II) ions it was found to be 4.6964lg^{-1}. Temkin isothermal constant (B) for Pb (II) ions and Cd (II) ions were found to be 0.7972 KJ/mol^{-1} and 1.6916l KJ/mol^{-1} respectively.

4.4 Kinetic studies

Various kinetic models were used to describe the mechanism of Pb (II) and Cd (II) ions adsorption. Raw data on the kinetic studies for Pb (II) and Cd (II) ions adsorption are shown in appendix XXXI.

4.4.1 Pseudo first order kinetics

The linearized form of pseudo first order is shown in equation 4.6.

$$\ln(q_e\text{-}q_t) = \ln(q_e\text{-}K_1t) \qquad (4.6)$$

Where q_e is adsorption capacity of the adsorbate at equilibrium(mg/g), q_t is the adsorption capacity at time t and K_1 is the first order rate constant(min). Values of K_1 and q_e are obtained from the slope and intercept respectively by plotting $\log(q_e\text{-}q_t)$ against t as shown in Figures 4.16 and 4.17 (Simonin., 2016).

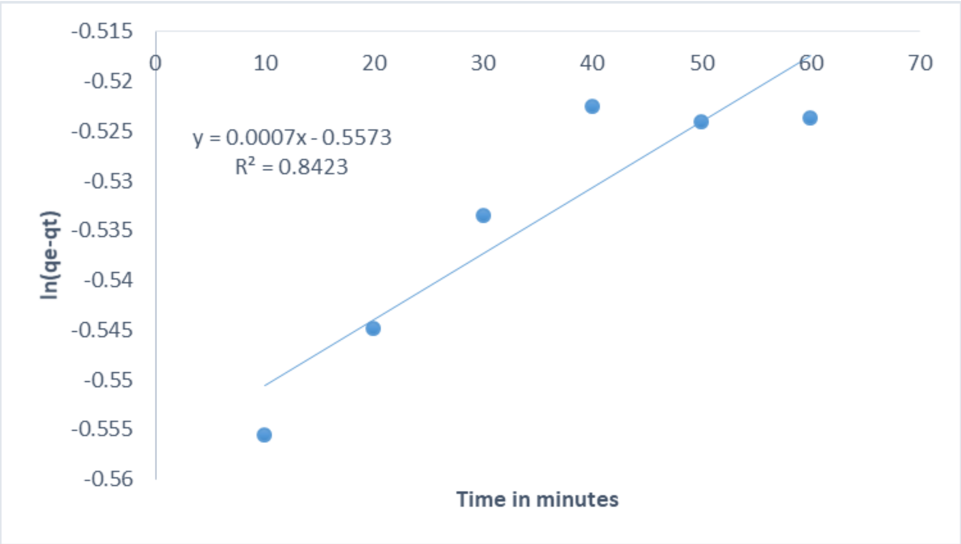

Figure 4.16: Linearized pseudo first order kinetics for Pb (II) ions adsorption onto activated carbon

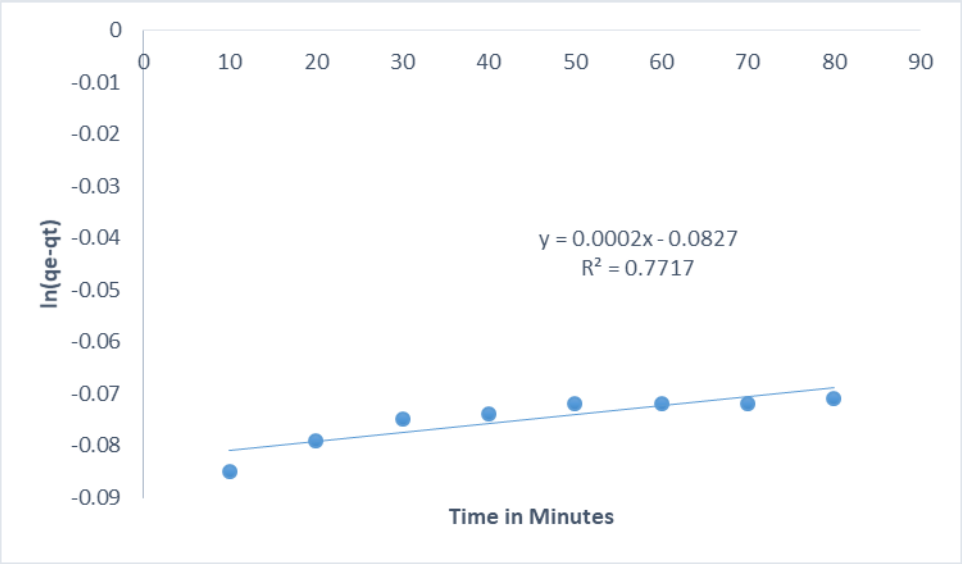

Figure 4.17: **Linearized pseudo first order kinetics for Cd (II) ions adsorption onto activated carbon**

Pseudo first order parameters are shown in Table 4.6.

Table 4.6: **Pseudo first order kinetic parameters for Pb (II) ions and Cd (II) ions adsorption**

Lead		**Cadmium**		
q_e	K_1	q_e	K_1	R^2
R^2				
0.0007	-0.5573	0.0002		-0.0827
0.8423		0.7717		

4.4.2 Pseudo second order kinetics

The linear form of pseudo second order rate equation is shown in equation 4.8.

$$\frac{t}{q_t} = \frac{t}{q_e} + \frac{1}{k_2 q_e^2} \quad \text{..... (4.8)}$$

Where K_2 is the pseudo second order rate constant, q_e is the adsorption capacity at equilibrium and q_t is the adsorption capacity at time t. A plot of t/q_t against t was used to determine pseudo second order rate constant and to determine q_e from the slope and intercept respectively as shown in Figures 4.18 and 4.19 (Yousef *et al.*, 2016).

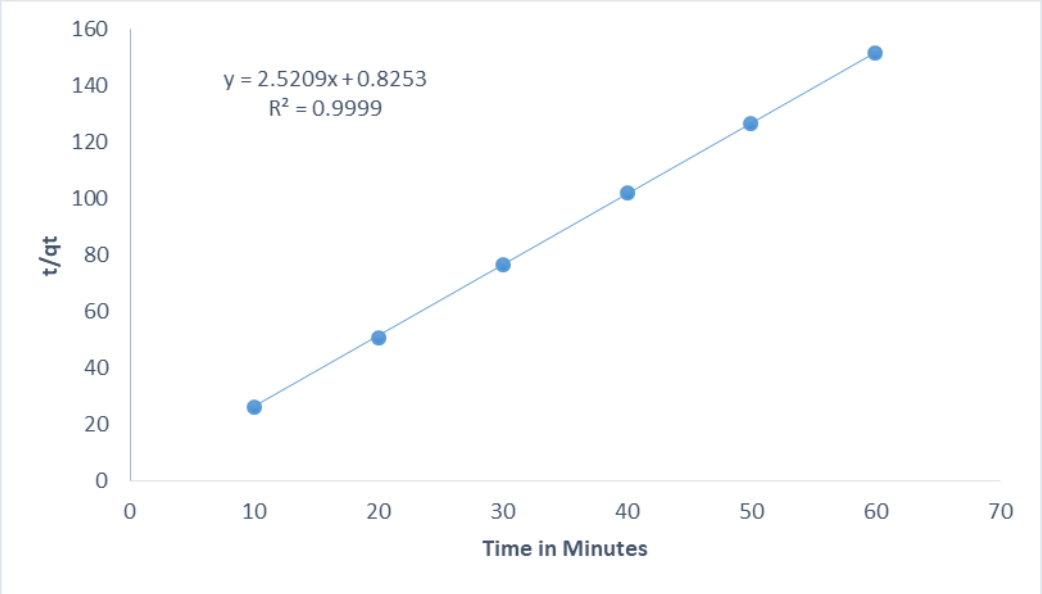

Figure 4.18: Linearized pseudo second order kinetics for Pb (II) Ions adsorption onto activated carbon

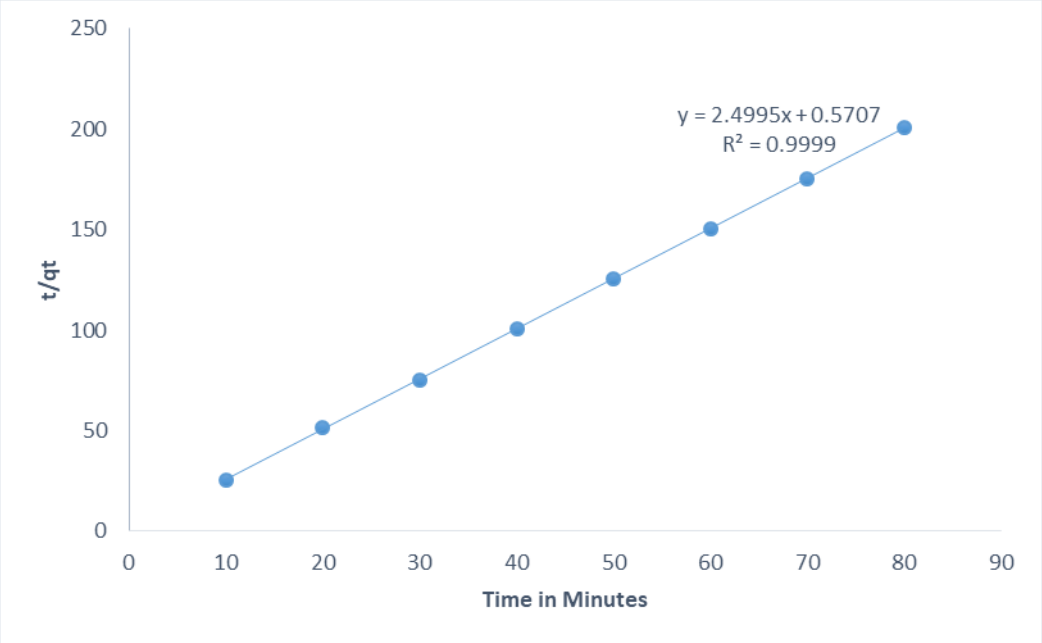

Figure 4.19: Linearized pseudo second order kinetics for Cd (II) ions adsorption onto activated carbon

Pseudo second order parameters are shown in Table 4.7.

Table 4.7*:* Pseudo second order kinetic parameters for Pb (II) ions and Cd (II) ions adsorption

Lead		**Cadmium**		
q_e	K_2	q_e	K_2	R^2
R^2				
2.5209	0.8253	2.4995	0.5707	0.9999
0.9999				

4.4.3 Intraparticle diffusion model

The linear form of intraparticle diffusion equation is shown in equation 4.9

$$q_t = a + K_{int} t^{0.5} \quad \text{.....(4.9)}$$

Where the plot of q_t vs $t^{0.5}$ for intraparticle diffusion plot was used in figures 4.20 and 4.21 to evaluate values of intraparticle diffusion rate (K_{int}) in units of mg/gmin$^{1/2}$ and a constant (C) which is proportional to the thickness of the boundary layer which is in the units of mg/g (Ofomaja 2010). A plot of q_t against t was used to determine the intraparticle diffusion rate and to determine constant C from the slope and intercept respectively as shown in Figures 4.20 and 4.21 (Yousef *et al*., 2016).

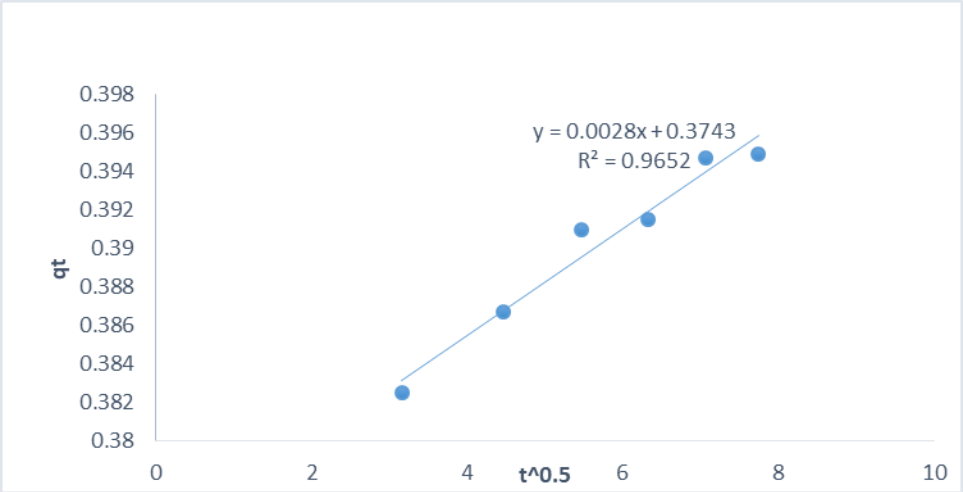

Figure 4.20: **Linearized intraparticle diffusion plot for Pb (II) ions adsorption onto activated carbon**

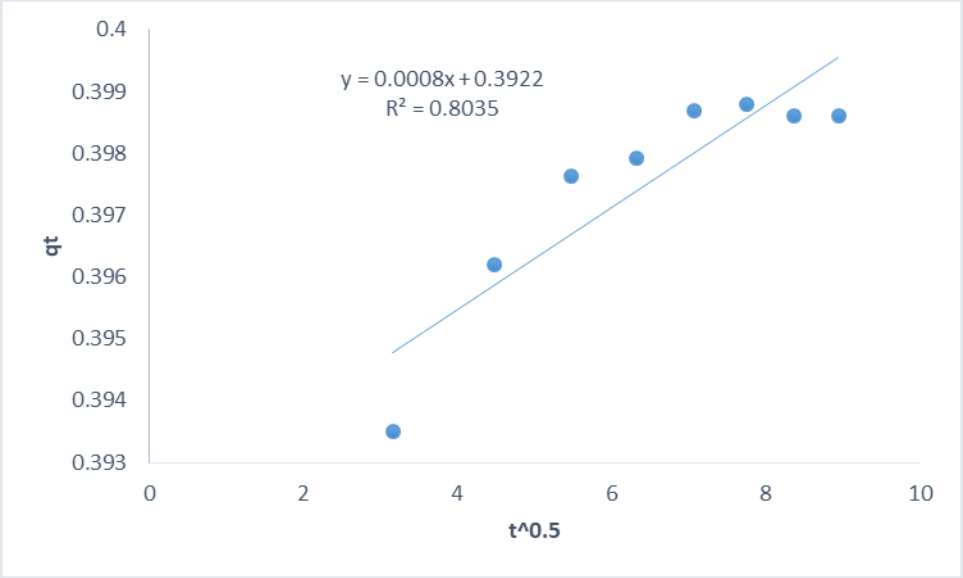

Figure 4.21: **Linearized intraparticle plot for Cd (II) ions adsorption onto activated carbon**

Intraparticle diffusion parameters are shown in Table 4.8.

Table 4.8: **Intraparticle diffusion kinetics parameters for Pb (II) ions and Cd (II) ions adsorption**

Lead	**Cadmium**

K_{int}	C	K_{int}	C	R^2
R^2				
0.0028	0.3743	0.0008	0.3922	0.8035
0.9652				

4.4.4 Elovich diffusion model

The linear form of Elovich equation is shown in eqaution 4.10

q_t= Bln(AB)+Blnt…….....(4.10)

A plot of q_t against lnt in Figures 4.22 and 4.23 was used to compute the initial rate of adsorption (A) which had the units of (g(mg/min) and the coefficient of desorption (B) which had the units of mg(g/mol) (Sen Gupta and Bhattacharyya., 2011).

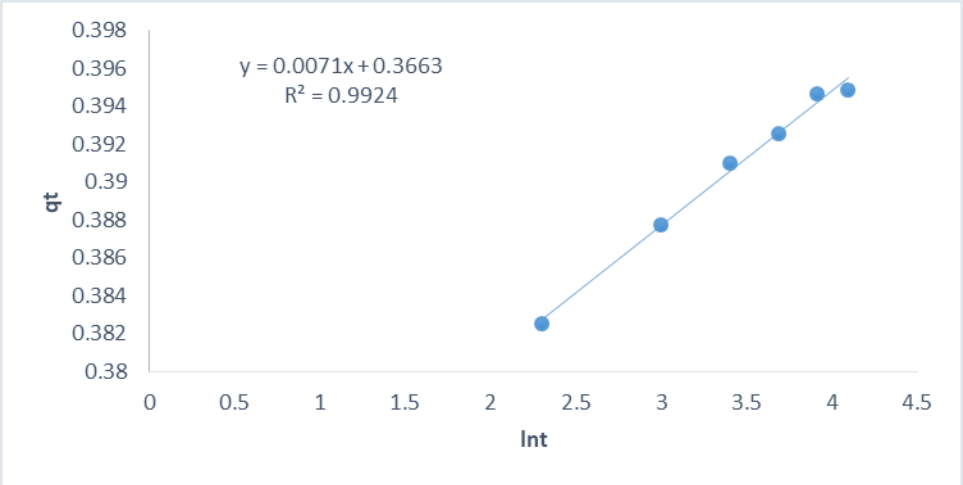

Figure 4.22: Linearized Elovich diffusion plot for Pb (II) ions adsorption onto activated carbon

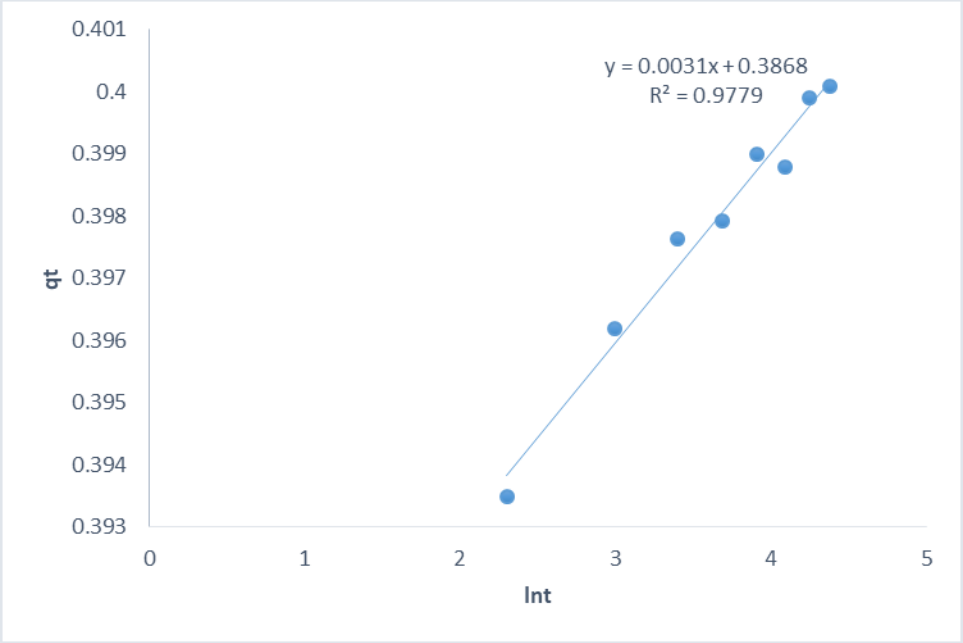

Figure 4.23: Linearized Elovich diffusion plot for Cd (II) ions adsorption onto activated carbon.

Elovich diffusion parameters are shown in Table 4.9.

Table 4.9: **Elovich diffusion kinetics parameters for Pb (II) ions and Cd (II) ions adsorption**

Lead			**Cadmium**		
A	B	R^2	A	B	R^2
0.0071		0.3663	0.0031	0.3868	0.9779
0.9924					

Comparison of various kinetic parameters is shown in Table 4.10.

Table 4.10: Comparison of various kinetic parameters for Pb (II) ions and Cd (II) ions adsorption

Lead			**Cadmium**		
Pseudo first order			**Pseudo first order**		
q_e	K1	R^2	q_e	K1	R^2
0.0007		-0.5573	0.0002	-0.0827	0.7717
0.8423					
Pseudo second order			**Pseudo second order**		
q_e	K_2	R^2	q_e	K_2	R^2
2.5209		0.8253	2.4995		0.5707
0.9999			0.9999		
Intraparticle diffusion model			**Intraparticle diffusion model**		
K_{int}		C	K_{int}	C	R^2
R^2			0.00008		0.3922
0.0028		0.3743	0.8035		
0.9652					
Elovich model			**Elovich model**		
A	B	R^2	A		B
0.0071		0.3663	R^2		
0.9924			0.0031	0.3868	0.9779

To fully determine the rate, path and the mechanism followed during the adsorption process, various kinetic adsorption models were used. Pseudo first order model for both metal ions gave the low values of regression coefficient Pb (II) ions was 0.8423 and Cd (II) ions was 0.7717. Therefore, pseudo first order model could not well describe the adsorption of Pb (II) ions and Cd (II) ions onto the activated carbon. Pseudo second order model gave the regression correlation coefficient of 0.9999 for both Pb (II) ions and Cd (II) ions. From the pseudo second order plot, values of

equilibrium adsorption capacity (qe) for Pb (II) ions and Cd (II) ions was 2.5209 mg/g and 2.4995 mg/g respectively. Pseudo second order rate constant for Pb (II) ions and Cd (II) ions was 0.8253 g/mg/min and 0.5707 g/mg/min respectively. Therefore, for both metal ions, adsorption mechanism through exchange of electrons between the adsorbent and the metal ions was prevalent. Elovich model gave the regression correlation coefficient of 0.9924 for Pb (II) ions and 0.9779 for Cd (II) ions. According to Elovich model initial rate of adsorption (A) was found to be 0.0071 g(mg/min) and 0.0031 g(mg/min) for Pb (II) ions and Cd(II) ions respectively. Coefficient of desorption (B) was found to be 0.3663 mg(g/mol) and 0.3868 mg(g/mol) for Pb (II) ions and Cd (II) ions respectively. Statistical analysis of the data revealed there was a significance difference ($P \leq 0.05$) in the Pb (II) ions and Cd (II) ions adsorbed at different time intervals. ANOVA test for both metal ions revealed that the value of F calculated was greater than F critical (Appendices I-J). This showed that there was significance difference between the means at different time intervals.

CHAPTER FIVE

CONCLUSION AND RECOMEDATIONS

5.1 CONCLUSION

From study the following conclusions were made

1. Activated carbon derived from *Macadamia intergrifolia* nutshell powder is an effective adsorbent for the removal of Pb (II) ions and Cd (II) ions from aqueous solution.

2. FTIR analysis revealed that the functional groups in activated carbon, O-H and C=O could be responsible for heavy metal ions adsorption. SEM micrograph revealed irregular distribution of pore sizes which gave a good possibility for the metal ions to be trapped and adsorbed.

3. Adsorption efficiency is affected by pH, sorbent mass, contact time and initial metal ions concentration. The optimum pH for Pb (II) ions and Cd (II) ions was found to be 4 and 5 respectively whereas the optimum sorbent mass for Pb (II) ions and Cd (II) ions was 0.4 and 0.3 grams respectively. The optimum contact time for Pb (II) ions and Cd (II) ions was 60 and 75 minutes respectively whereas the optimum initial metal ions concentration for both metal ions was found to be 8 mg/l.

4. Adsorption isotherm for both metal ions were found to fit well in the Langmuir model which had a correlation coefficient greater than 0.9978 for Pb^{2+} and 0.9983 for Cd^{2+}. This was an indication that monolayer adsorption on a homogenous material was prevalent in both metal ions. Futhermore, kinetic studies for both metal ions were found to fit well in the pseudo second order kinetics with a correlation coefficient greater than 0.999, indicating that chemisorption mechanism was prevalent in both metal ions.

5.2 RECOMMENDATION

1. Studies should be conducted on the effect of particle size, temperature and shaking speed for the removal of Pb (II) ions and Cd (II) ions from aqueous

solutions using activated carbon derived from *Macadamia Intergrifolia* nutshell powder should be done.

2. Consuming water contaminated with pesticides and pharmaceutical products beyond the required concentration lead to detrimental effects on human health. Adsorption studies on removal of pharmaceuticals and pesticides in aqueous solutions using activated carbon should be therefore done.
3. Heavy metals ions such as arsenic and chromium ions are harmful to human health even in minute concentrations. Studies on the removal of such metal ions using activated carbon should therefore be done.

REFERENCES

Adamczuk, Agnieszka, & Dorota Kołodyńska. (2015). Equilibrium, Thermodynamic and Kinetic Studies on Removal of Chromium, Copper, Zinc and Arsenic from Aqueous Solutions onto Fly Ash Coated by Chitosan. *Chemical Engineering Journal* 274: 200–212.

Afroze, Sharmeen, Tushar Kanti Sen, & Ha Ming Ang. (2016). Adsorption Removal of Zinc (II) from Aqueous Phase by Raw and Base Modified Eucalyptus Sheathiana Bark: Kinetics, Mechanism and Equilibrium Study. *Process Safety and Environmental Protection* 2(1): 336–52.

Akenga, A., Kerich, E., & Kiplangat, A., (2019). "Investigation of Selected Heavy Metal Ions in Irrigation Water, Soil and Managu; (Solanum Nigrum); from Homahills, Homabay County, Kenya." *Journal of Health and Environmental Research* 5(4): 101-105

Al Bsoul, A., Zeatoun, L., Abdelhay, A., & Chiha, M. (2014). Adsorption of copper ions from water by different types of natural seed materials. *Desalination and Water Treatment*, 52(*31–33*), 5876–5882.

Ali, Hazrat, Ezzat Khan & Muhammad Anwar Sajad. (2013). Phytoremediation of Heavy Metals-Concepts and Applications. *Chemosphere* 91(7): 869–81.

Alslaibi, Tamer M., Ismail Abustan, Mohd Azmier Ahmad & Ahmad Abu Foul. (2013). "Cadmium Removal from Aqueous Solution Using Microwaved Olive Stone Activated Carbon." *Journal of Environmental Chemical Engineering* 1(3): 589–99.

Amorim Filho, Volnei Resta & José Anchieta Gomes Neto. (2009). Evaluation of Lubricating Oil Preparation Procedures for the Determination of Al, Ba, Mo, Si and V by High-Resolution Continuum Source FAAS. *Analytical Sciences* 25(1): 95–100.

Araújo, T., Cleide S., & Rezende C. (2018). Elucidation of Mechanism Involved in

Adsorption of Pb(II) onto Lobeira Fruit (Solanum Lycocarpum) Using Langmuir, Freundlich and Temkin Isotherms. *Microchemical Journal* 137(12): 348–54.

Assi, M., Mohammed, A., Hezmee, M., Sabri, M., & Rajen, M. (2016). The Detrimental Effects of Lead on Human and Animal Health. *Veterinary World* 9(6): 660–71.

Asuquo, E., Martin, A, & Nzerem, P. (2017). Adsorption of Cd(II) and Pb(II) Ions from Aqueous Solutions Using Mesoporous Activated Carbon Adsorbent: Equilibrium, Kinetics and Characterisation Studies. *Journal of Environmental Chemical Engineering* 5(1): 679–98.

Paula, B. N., Chandaa S., Dasa S., Singha P., Pandeya B.K & Girib S.S. (2016). Mineral Assay in Atomic Absorption Spectroscopy Mineral Assay in Atomic Absorption Spectroscopy. 1(12): 1–17.

Bernhoft, Robin A. (2013). Cadmium Toxicity and Treatment- A Review. *The Scientific World Journal* 2013(6), 1-8.

Birry, L., Mehta, P., Jaouen, E., Dodelet, P., & Guiot, S. (2011). Application of Iron-Based Cathode Catalysts in a Microbial Fuel Cell. *Electrochimica Acta* 56(3): 1505–11.

Boeykens, S. P., Redondo, N., Obeso, R. A., Caracciolo, N., & Vázquez, C. (2019). Chromium and Lead adsorption by avocado seed biomass study through the use of Total Reflection X-Ray Fluorescence analysis. *Applied Radiation and Isotopes*.12(*6*) 974-986

Boss, C. B., & Fredeen, K. J. (1997). Concepts, Instrumentation and Techniques in Atomic Absorption Spectrophotometry. 14: 2–12.

Cai, L., Xu, Z., Qi, J., Feng, Z., and Xiang, T. (2015). Assessment of Exposure to Heavy Metals and Health Risks among Residents near Tonglushan Mine in Hubei, China. *Chemosphere* 127: 127–35.

Calvin C.Willite., Gwedolyn L. Bell & Clifton J. Mclellan. (2012). Total Allowable Concentration of Momomeic Alminium Silicates in Drinking Water. Critical Review in Toxicology 42(*5*) 358-442

Can, Nursel, Birsel Can Ömür & Ahmet Altındal. (2016). Modeling of Heavy Metal Ion Adsorption Isotherms onto Metallophthalocyanine Film. *Sensors and Actuators, B: Chemical* 237: 953–61.

Chand, Piar, Arun Kumar Shil, Mohit Sharma & Yogesh B. Pakade. (2014). Improved Adsorption of Cadmium Ions from Aqueous Solution Using Chemically Modified Apple Pomace: Mechanism, Kinetics, and Thermodynamics. *International Biodeterioration and Biodegradation* 90: 8–16.

Chaney, Rufus L. (2015). How Does Contamination of Rice Soils with Cd and Zn Cause High Incidence of Human Cd Disease in Subsistence Rice Farmers. *Current Pollution Reports* 1(1): 13–22.

Cheng, Q., Xu, L., & Zhai, L. (2011). Adsorption of Cr(VI) Ions Using the Amphiphilic Gels Based on 2-(Dimethylamino)Ethyl Methacrylate Modified with 1-Bromoalkanes. *Chemical Engineering Journal* 173(1): 42–48.

Chotpantarat, Srilert, Say Kee Ong, Chakkaphan Sutthirat & Khemarath Osathaphan. (2011) Effect of PH on Transport of Pb^{2+}, Mn^{2+}, Zn^{2+} and Ni^{2+} through Lateritic Soil: Column Experiments and Transport Modeling. *Journal of Environmental Sciences* 23(4): 640–48.

Ciftci, Harun & Cigdem Er. (2013). Solid-Phase Extraction and Separation Procedure for Trace Aluminum in Water Samples and Its Determination by High-Resolution Continuum Source Flame Atomic Absorption Spectrometry (HR-CS FAAS). : 2745–53.

Colina, J., Suwalsky, M., Marique, M., and Moreno M. (2019). An in Vitro Study of the Protective Effect of Caffeic Acid on Erythrocytes. *Archives of Biochemistry and Biophysics* 662(9): 75–82.

Deliyanni, Eleni A., George Z. Kyzas & Kostas A. Matis. (2017).Various Flotation Techniques for Metal Ions Removal. *Journal of Molecular Liquids* 225: 260–

64.

Demiral, Hakan. (2016). Adsorption of Copper (II) from Aqueous Solutions on Activated Carbon Prepared from Grape Bagasse ; Journal of cleaner production 124(15), 103-113.

Desta, Mulu Berhe. (2013). Batch Sorption Experiments: Langmuir and Freundlich Isotherm Studies for the Adsorption of Textile Metal Ions onto Teff Straw (Eragrostis Tef) Agricultural Waste. *Journal of Thermodynamics* 1(1).

Doroodmand, Mohammad Mahdi & Maryam Mehrtash. (2015). Micro/Nano Bubble-Modified Flame Atomic Spectrometry as a New Technique for Promotion of the Figures of Merit during Determination of Metal Species: Improvement in the Performance of Pre-Mixed Burner. *Sensors and Actuators, A: Physical* 232, 84–93.

El-Ghussein, M., Mastanduno, S., Shundong, T., Pogue, W., & Paulsen, K. (2013). Hybrid Photomultiplier Tube and Photodiode Parallel Detection Array for Wideband Optical Spectroscopy of the Breast Guided by Magnetic Resonance Imaging. *Journal of Biomedical Optics* 19(1): 011010.

Fakayode, S., Yakubu. A., Mohammed, A., & Pollard, D. (2012). Determination of Fe Content of Some Food Items by Flame Atomic Absorption Spectroscopy (FAAS): A Guided-Inquiry Learning Experience in Instrumental Analysis Laboratory. *Journal of Chemical Education* 89(1): 109–13.

Fawzy, Manal, Mahmoud Nasr, Ashraf Abdel-Gaber & Shaimaa Fadly. (2016). Biosorption of Cr(VI) from Aqueous Solution Using Agricultural Wastes, with Artificial Intelligence Approach. *Separation Science and Technology (Philadelphia)* 51(3): 416–26.

Feng, N., Guo, X., Liang, S., Zhu, S., & Liu, J. (2011). Biosorption of Heavy Metals from Aqueous Solutions by Chemically Modified Orange Peel. *Journal of Hazardous Materials* 185(1): 49–54.

Ganzoury, Mohamed A., Nageh K. Allam, Thermo Nicolet & Corporation All. (2015). Introduction to Fourier Transform Infrared Spectrometry. *Renewable and*

Sustainable Energy Reviews 50: 1–8.

Ge, H., & X. Fan. (2011). Adsorption of Pb^{2+} and Cd^{2+} onto a Novel Activated Carbon-Chitosan Complex. *Chemical Engineering and Technology* 34(10): 1745–52.

Gherasim, Cristina Veronica, Jirí Cuhorka & Petr Mikulášek. (2013). Analysis of Lead(II) Retention from Single Salt and Binary Aqueous Solutions by a Polyamide Nanofiltration Membrane: Experimental Results and Modelling. *Journal of Membrane Science* 436: 132–44.

Greenwood, Ted & Alvin Streeter. (2019). 2 Natural Resources in U.S.-canadian Relations, Volume 2: Patterns and Trends in Resource Supplies and Policies *Uranium*.

Gupta, R., Tinda, T., Khan, A., Srivastava, P., & Kanaujia, A. (2019). Assessment Of Ground Water Quality And Its Suitability For Drinking In Industrial Area Jajmau , Kanpur , India. 19(1): 1569–71.

Sen Gupta, Susmita & Krishna G. Bhattacharyya. (2011). Kinetics of Adsorption of Metal Ions on Inorganic Materials: A Review. *Advances in Colloid and Interface Science* 162(1–2): 39–58.

Gupta, Vinod Kumar, Deepak Pathania, Shikha Sharma & Pardeep Singh. (2013). Preparation of Bio-Based Porous Carbon by Microwave Assisted Phosphoric Acid Activation and Its Use for Adsorption of Cr(VI). *Journal of Colloid and Interface Science* 401: 125–32.

Hans Wedepohl, K. (1995). "The Composition of the Continental Crust." *Geochimica et Cosmochimica Acta* 59(7): 1217–32.

Hashim, D., Man Che, Y., Nokarasha, R., Shuhaimi, M., Salama, Y., & Syahariza, Z., (2010). Potential Use of Fourier Transform Infrared Spectroscopy for Differentiation of Bovine and Porcine Gelatins. *Food Chemistry* 118(3): 856–60.

Hossain, M A, M Kumita & S Mori. (2010). SEM Characterization of the Mass Transfer of Cr(VI) during the Adsorption on Used Black Tea Leaves. *African*

Journal of Pure and Applied Chemistry 4(7): 135–41.

Huang, Yuxiang, Erni Ma & Guangjie Zhao. (2015). Thermal and Structure Analysis on Reaction Mechanisms during the Preparation of Activated Carbon Fibers by KOH Activation from Liquefied Wood-Based Fibers. *Industrial Crops and Products* 69: 447–55.

Jadia, Chhotu D., & M. H. Fulekar. (2009). Phytoremediation of Heavy Metals: Recent Techniques. *African Journal of Biotechnology* 8(6): 921–28.

Jain, Ravi. (2012). Providing Safe Drinking Water: A Challenge for Humanity. *Clean Technologies and Environmental Policy* 14(1): 1–4.

Järup, Lars, & Agneta Åkesson. 2009. Current Status of Cadmium as an Environmental Health Problem. *Toxicology and Applied Pharmacology* 238(3): 201–8.

Kakoi, B., Kaluli, J. W., Ndiba, P., & Thiong, G. (2016). Removal of Lead (II) from Aqueous Solution using Natural Materials : A Kinetic and Equilibrium Study *Journal of Sustainable Research and Engineering.* 3(*3*), 53–62.

Kariuki, Zacharia., Kiptoo, Jackson & Onyancha, Douglas. (2017). Biosorption Studies of Lead and Copper Using Rogers Mushroom Biomass (Lepiota Hystrix). *South African Journal of Chemical Engineering* 23: 62–70.

Kim, H. S., Kim, Y. J., & Seo, Y. R. (2015). An Overview of Carcinogenic Heavy Metal: Molecular Toxicity Mechanism and Prevention. *Journal of Cancer Prevention*, 20(*4*), 232–240.

Kim, J., & Benjamin, M. M. (2004). Modeling a novel ion exchange process for arsenic and nitrate removal. *Water Research*, 38(*8*), 2053–2062.

Kinuthia, G., Ngure, V., Beti, D., Lugalia, R., Wanjila, A., & Kamau, L. (2020). Levels of Heavy Metals in Wastewater and Soil Samples from Open Drainage Channels in Nairobi , Kenya : *Community Health Implication.* : 1–13.

Kokot, F. (1955). Flame photometry. *Polski Tygodnik Lekarski*, 10(*36*), 1188–1195.

Kosgei, P J, Mwaniki, D. M., & Liti D M. (2019). Concentration of Selected Heavy Metals in Water and the Cummulative Effect on Selected Organs of Oreochromis Niloticus and Clarias Gariepinus from Lake Victoria . *The Journal of Applied Sience*, 9(4): 80–91.

Kowanga, K. D., Gatebe, E., Mauti, G. O., & Mauti, E. M. (2016). Kinetic , sorption isotherms , pseudo-first-order model and pseudo-second-order model studies of Cu(II) and Pb(II) using defatted Moringa oleifera seed powder. *The Journal of Phytopharmacology*, 5(*2*), 71–78.

Kumar, S., Meena, H. M., & Verma, K. (2017). Water Pollution in India: Its Impact on the Human Health: Causes and Remedies. *International Journal of Applied Environmental Sciences*, *12*(*2*), 275–279.

Kyzas, G. Z., & Matis, K. A. (2018). Flotation in water and wastewater treatment- A Review. *Processes*, 6(8), 1-16.

Lagalante, A. F. (1999). Atomic absorption spectroscopy: A tutorial review. *Applied Spectroscopy Reviews*, 34(*3*), 173–189.

Li, D., Ding, Y., Li, L., Chang, Z., Rao, Z., & Lu, L. (2015). Removal of hexavalent chromium by usSing red mud activated with cetyltrimethylammonium bromide. *Environmental Technology (United Kingdom)*, *36*(*9*), 1084–1090.

Li, Z., Ma, Z., Jan, T., Kuijp, V. Der, Yuan, Z., & Huang, L. (2014). Science of the Total Environment A review of soil heavy metal pollution from mines in China : Pollution and health risk assessment. *Science of the Total Environment, 39(468–469)*, 843–853.

Lombi, E., Zhao, F. J., Dunham, S. J., & McGrath, S. P. (2001). Phytoremediation of Heavy Metal–Contaminated Soils. *Journal of Environment Quality*, 30(*6*), 1919.

Lu, Y., Song, S., Wang, R., Liu, Z., Meng, J., Sweetman, A. J., Jenkins, A., Ferrier, R. C., Li, H., Luo, W., & Wang, T. (2015). Impacts of soil and water pollution on food safety and health risks in China. *Environment International*, 77(*16)*, 5–15.

Lung, K., Arisaka, K., Bargetzi, A., Beltrame, P., Cahill, A., Genma, T., Ghag, C., Gordon, D., Sainz, J., Teymourian, A., & Yoshizawa, Y. (2012). Characterization of the Hamamatsu R11410-10 3-in. photomultiplier tube for liquid xenon dark matter direct detection experiments. *Nuclear Instruments and Methods in Physics Research, Section A: Accelerators, Spectrometers, Detectors and Associated Equipment*, 696*(7)*, 32–39.

Lyu, M., Yun, J. H., Chen, P., Hao, M., & Wang, L. (2017). Addressing Toxicity of Lead: Progress and Applications of Low-Toxic Metal Halide Perovskites and Their Derivatives. *Advanced Energy Materials*, 7(15), 131-145.

Ma, J., Qin, G., Zhang, Y., Sun, J., Wang, S., & Jiang, L. (2018). Heavy metal removal from aqueous solutions by calcium silicate powder from waste coal fly-ash. *Journal of Cleaner Production*, *182*, 776–782.

Madivoli, E., Kareru, P., Gachanja, A., Mugo, S., Murigi, M., Kairigo, P., Kipyegon, C., Mutembei, J., & Njonge, F. (2016). Adsorption of Selected Heavy Metals on Modified Nano Cellulose. *International Research Journal of Pure and Applied Chemistry*, 12(3), 1–9.

Mahar, A., Wang, P., Ali, A., Awasthi, M. K., Lahori, A. H., Wang, Q., Li, R., & Zhang, Z. (2016). Challenges and opportunities in the phytoremediation of heavy metals contaminated soils: A review. *Ecotoxicology and Environmental Safety*, *126*, 111–121.

Malakahmad, A., Tan, S., & Yavari, S. (2016). Valorization of Wasted Black Tea as a Low-Cost Adsorbent for Nickel and Zinc Removal from Aqueous Solution. *Journal of Chemistry*, *2016*.

Malik, D. S., & Yadav, A. K. (2015). Preparation and Characterization of Low Cost Adsorbants. *Journal of Global Biosciences*, 4(1), 1824–1829.

Mason, L. H., Harp, J. P., & Han, D. Y. (2014). Pb neurotoxicity: Neuropsychological effects of lead toxicity-A Review. *BioMed Research International*, 2014(47), *1-8*.

Meharg, A. A., Norton, G., Deacon, C., Williams, P., Adomako, E. E., Price, A., Zhu, Y., Li, G., Zhao, F. J., McGrath, S., Villada, A., Sommella, A., De Silva, P. M. C. S., Brammer, H., Dasgupta, T., & Islam, M. R. (2013). Variation in rice cadmium related to human exposure. *Environmental Science and Technology*, 47(11), 5613–5618.

Meunier, N., Drogui, P., Montané, C., Hausler, R., Mercier, G., & Blais, J. F. (2006). Comparison between electrocoagulation and chemical precipitation for metals removal from acidic soil leachate. *Journal of Hazardous Materials*, 137(1), 581–590.

Mishra, V., Majumder, C. B., & Agarwal, V. K. (2012). Sorption of Zn(II) ion onto the surface of activated carbon derived from eucalyptus bark saw dust from industrial wastewater: Isotherm, kinetics, mechanistic modeling, and thermodynamics. *Desalination and Water Treatment*, 46(1–3), 332–351.

Mohammadi, S. Z., Karimi, M. A., Afzali, D., & Mansouri, F. (2010). Removal of Pb(II) from aqueous solutions using activated carbon from Sea-buckthorn stones by chemical activation. *Desalination and Water Treament*, 26s2(1–3), 86–93.

Moloukhia, H., Hegazy, W. S., & Mahrous, S. S. (2016). Removal of Eu , Ce , Sr , and Cs ions from radioactive waste solutions by modified activated carbon prepared from coconut shells.

Momčilović, M., Purenović, M., Bojić, A., Zarubica, A., & Randelovid, M. (2011). Removal of lead(II) ions from aqueous solutions by adsorption onto pine cone activated carbon. *Desalination and Water Treaatment*, 276(1–3), 53–59.

Moreno-Piraján, J. C., & Giraldo, L. (2012). Heavy metal ions adsorption from wastewater using activated carbon from orange peel. *E-Journal of Chemistry*, 9(2), 926–937.

Moussout, H., Ahlafi, H., Aazza, M., & Maghat, H. (2018). Critical of linear and nonlinear equations of pseudo-first order and pseudo-second order kinetic models. *Karbala International Journal of Modern Science*, 4(2), 244–254.

Muvengei, D., Mbuvi, H., & Nganga, M. (2017) . Removal of Pb(II) and Cd(II) ions, colour and turbidity from water using carbon and ash derived products from maize cobs. J*ournal of Applied Chemistry*, 10(6), 56-68

Nagy, A., Baranyai, E., & Gaspar, A. (2014). Interfacing microfluidic chip-based chromatography with flame atomic absorption spectrometry for the determination of chromium(VI). *Microchemical Journal*, 114, 216–22

Ndungu, S., Wanja, E., & Nduta, R. (2014). Kinetic modelling for Cu^{2+}, Cd^{2+} amd Pb^{2+} onto a raw and modified Artocarpus heterophyllus seed from a model solution. *Asian Journal of Research in Chemistry,* 2, 89-95.

NEMA., (2006). Quality Standards For Domestic Water, *National Environmental Management Authority*: Nairobi Kenya 8-9.

Nethaji, S., Sivasamy, A., & Mandal, A. B. (2013). Adsorption isotherms, kinetics and mechanism for the adsorption of cationic and anionic dyes onto carbonaceous particles prepared from Juglans regia shell biomass. *International Journal of Environmental Science and Technology*, 10(2), 231–242.

Njuguna, S. M., Yan, X., Gituru, R. W., Wang, Q. &Wang, J. (2017). Assessment of macrophyte , heavy metal , and nutrient concentrations in the water of the Nairobi River. *Environmental Monitoring and Assesment* , 189(454). 1-14

Ochongo. E.A, Ouma G.O., Obiero P.O., & Odero. N.A., (2019) Improved Response to Water Shortage. A discrete study of Lang'ata sub county Nairobi city, Kenya. *Journal of Water Resource and Protection*, 11(9), 1161-1187.

Ofomaja, A. E. (2010). Intraparticle diffusion process for lead(II) biosorption onto mansonia wood sawdust. *Bioresource Technology*, 101(15), 5868–5876.

Onyancha, D., Mavura, W., Ngila, J. C., Ongoma, P., & Chacha, J. (2008). Studies of chromium removal from tannery wastewaters by algae biosorbents, Spirogyra condensata and Rhizoclonium hieroglyphicum. *Journal of Hazardous Materials*, 158(2–3), 605–614.

Ortega, L. M., Lebrun, R., Blais, J. F., Hausler, R., & Drogui, P. (2008). Effectiveness of soil washing, nanofiltration and electrochemical treatment for the recovery of metal ions coming from a contaminated soil. *Water Research*, 42(8–9), 1943–1952.

Pan, J., Plant, J. A., Voulvoulis, N., Oates, C. J., & Ihlenfeld, C. (2010). Cadmium levels in Europe: implications for human health. *EnvironmentalS Geochemistry and Health*, 32(1), 1–12.

Pastorelli, A. A., Baldini, M., Stacchini, P., Baldini, G., Morelli, S., Sagratella, E., Zaza, S., & Ciardullo, S. (2012). Human exposure to lead, cadmium and mercury through fish and sea food product consumption in Italy: a pilot evaluation. *Food Additives and Contaminants - Part A Chemistry, Analysis, Control, Exposure and Risk Assessment*, 29(12), 1913–1921.

Paul, V., Pandey, R., & C Meena, R. (2017). Atomic absorption spectroscopy (AAS) for elemental analysis of plant samples. *Manual of ICAR Sponsored Training Programme on "Physiological Techniques to Analyze the Impact of Climate Change on Crop Plants,"*11, 84–86.

Paz-Rodríguez, B., Domínguez-González, M. R., Aboal-Somoza, M., & Bermejo-Barrera, P. (2015). Application of High Resolution-Continuum Source Flame Atomic Absorption Spectrometry (HR-CS FAAS): Determination of trace elements in tea and tisanes. *Food Chemistry*, 170, 492–500.

Pizzol, M., Thomsen, M., & Andersen, M. S. (2010). Long-term human exposure to lead from different media and intake pathways. *Science of the Total Environment*, 408(22), 5478–5488.

Qiu, Y. R., & Mao, L. J. (2013). Removal of heavy metal ions from aqueous solution by ultrafiltration assisted with copolymer of maleic acid and acrylic acid. *Desalination*, 329, 78–85.

Rahimzadeh, M. R., Rahimzadeh, M. R., Kazemi, S., & Moghadamnia, A. A. (2017). Cadmium toxicity and treatment: An update. *Caspian Journal of Internal Medicine*, 8(3), 135–145.

Ran, J., Wu, L., He, Y., Yang, Z., Wang, Y., Jiang, C., Ge, L., Bakangura, E., & Xu, T. (2017). Ion exchange membranes: New developments and applications. *Journal of Membrane Science*, 522, 267–291.

Ravindra, K.G; Pavan,K.G; Shushmita,B; Vandani, R; Shivani, S; Sanjay, K.S; & Mahes,C.C; Removal of tartrazine by activated carbon biosorbents of Lantana camara: Kinetics, equilibrium modeling and spectroscopic analysis. *Journal of Environmental Chemical Engineering*, 20(3), 79-88.

Rao, K. S., Chaudhury, G. R., & Mishra, B. K. (2010). Kinetics and equilibrium studies for the removal of cadmium ions from aqueous solutions using Duolite ES 467 resin. *International Journal of Mineral Processing*, 97(1–4), 68–73.

Rengaraj, S., Yeon, K. H., & Moon, S. H. (2001). Removal of chromium from water and wastewater by ion exchange resins. *Journal of Hazardous Materials*, 87(1–3), 273–287.

Renu, M. A., Singh, K., Upadhyaya, S., & Dohare, R. K. (2017). Removal of heavy metals from wastewater using modified agricultural adsorbents. *Materials Today: Proceedings*, 4(9), 10534–10538.

Repo, E., Warchoł, J. K., Bhatnagar, A., & Sillanpää, M. (2011). Heavy metals adsorption by novel EDTA-modified chitosan-silica hybrid materials. *Journal of Colloid and Interface Science*, 358(1), 261–267.

Rocha, M. S., Mesko, M. F., Silva, F. F., Sena, R. C., Quaresma, M. C. B., Araújo, T. O., & Reis, L. A. (2011). Determination of Cu and Fe in fuel ethanol by ICP OES using direct sample introduction by an ultrasonic nebulizer and membrane desolvator. *Journal of Analytical Atomic Spectrometry*, 26(2), 456–461.

Rubio, F., Gonçalves, A. C., Meneghel, A. P., Teixeira Tarley, C. R., Schwantes, D., & Coelho, G. F. (2013). Removal of cadmium from water using by-product Crambe abyssinica Hochst seeds as biosorbent material. *Water Science and Technology*, *68*(1), 227–233.

Sahu, A., Chatterjee Mitra, J., & Author, C. (2018). Preparation of Thermo-Modified Tea waste and Its Use to Study the Heavy Metal Adsorption from Waste Water. *IOSR Journal of Applied Chemistry (IOSR-JAC*, 11(7), 40–46.

Saini, V. K., Kak, A., & Dixit, S. K. (2018). Selective photoionization of lithium isotopes in a hollow cathode lamp: a feasibility study for a laser ion source and detector. *Applied Optics*, *57*(23), 6808.

Salehzadeh, J. (2013). Removal of Heavy Metals Pb^{2+}, Cu^{2+}, Zn^{2+}, Cd^{2+}, Ni^{2+}, Co^{2+} and Fe^{3+} from Aqueous Solutions by using Xanthium Pensylvanicum. *Leonardo Journal of Sciences*, 12(23), 97–104.

Sari, A., & Tuzen, M. (2009). Kinetic and equilibrium studies of biosorption of Pb(II) and Cd(II) from aqueous solution by macrofungus (Amanita rubescens) biomass. *Journal of Hazardous Materials*, 164(2–3), 1004–1011.

Satarug, S., Garrett, S. H., Sens, M. A., & Sens, D. A. (2010). Cadmium, environmental exposure, and health outcomes. *Environmental Health Perspectives*, 118(2), 182–190.

Sekhararao Gulipalli, C., Prasad, B., & Wasewar, K. L. (2011). Batch study, Equilibirum and kinetics of adsorption of selenium using rice husk ash (RHA). *Journal of Engineering Science and Technology*, 6(5), 590–609.

Sen Gupta, S., & Bhattacharyya, K. G. (2011). Kinetics of adsorption of metal ions on inorganic materials: A review. *Advances in Colloid and Interface Science*, 162(1–2), 39–58.

Seyed Masoud Seyedi, Bagher Anvaripour & Mohsen Motavassel, N. J. (2013). Comparative Cadmium Adsorption from water by nanochitosan and chitosan. *International Journal of Engineering and Innovative Technology*, 5(9), 145–148.

Shamsuddin, M. S., Yusoff, N. N. & Sulaiman, M. A. (2016). Synthesis and characterization of activated carbon produced from kenaf core fiber using H_3PO_4 activation. *Procedia Chemistry*, 19*(6)*, 558–565.

Sharma, B., & Tyagi, S. (2013). Simplification of Metal Ion Analysis in Fresh Water Samples by Atomic Absorption Spectroscopy for Laboratory Students. *Journal of Laboratory Chemical Education*, 1(3), 54–58.

Simonin, J. P. (2016). Comparison of pseudo-first order and pseudo-second order rate laws in the modeling of adsorption kinetics. *Chemical Engineering Journal*, 300(24), 254–263.

Singh, R., Gautam, N., Mishra, A., & Gupta, R. (2011). Heavy metals and living systems: An overview. *Indian Journal of Pharmacology*, 43(3), 246–253.

Sudha, R., Kalpana, K., Rajachandrasekar, T., & Arivoli, S. (2007). Comparative study on the adsorption kinetics and thermodynamics of metal ions onto acid activated low cost pandanus carbon. *E-Journal of Chemistry*, 4(2), 238–254.

Surchi, K. M. S. (2011). Agricultural Wastes as Low Cost Adsorbents for Pb Removal: Kinetics, Equilibrium and Thermodynamics. *International Journal of Chemistry*, 3(3), 103–112.

Suryawanshi S.B. (2019). Atomic Absorption Spectroscopy. *Analytical Chemistry*, 6, 8-9

Sych, N. V., Trofymenko, S. I., Poddubnaya, O. I., Tsyba, M. M., Sapsay, V. I., Klymchuk, D. O., & Puziy, A. M. (2012). Porous structure and surface chemistry of phosphoric acid activated carbon from corncob. *Applied Surface Science*, 261*(5)*, 75–82.

Smolyakov, S.B., (2012) . Uptake of Zn., Cu, Pb and Cd by water hyacinth in the initial stage of water system remediation. *Journal of applied geochemistry* 27(6), 1214-1219.

Taboada-Castro, M., Diéguez-Villar, A., Rodríguez-Blanco, M. L., & Taboada-Castro, M. T. (2012). Agricultural Impact of Dissolved Trace Elements in Runoff Water from an Experimental Catchment with Land-Use Changes. *Communications in Soil Science and Plant Analysis*, 43(1–2), 81–87.

Taha, A., & Dakroury, A. (2007). Assessment removal of heavy metals ions from wastewater by cement kiln dust (CKD). *Journal of American Science*, 6(12), 910-917.

Tao, B., & Fletcher, A. J. (2013). Metaldehyde removal from aqueous solution by adsorption and ion exchange mechanisms onto activated carbon and polymeric sorbents. *Journal of Hazardous Materials*, 2011 (*244–245)*, 240–250.

Tongpoothorn, W., Sriuttha, M., Homchan, P., Chanthai, S., & Ruangviriyachai, C. (2011). Preparation of activated carbon derived from Jatropha curcas fruit shell by simple thermo-chemical activation and characterization of their physico-chemical properties. *Chemical Engineering Research and Design*, 89(3), 335–340.

Tripathi, A., & Ranjan, M. R. (2015) Heavy Metal Removal from Wastewater Using Low Cost Adsorbents. *Journal of Bioremediation and Biodegradation* 6(6) 1-5.

Ullah, A., Heng, S., Munis, M. F. H., Fahad, S., & Yang, X. (2015). Phytoremediation of heavy metals assisted by plant growth promoting (PGP) bacteria: A review. *Environmental and Experimental Botany*, 117, 28–40.

UNICEF (2008). Water Sanitation and Hygiene Annual Report (14-23)

Vijayaraghavan, G.; & Sivakumar, T. V. (2011). Application of Plant Based Coagulants for Waste Water Treatment. *International Journal of Advanced Engineering Research and Studies*, 1(1), 88–92.

Vrhovnik, P., Dolenec, T., Serafimovski, T., Dolenec, M., & Šmuc, N. R. (2013). The occurrence of heavy metals and metalloids in surficial lake sediments before and after a tailings dam failure. *Polish Journal of Environmental Studies*, 22(5), 1525–1538.

Wang, L. K., Vaccari, D. A., Li, Y., & Shammas, N. K. (2005). Chemical Precipitation. *Physicochemical Treatment Processes*, 3, 141–197.

Wani, Ab Latif, Anjum Ara & Jawed Ahmad Usmani. (2015). “Lead Toxicity: A Review.” *Interdisciplinary Toxicology* 8(2): 55–64.

Wanja, E.., Murungi, J., Wanjau, R., & Hassan, A. (2015). Application of chemically modified avocado seed in the removal of Cu(II) and Cd(II) ions from aqueous solution. Internation Journal of Research in Engineering and Applied Sciences. 6(8): 1-15

Wasewar, K. (2010). Adsorption of metals onto tea factory waste: a review. *International Journal of Research and Reviews in Applied Sciences*, 3(6), 303–322.

Wei, Y., Van Houten, R. T., Borger, A. R., Eikelboom, D. H., & Fan, Y. (2003). Minimization of excess sludge production for biological wastewater treatment. *Water Research*, 37(18), 4453–4467.

WHO., (2006). Geneva, *Guidelines for drinking water quality*, World Health Organisation: Geneva Switzerland 296-31.

Yousef, N. S., Farouq, R., & Hazzaa, R. (2016). Adsorption kinetics and isotherms for the removal of nickel ions from aqueous solutions by an ion-exchange resin: application of two and three parameter isotherm models. *Desalination and Water Treatment*, *57*(46), 21925–21938.

Yu, M., Gong, H., Chen, Z., & Zhang, M. (2013). Adsorption characteristics of activated carbon for siloxanes. *Journal of Environmental Chemical Engineering*, *1*(4), 1182–1187.

Yu, S. M., Ren, A. P., Chen, C. L., Chen, Y. X., Wang, X., Ozsoy, O., Bekbolet, M., Missana, T & García-Gutiérrez.;(2013). The Removal Of Heavy Metal Ions (Copper, Zinc, Nickel And Cobalt) By Natural Bentonite. *Applied Radiation and Isotopes*, 26(1), 288–294.

Zewail, T. M., & Yousef, N. S. (2015). Kinetic study of heavy metal ions removal by ion exchange in batch conical air spouted bed. *Alexandria Engineering Journal*, 54(1), 83–90.

Zhang, D., Wang, C., Bao, Q., Zheng, J., Deng, D., Duan, Y., & Shen, L. (2018). The physicochemical characterization, equilibrium, and kinetics of heavy metal ions

adsorption from aqueous solution by arrowhead plant (Sagittaria trifolia L.) stalk. *Journal of Food Biochemistry*, 42(1), 1–12.

Zhu, S. G., He, W. Z., Li, G. M., Zhou, X., Zhang, X. J., & Huang, J. W. (2012). Recovery of Co and Li from spent lithium-ion batteries by combination method of acid leaching and chemical precipitation. *Transactions of Nonferrous Metals Society of China (English Edition)*, 22(9), 2274–2281.

APPENDICES

Appendix I: Effect of pH on Pb (II) ions removal

Initial concentration = 4 mg/L

pH	Eq (mg/L)	Av (mg/L)	SD	% Removal
2	0.2851,0.3041, 0.2972	0.2953	± 0.0096	96.15
3	0.1432,0.1476, 0.1496	0.1468	± 0.0033	98.16
4	0.0701,0.0739, 0.0761	0.0733	± 0.0030	99.10
5	0.0542,0.0582, 0.053	0.0551	± 0.0027	99.13
6	0.121,0.1361, 0.128	0.1286	± 0.0072	98.23
7	0.1476, 0.1458 0.1446	0.1460	± 0.0015	97.51
8	1.1788 1.1677 1.1724	1.1727	± 0.0056	81.77
10	1.1765 1.179 1.1771	1.1775	± 0.0013	81.39

Appendix II: Effect of adsorbent dosage on Pb (II) ions removal

Initial concentraion = 4 mg/L

Ad (g)	Eq (mg/L)	Av (mg/L)	SD	% Removal
0.1	0.2270, 0.2231, 0.2246	0.2249	± 0.0020	97.49
0.2	0.0993, 0.1056, 0.0961	0.1003	± 0.0048	98.90
0.3	0.0397, 0.0375, 0.0381	0.0384	± 0.0012	99.36
0.4	0.0624, 0.0615, 0.0617	0.0618	± 0.0005	99.31
0.5	0.0761, 0.0773, 0.0764	0.0765	± 0.0005	99.15
0.6	0.0785, 0.0782, 0.0782	0.0782	± 0.0003	99.13
0.7	0.0781, 0.0782, 0.0779	0.0783	± 0.0002	99.14

Appendix III: Effect of Contact Time on Cd (II) Ions Adsorption

Initial concentration = 4 mg/L

Time (min)	Eq (mg/L)	AV (mg/L)	SD	% Removal
15	0.1216, 0.1214, 0.120	0.1211	± 0.0007	98.70
30	0.0710, 0.0747, 0.0727	0.0730	±0.0035	99.22
45	0.0469, 0.0432, 0.0450	0.0450	± 0.0019	99.51
60	0.0403, 0.0412, 0.0393	0.0399	± 0.0005	99.56
75	0.0204, 0.0190, 0.0211,	0.0201	± 0.0010	99.78
90	0.0252, 0.0232, 0.0244	0.0242	± 0.0011	99.74
105	0.0236, 0.0247, 0.0251	0.0244	± 0.0008	99.73
120	0.0242, 0.0247, 0.0238	0.0242	± 0.0005	99.74

Appendix IV: Effects on initial metal ions concentration on Cd (II) ions removal

In (mg/l)	Eq (mg/L)	Av (mg/L)	SD	% Removal
4	0.1509, 0.1549,0.1561	0.1540	± 0.0027	96.15
8	0.0239, 0.0193, 0.0210	0.0214	± 0.0023	99.49
12	0.2135, 0.2161, 0.2170	0.2155	± 0.0018	98.20
16	0.3228, 0.3298,0.3251	0.3257	± 0.0033	97.95
20	0.4102, 0.4114, 0.4146	0.4121	± 0.0022	97.93
24	0.6694, 0.6621, 0.6675	0.6663	± 0.0038	97.22
28	0.8149 , 0.8178, 0.8164	0.8164	± 0.0015	97.08
32	0.9846 , 0.9872, 0.9864	0.9861	± 0.0013	96.91

Appendix V: Kinetic data for Cd (II) Ions Removal

Initial concentration = 8 mg/L

Time (mins)	Eq (mg/L)	Av (mg/L)	SD
15	0.1259, 0.1273, 0.1372	0.1301	±0.0062
30	0.0758 , 0.0772, 0.0783	0.0771	±0.0013
45	0.0493 , 0.0424, 0.0498	0.0472	±0.0054
60	0.0412 , 0.0419, 0.0415	0.0415	±0.0004
75	0.0298 , 0.0252, 0.0226	0.0259	±0.0027
90	0.027, 0.0213, 0.0233	0.0239	±0.0029
105	0.0241 , 0.0283, 0.0306	0.0277	±0.0035
120	0.028 , 0.0228, 0.0333	0.0280	±0.0053

Appendix VI: Effect of pH on Pb (II) ions removal

Initial concentration = 8 mg/L

Ph	Eq (mg/L)	Av (mg/L)	SD	% Removal
2	1.5711, 1.6009, 1.5803	1.5833	0.0153	60.5
3	0.7269, 0.7269, 0.7266	0.7268	0.0002	81.83
4	0.2254, 0.2253, 0.2251	0.2253	0.0002	94.37
5	0.6714, 0.6720, 0.6717	0.6717	0.0003	83.21
6	0.8002, 0.8007, 0.8004	0.8004	0.0003	79.99
7	1.4646, 1.4646, 1.4642	1.4648	0.0004	68.38
8	1.2969, 1.2964, 1.2963	1.2965	0.0004	67.59
10	1.3193, 1.3201, 1.3193	1.3196	0.0005	67.01

Appendix VII: Effect of sorbent mass on Pb (II) ions removal

Initial concentration = 8 mg/L

Ad (g)	Av (mg/L)	Av (mg/L)	SD	% removal
0.1	0.7092, 0.7080, 0.7098	0.709	0.0009	90.71
0.2	0.3664, 0.3657, 0.3652	0.3658	0.0006	95.45
0.3	0.3295, 0.3288, 0.3284	0.3289	0.0006	95.91
0.4	0.2446, 0.2438, 0.2432	0.2439	0.0007	96.91
0.5	0.2592, 0.2584, 0.2587	0.2588	0.0004	96.78
0.6	0.2807, 0.2804, 0.2809	0.2805	0.0001	96.51
0.7	0.2822, 0.2822, 0.2817	0.2820	0.0003	96.49
0.8	0.2874, 0.2876, 0.2881	0.2877	0.0003	96.42
0.9	0.3443, 0.3437, 0.3442	0.3441	0.0003	95.72
1.0	0.3049, 3055, 0.3059	0.3054	0.0005	95.46

Appendix VIII: Effect of initial metal ion concentration on Pb (II) ions adsorption

In (mg/L)	Eq (mg/L)	Av (mg/L)	SD	% Removal
2.3826	0.9459, 0.9446, 0.9439	0.9448	0.0010	60.35
4.0427	0.1441, 0.1390, 0.1419	0.1416	0.0026	96.52
9.6203	0.2735, 0.2733, 0.2728	0.2732	0.0004	97.16
12.1408	0.8752, 0.8755, 0.8759	0.8755	0.0004	92.78
15.0041	1.1115, 1.1119, 1.1121	1.1118	0.0003	92.59
19.2991	1.9284, 1.9279, 1.9275	1.9280	0.0005	90.01
23.9864	2.6823, 2.6818, 2.6814	2.6818	0.0004	88.82
28.1833	3.9877, 3.9921, 3.9937	3.9878	0.0004	85.85

Appendix IX: Effects of contact time on Pb (II) ions adsorption

Initial concentration = 8 mg/L

Time	Eq (mg/L)	Av (mg/L)	SD	% Removal
15	1.5784, 1.5791, 1.5787	1.5787	0.0003	80.37
30	0.6799, 0.6793, 0.6796	0.6796	0.0003	91.55
45	0.3309, 0.3303, 0.3301	0.3306	0.0003	95.89
60	0.1847, 0.1851, 0.1849	0.1849	0.0002	97.70
75	0.2008, 0.2012, 0.2011	0.2010	0.0002	97.50
90	0.2254, 0.2251, 0.2247	0.2251	0.0003	97.21
105	0.2296, 0.2292, 0.228	0.2292	0.000451	97.15
120	0.2335, 0.2329, 0.2332	0.2332	0.0003	97.09

Appendix X: Variation (ANOVA) for the effect of pH for Pb(II) ions removal

Source of Variation	SS	Df	MS	F	P-value	F crit
Between Groups	110.2841	1	110.2841	59.8736	1.24E-08	4.1708
Within Groups	55.2585	30	1.8419			
Total	165.5427	31				

Appendix XI: Variation (ANOVA) for the effect of pH for Cd (II) ions removal

Source of Variation	SS	Df	MS	F	P-value	F crit
Between Groups	163.8369	1	163.8369	89.6950	1.6E-10	4.1709
Within Groups	54.7981	30	1.826601			
Total	218.635	31				

Appendix XII: Variation (ANOVA) for the effect of sorbent mass for Pb (II) ions removal

Source of Variation	*SS*	*Df*	*MS*	*F*	*P-value*	*F crit*
Between Groups	1.0565	1	1.0565	39.5903	2.26E-07	4.0981
Within Groups	1.0141	38	0.0266			
Total	2.0706	39				

Appendix XIII: Variation (ANOVA) for the effect of sorbent mass on Cd (II) ions removal

Source of Variation	*SS*	*Df*	*MS*	*F*	*P-value*	*F crit*
Between Groups	1.6085	1	1.6085	67.9667	5.46E-10	4.0981
Within Groups	0.8993	38	0.0236			
Total	2.5078	39				

Appendix XIV: Variation (ANOVA) for the effect of contact time on Pb (II) ions removal

Source of Variation	*SS*	*Df*	*MS*	*F*	*P-value*	*F crit*
Between Groups	27079.37	1	27079.37	85.9607	2.58E-10	4.1709
Within Groups	9450.615	30	315.0205			
Total	36529.98	31				

Appendix XV: Variation (ANOVA) for the effect of contact time on Cd (II) ions removal

Source of Variation	*SS*	*Df*	*MS*	*F*	*P-value*	*F crit*
Between Groups	27299.85	1	27299.85	86.66595	2.36E-10	4.170877
Within Groups	9450.025	30	315.0008			
Total	36749.87	31				

Appendix XVI: Variation (ANOVA) for the effect of initial metal ions concentration and adsorption isotherms on Pb(II) ions removal

Source of Variation	*SS*	*Df*	*MS*	*F*	*P-value*	*F crit*
Between Groups	1097.589	1	1097.589	62.3221	2.27E-08	4.2252
Within Groups	457.9004	26	17.61155			
Total	1555.49	27				

Appendix XVII: Variation (ANOVA) for the effect of initial metal ions concentration and adsorption isotherms on Cd (II) ions removal

Source of Variation	*SS*	*Df*	*MS*	*F*	*P-value*	*F crit*
Between Groups	1282.058	1	1282.058	74.1654	4.32E-09	4.2252
Within Groups	449.4485	26	17.28648			
Total	1731.506	27				

Appendix XVIII: Variation (ANOVA) for the kinetic studies on Pb (II) ions removal

Source of Variation	*SS*	*Df*	*MS*	*F*	*P-value*	*F crit*
Between Groups	5276.701	1	5276.701	66.2855	4.41E-08	4.3010
Within Groups	1751.326	22	79.60571			
Total	7028.026	23				

Appendix XIX: Variation (ANOVA) for the kinetic studies on Cd (II) ions removal

Source of Variation	*SS*	*Df*	*MS*	*F*	*P-value*	*F crit*
Between Groups	12122.92	1	12122.92	86.5917	2.38E-10	4.1709
Within Groups	4200.029	30	140.001			
Total	16322.95	31				

Appendix XX: Calibration curve for the effect of pH on Pb (II) ions removal

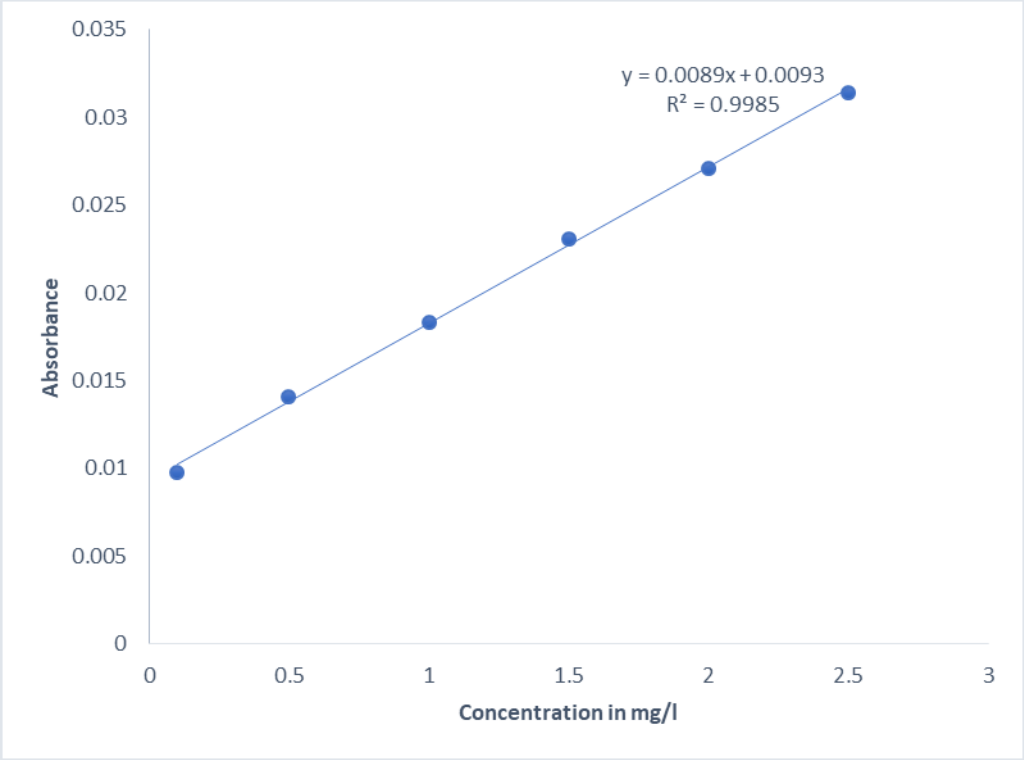

Appendix XXI: Calibration curve for the effect of pH on Cd (II) ions removal

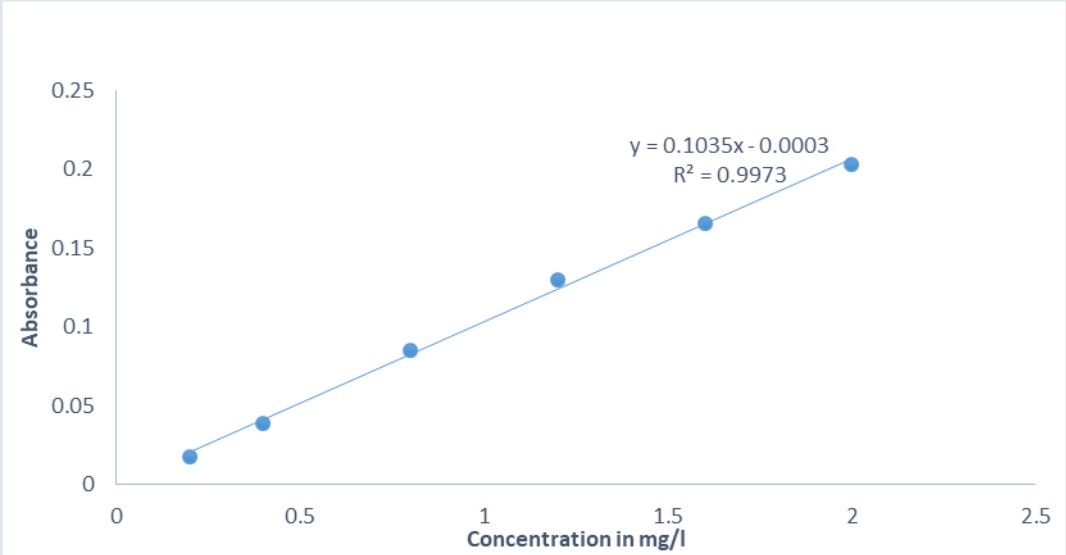

Appendix XXII: Calibration curve for the effect of sorbent mass on Pb (II) ions removal

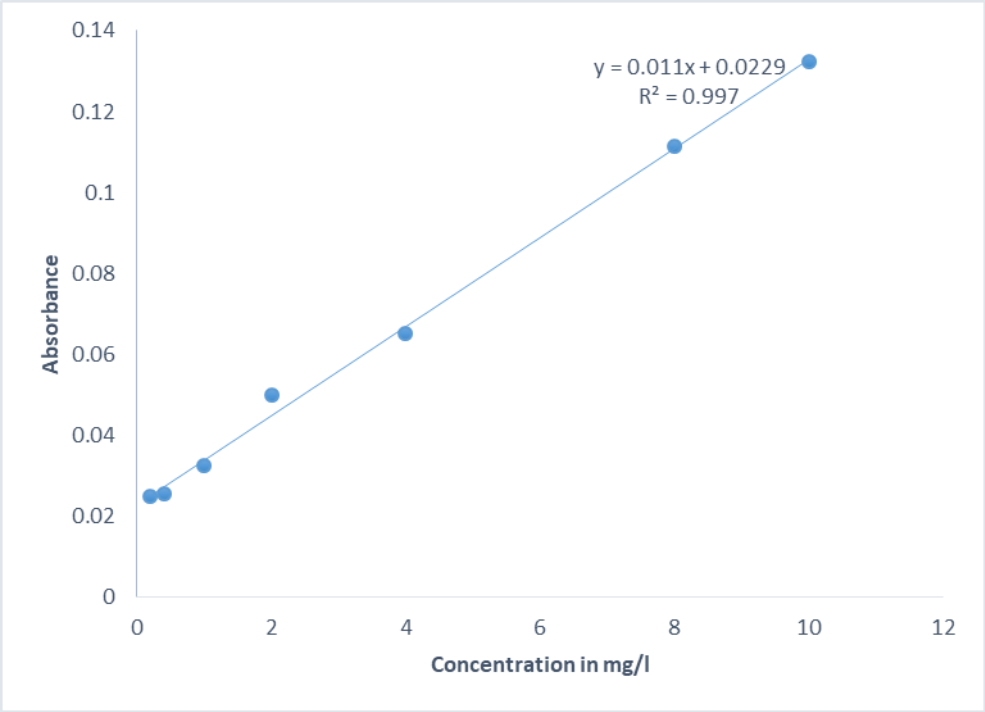

Appendix XXIII: Calibration curve for the effect of sorbent mass on Cd (II) ions removal

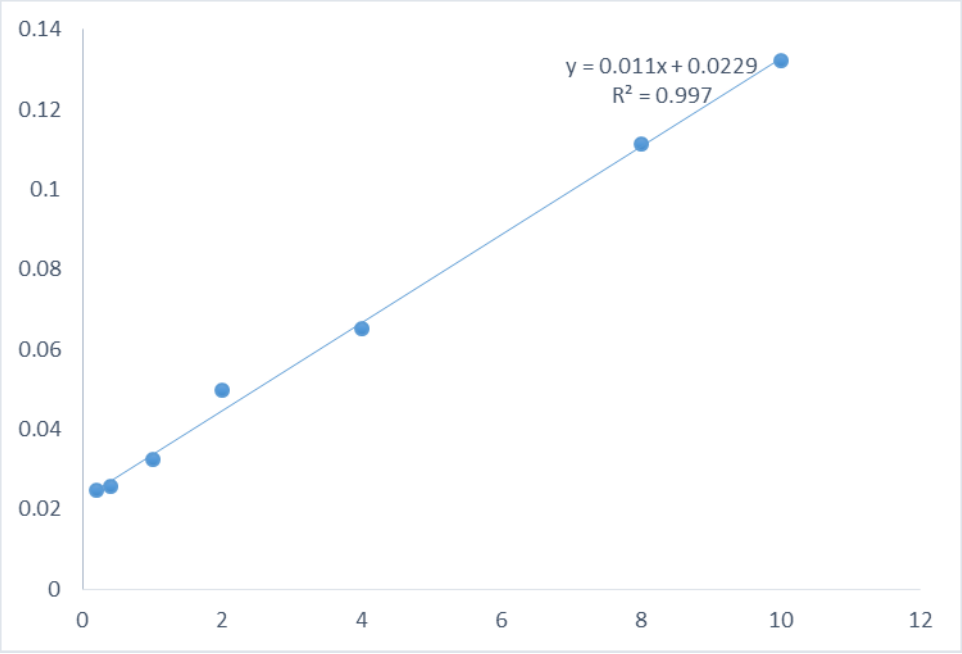

Appendix XXIV: Calibration curve for the effect of contact time on Pb (II) ions removal

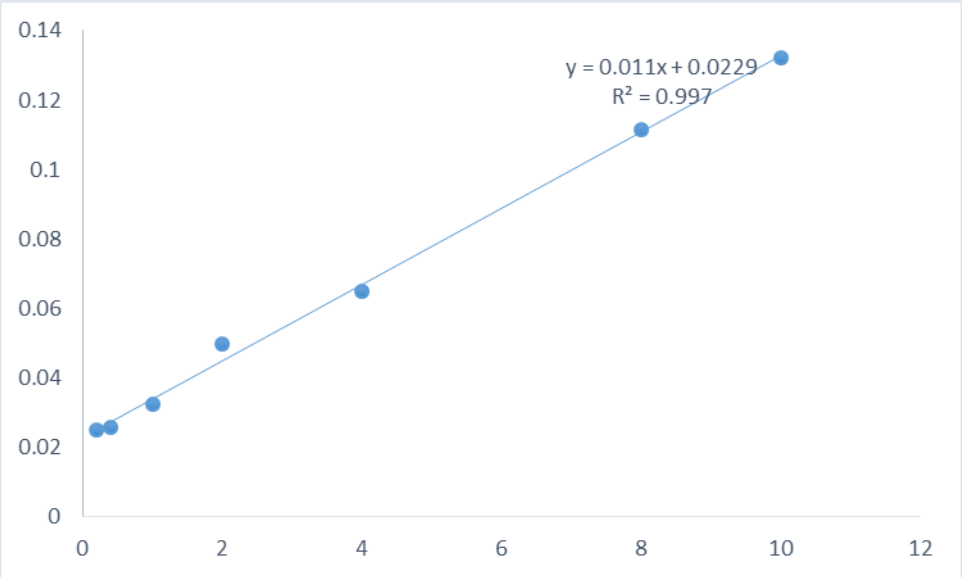

Appendix XXV: Calibration curve for the effect of contact time on Cd (II) ions removal

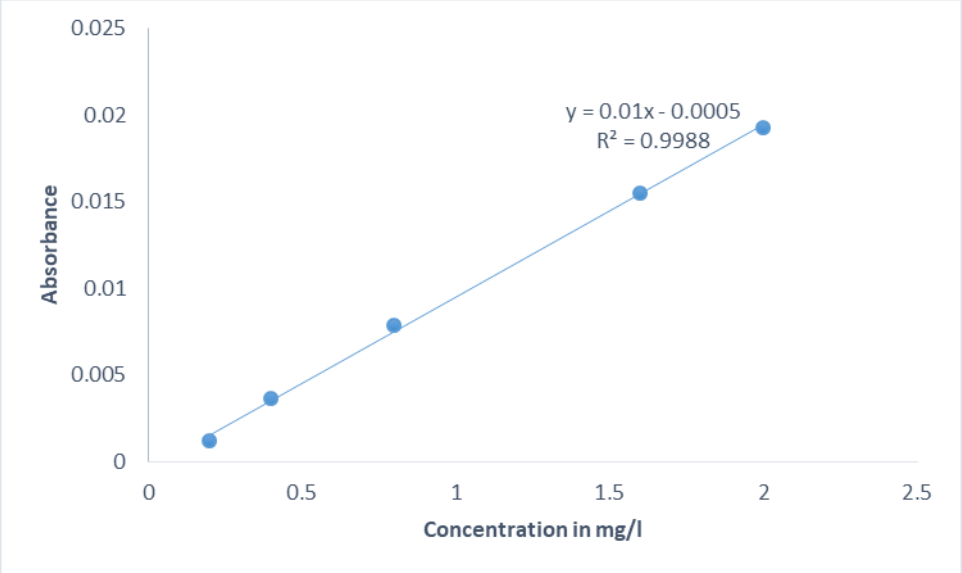

Appendix XXVI: Calibration curve for the effect of initial metal ions concentration and adsorption isotherms on Pb (II) ions removal

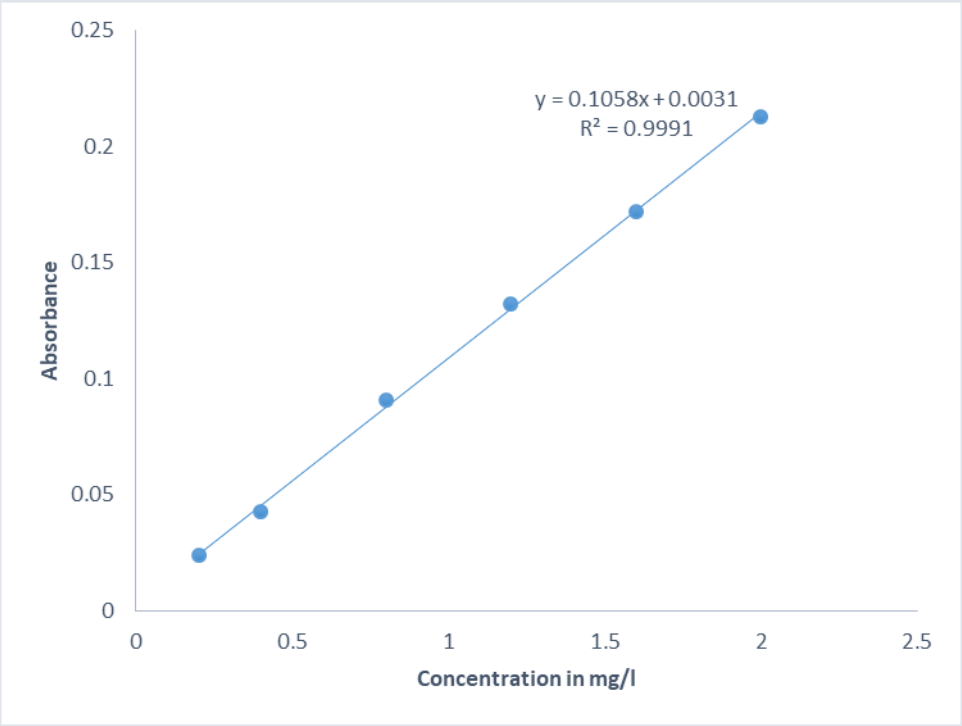

Appendix XXVII: Calibration curve for the effect of initial metal ions concentration and adsorption isotherms on Cd (II) ions removal

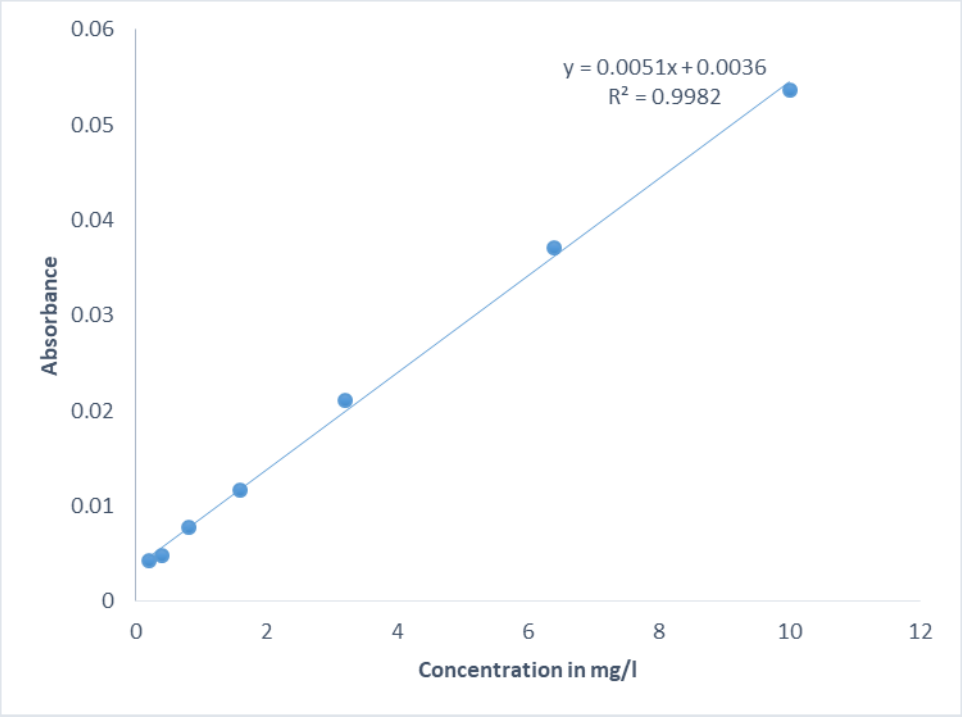

Appendix XXVIII: Calibration curve for the kinetic studies on Pb (II) ions removal

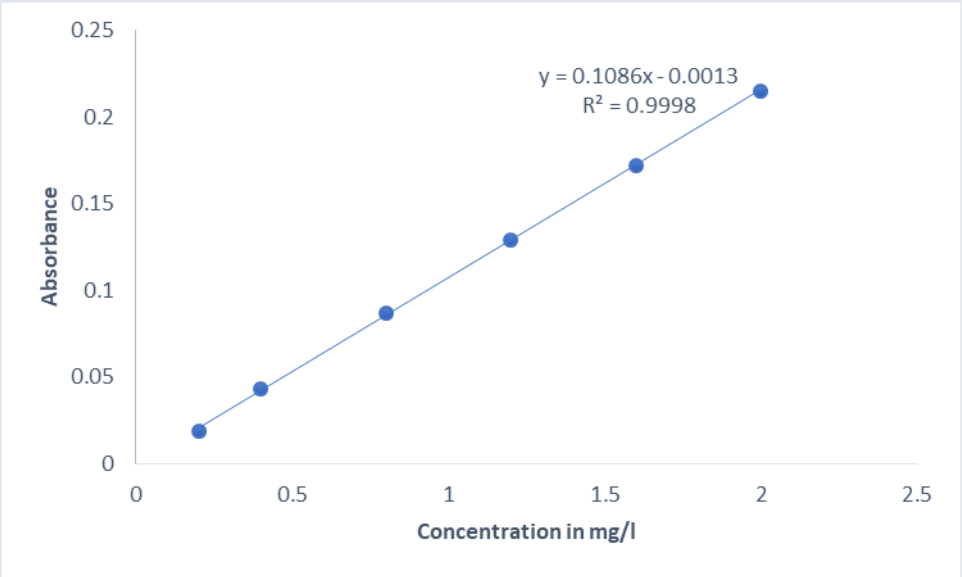

Appendix XXIX: Calibration curve for the kinetic studies on Cd(II) ions removal

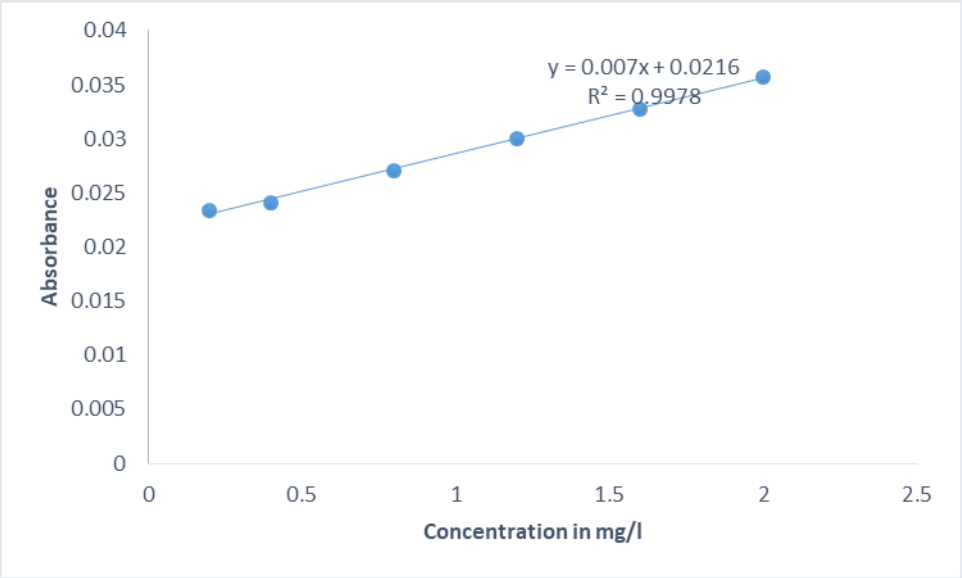

Appendix XXX: Adsorption isotherm data for Pb (II) ions and Cd(II) ions

Lead					Cadmium				
Ce	**qe**	**Ce/qe**	**lnce**	**lnqe**	**Ce**	**qe**	**Ce/qe**	**lnce**	**lnqe**
0.140	0.382	0.367	-1.966	-0.963	0.154	1.638	0.094	-1.871	0.493
0.273	0.630	0.433	-1.298	-0.462	0.189	1.871	0.101	-1.666	0.626
0.877	1.558	0.563	-0.131	0.443	0.215	2.087	0.103	-1.537	0.736
1.136	1.734	0.655	0.127	0.550	0.326	2.612	0.12	-1.121	0.960
1.902	2.174	0.875	0.643	0.777	0.412	3.169	0.126	-0.886	1.153
2.748	2.655	1.035	1.011	0.976	0.666	3.889	0.171	-0.406	1.358
3.987	3.024	1.318	1.383	1.107	0.816	4.531	0.180	-0.203	1.511

Appendix XXXI: Kinetics data for Pb (II) ions and Cd (II) ions

Lead					Cadmium				
Ce	**qe**	**t/qt**	**qt**	**ln(qe-qt)**	**Ce**	**qe**	**t/qt**	**qt**	**ln(qe-qt)**
0.350	0.9563	26.14	0.3825	-0.5555	0.1301	1.3116	25.41	0.3935	-0.085
0.265	0.9667	51.71	0.38675	-0.5448	0.0771	1.3205	50.48	0.3962	-0.079
0.180	0.9775	76.73	0.391	-0.5335	0.0472	1.3255	75.45	0.39764	-0.075
1.169	0.9828	102.15	0.39155	-0.5255	0.0415	1.3264	100.52	0.39792	-0.074
0.106	0.9868	126.68	0.3947	-0.5241					

0.102 0.9873 151.94 0.3949 -0.5236	0.0259 1.3290 125.41 0.3987 -0.072 0.0239 1.3294 150.45 0.3988 -0.0719 0.0277 1.3287 175.61 0.3986 0.0280 1.3299 200.71 0.3986